NASA/TM—2007–215131

Numerical Modeling of Propellant Boiloff in Cryogenic Storage Tank

A.K. Majumdar
Marshall Space Flight Center, Marshall Space Flight Center, Alabama

T.E. Steadman and J.L. Maroney
Sverdrup Technology, Inc., Huntsville, Alabama

November 2007

The NASA STI Program Office…in Profile

Since its founding, NASA has been dedicated to the advancement of aeronautics and space science. The NASA Scientific and Technical Information (STI) Program Office plays a key part in helping NASA maintain this important role.

The NASA STI Program Office is operated by Langley Research Center, the lead center for NASA's scientific and technical information. The NASA STI Program Office provides access to the NASA STI Database, the largest collection of aeronautical and space science STI in the world. The Program Office is also NASA's institutional mechanism for disseminating the results of its research and development activities. These results are published by NASA in the NASA STI Report Series, which includes the following report types:

- TECHNICAL PUBLICATION. Reports of completed research or a major significant phase of research that present the results of NASA programs and include extensive data or theoretical analysis. Includes compilations of significant scientific and technical data and information deemed to be of continuing reference value. NASA's counterpart of peer-reviewed formal professional papers but has less stringent limitations on manuscript length and extent of graphic presentations.

- TECHNICAL MEMORANDUM. Scientific and technical findings that are preliminary or of specialized interest, e.g., quick release reports, working papers, and bibliographies that contain minimal annotation. Does not contain extensive analysis.

- CONTRACTOR REPORT. Scientific and technical findings by NASA-sponsored contractors and grantees.

- CONFERENCE PUBLICATION. Collected papers from scientific and technical conferences, symposia, seminars, or other meetings sponsored or cosponsored by NASA.

- SPECIAL PUBLICATION. Scientific, technical, or historical information from NASA programs, projects, and mission, often concerned with subjects having substantial public interest.

- TECHNICAL TRANSLATION. English-language translations of foreign scientific and technical material pertinent to NASA's mission.

Specialized services that complement the STI Program Office's diverse offerings include creating custom thesauri, building customized databases, organizing and publishing research results…even providing videos.

For more information about the NASA STI Program Office, see the following:

- Access the NASA STI Program Home Page at ***http://www.sti.nasa.gov***

- E-mail your question via the Internet to help@sti.nasa.gov

- Fax your question to the NASA Access Help Desk at 301–621–0134

- Telephone the NASA Access Help Desk at 301–621–0390

- Write to:
  NASA Access Help Desk
  NASA Center for AeroSpace Information
  7121 Standard Drive
  Hanover, MD 21076–1320
  301–621–0390

NASA/TM—2007–215131

Numerical Modeling of Propellant Boiloff in Cryogenic Storage Tank

A.K. Majumdar
Marshall Space Flight Center, Marshall Space Flight Center, Alabama

T.E. Steadman and J.L. Maroney
Sverdrup Technology, Inc., Huntsville, Alabama

National Aeronautics and
Space Administration

Marshall Space Flight Center • MSFC, Alabama 35812

November 2007

Acknowledgments

The authors would like to acknowledge James Fesmire, Jared Sass, Alexis Hongamen, Steve Sojourner, and Zoltan Nagy of the Cryogenic Test Laboratory, Kennedy Space Center, for their valuable contribution to this effort through many technical interchange meetings, transmission and discussions of test data, laboratory and facility visits, and several administrative processes during the entire period of investigation.

Available from:

NASA Center for AeroSpace Information
7115 Standard Drive
Hanover, MD 21076–1320
301–621–0390

This report is also available in electronic form at
<https://www2.sti.nasa.gov>

TABLE OF CONTENTS

TABLE OF CONTENTS (Continued)

LIST OF FIGURES

LIST OF FIGURES (Continued)

LIST OF TABLES

LIST OF ACRONYMS AND SYMBOLS

CESAT	Cost-Efficient Storage And Transfer
GFSSP	Generalized Fluid System Simulation Program
ID	Inside Diameter
IRAD	Independent Research and Development
KSC	Kennedy Space Center
LC	Launch Complex
LH_2	Liquid Hydrogen
MSFC	Marshall Space Flight Center
OD	Outside Diameter
SASS	Simultaneous Adjustment with Successive Substitution
TM	Technical Memorandum
VTASC	Visual Thermo-fluid Analyzer of Systems and Components

NOMENCLATURE

A	area (m^2)
$A_{u\text{-}p}$	ullage-propellant interface heat transfer area
$A_{u\text{-}p,cond}$	conduction area between the tank wall sections exposed to ullage and propellant
BR	boiloff rate (gallons/day)
CF	conversion factor (613 s-Btu-gal/day-J-ft^3)
D	diameter of inner wall (1.245 m); diameter of the outer tank wall (1.524 m)
D_t	diameter of spherical tank
g	acceleration of gravity (39.8067 m/s^2)
h	height of either propellant or ullage space
h_{fg}	enthalpy (BTU/lb)
h_i	heat transfer coefficient through inner wall (17.361 W/(m^2-K))
h_o	heat transfer coefficient through outer wall (9.068 W/(m^2-K))
h_x	height of either propellant or ullage space
K	thermal conductivity (Btu/s-ft-R)
k	thermal conductivity of fluid (0.1164 W/m-K)
k_p	thermal conductivity of insulation material (W/(m-K))
k_s	thermal conductivity of stainless steel (15.5636 W/(m-K))
L	length (ft)
Nu	Nusselt number
$\dot{Q}$	heat rate (W)
$\dot{Q}_{a\text{-}p}$	ambient to propellent heat rate (W)
$\dot{Q}_{a\text{-}u}$	ambient to ullage heat rate (W)
$\dot{Q}_{s\text{-}p}$	solid to propellent heat rate (W)
$\dot{Q}_{u\text{-}p}$	ullage to propellent heat rate (W)

NOMENCLATURE (Continued)

q	heat transfer rate (Btu/s)
Ra	Rayleigh Number (dimensionless)
Re	Reynolds number (dimensionless)
$R_{u\text{-}p}$	radius calculated using either the ullage or propellant height
T	temperature
t_{wall}	wall thickness of the tank
U	overall heat transfer through the system (W/m^2-K)
V_t	volume of spherical tank
V_x	corresponding volume
v	velocity of air (assume 5 mph wind = 2.235 m/s); kinematic viscosity of fluid (1.96E-7 m^2/s)
w	wall
x	ullage or propellant
α	thermal diffusivity of fluid (1.75E-7 m^2/s).
β	thermal expansion coefficient (9.5E-6 m/m-K)
ΔT	temperature difference between liquid and wall (assume 0.55K)
δ_p	thickness of insulation material (0.12509 m)
δ_{si}	thickness of inner sphere wall (0.004755 m)
δ_{so}	thickness of outer sphere wall (0.004755 m)
μ	viscosity of air (1.86E-5 kg/m-s)
ρ	density (lb/ft^3); density of air (1.2 kg/m^3)

TECHNICAL MEMORANDUM

NUMERICAL MODELING OF PROPELLANT BOILOFF IN CRYOGENIC STORAGE TANK

1. INTRODUCTION

1.1 Purpose and Objective

The cost of boiloff of propellants in cryogenic storage tanks at launch complex 39 (LC-39) at Kennedy Space Center (KSC) is in the order of $1M per year. The LC-39A and LC-39B storage tanks for liquid hydrogen (LH_2) are spherical (fig. 1). The vacuumed annulus space between the inner and outer spheres of each storage tank is filled with perlite insulation. Perlite is susceptible to compaction after repeated thermal cycles. It is widely believed that the compaction has led to decreased thermal performance.

Figure 1. Liquid hydrogen tank in LC-39A at Kennedy Space Center.

The Cryogenic Test Laboratory at KSC has undertaken a study of insulation materials for cryogenic tanks in order to reduce boiloff from liquid hydrogen and oxygen tanks. Fesmire and Augustynowicz[1] have measured apparent thermal conductivity of several bulk-fill insulation materials and have found that the thermal conductivity of glass bubbles is 67% less than perlite in vacuum. In another study, Fesmire et al.[2] studied the vibration and thermal cycling effects on several bulk-fill insulation materials and found that glass bubbles are not susceptible to compaction due to thermal cycling. As a part of the Independent Research and Development (IRAD) project entitled, "New Materials and Technology for Cost Efficient Storage and Transfer (CESAT)," KSC has built two 1,000-L demonstration tanks (fig. 2) and tested the performance of perlite and glass bubble insulation for liquid nitrogen and hydrogen.

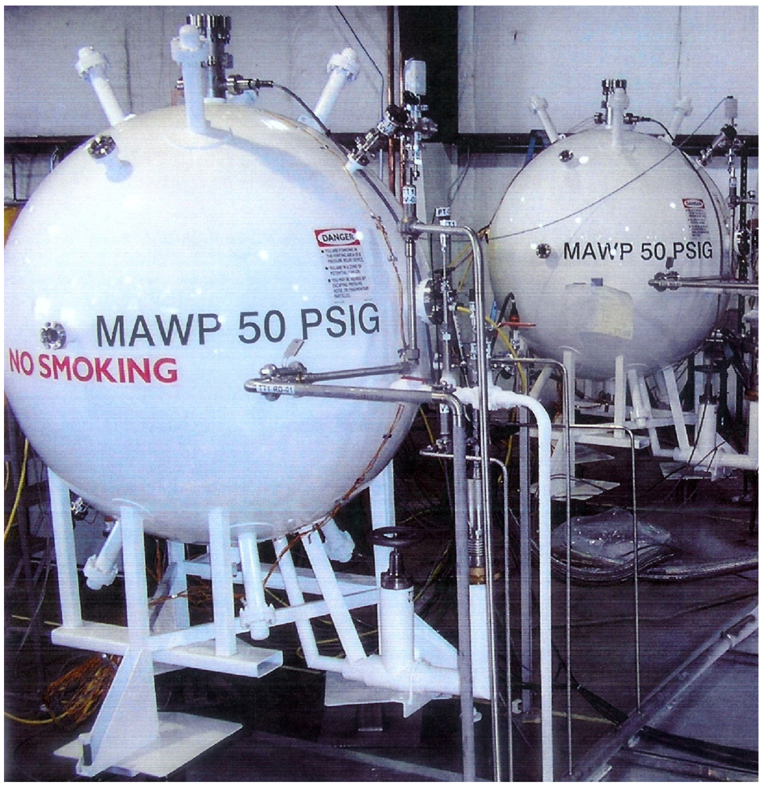

Figure 2. Two 1,000-L demonstration tanks for measuring boiloff of liquid hydrogen and nitrogen using glass bubbles and perlite insulation.

Marshall Space Flight Center (MSFC) was responsible for developing numerical models to calculate boiloff for the demonstration and full-scale tanks. The main objective of the thermal modeling effort is to numerically predict the boiloff rate of stored propellants in a cryogenic tank with different insulation materials. The intent is to compare the boiloff rate when using two different insulation materials—glass bubbles and perlite. The scope of the thermal modeling effort includes (1) development, testing, and running models for the 1,000-L demonstration tanks with liquid nitrogen and hydrogen, (2) comparison of numerical predictions with test data, and (3) development, testing, and running models for the liquid hydrogen tanks of LC-39 at KSC.

1.2 Numerical Approach

Boiloff calculation requires the calculation of heat leak through metal walls and insulation. A simple one-dimensional calculation of heat conduction through a composite layer consisting of metal and insulation is not adequate for estimating the boiloff because the heat leak process is not entirely one dimensional. The tanks are partially filled with vapor at a temperature higher than the liquid propellant. This vapor space, called the ullage, is also stratified due to gravitational effects. In addition to heat conduction through metal and insulation, the thermodynamics and fluid mechanics of the propellant also play a role in determining boiloff rate. Therefore, it is essential to use a code that has the capability to model all of the processes that influence boiloff.

The Generalized Fluid System Simulation Program (GFSSP), developed at MSFC,[3,4] has been used to develop the thermal models for estimating boiloff in the demonstration tanks and the liquid hydrogen storage tank at LC-39. GFSSP is a finite volume-based computer code for analyzing fluid flow in a complex flow circuit. The program is capable of modeling phase changes, compressibility, mixture thermodynamics, pumps, compressors, and external body forces such as gravity and centrifugal. Recently, the code has been upgraded to model conjugate heat transfer[5] that allows simultaneous calculation of solid temperatures accounting for the heat transfer between solid and fluid.

The computational effort was first focused to develop a model for the demonstration tank in order to verify the numerical predictions by comparing with test data. During this effort, two models were developed. In the first model, the internal volume of the tank was modeled by a single node. This node was connected with multiple solid nodes. Each solid node in turn was connected with other solid nodes to model the heat leak path. The underlying assumption of this single fluid node tank model is that vapor and liquid have the same temperature. The second model of the demonstration tank uses two fluid nodes to represent ullage and liquid propellant volume. Both ullage and liquid propellant nodes are connected to solid nodes that have separate heat leak paths. This model allows calculation of ullage temperature different from propellant temperature and also calculates ullage to propellant heat transfer that contributes to boiloff of propellants. This model was verified by comparing with test data for liquid nitrogen and hydrogen. After the verification of the model, the second model was scaled up to represent the full-scale hydrogen tank of LC-39. In addition, the ullage space was further subdivided into eight control volumes to model stratification.

1.3 Outline of the Report

The remaining report consists of five additional sections. Section 2 provides a brief description of the numerical modeling tool, GFSSP, which includes network definition, program structure, mathematical formulation, solution scheme, thermodynamic property program, and fluid resistance options. The cryogenic propellant tanks modeled in this Technical Memorandum (TM) are described in section 3. The tank geometry and instrumentation for the demonstration tanks and the geometry of the full-scale tank has been described. The details of the three numerical models described in section 1.2 have been described in section 4. The results of all three numerical models are described in section 5. This section also describes the comparison of numerical predictions with test data. Section 6 describes the conclusions, which includes a summary of the present investigation and proposed future work.

2. DESCRIPTION OF NUMERICAL MODELING TOOL (GFSSP)

2.1 Network Definition

GFSSP is a general-purpose computer program for analyzing fluid flow and heat transfer in a complex network of fluid and solid systems. Figure 3 shows a network of fluid and solid nodes to model fluid flow and heat transfer in a counter flow heat exchanger. The nodes in the upper leg are representative of flow through the inner pipe and the lower leg represents flow through the annulus. The convective and conduction heat transfer between these streams occurs through solid-fluid and solid-solid conductors. In constructing the flow network, the program uses boundary and internal nodes connected by branches. At the boundary nodes, pressure, temperature, and concentrations are specified. At the internal nodes, all scalar properties such as pressure, temperature, density, compressibility factor, and viscosity are computed. Mass, energy, and species conservation equations are solved at the internal nodes in conjunction with the thermodynamic equation of state for a real fluid. Flow rates are computed at the branches by solving the momentum conservation equation. In constructing the network of solid nodes, the program uses solid nodes and ambient nodes (not shown in the figure). Solid nodes are connected with other solid nodes by solid-solid conductors and with fluid nodes by solid-fluid conductors. Temperatures of solid nodes are calculated by solving energy conservation in solid nodes.

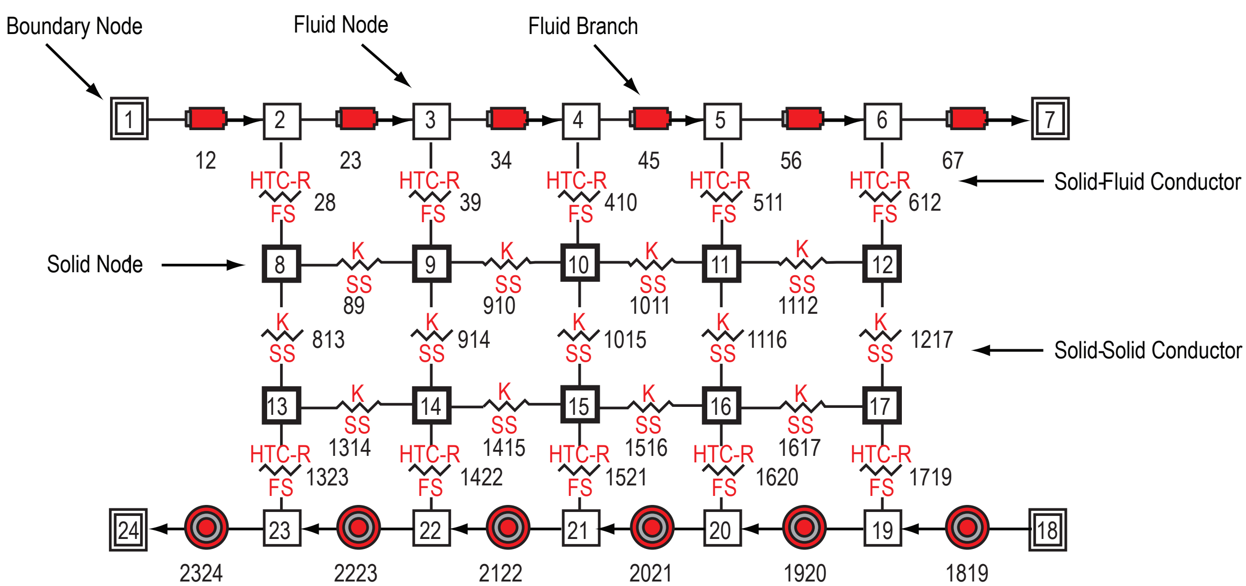

Figure 3. GFSSP network of fluid and solid nodes for a counter flow heat exchanger.

2.2 Program Structure

GFSSP has three major parts (fig. 4). The first part is the graphical user interface, the visual thermo-fluid analyzer of systems and components (VTASC). VTASC allows users to create a flow circuit by a 'point and click' paradigm. It creates the GFSSP input file after the completion of the model building process. It can also create a customized GFSSP executable by compiling and linking user subroutines with the solver module of the code. The user can run GFSSP from VTASC and postprocess the results in the same environment. The second major part of the program is the solver and property module. This is the heart of the program that reads the input data file and generates the required conservation equations for fluid and solid nodes and branches with the help of thermodynamic property programs. It also interfaces with user subroutines to receive any specific inputs from users. Finally, it creates output files for VTASC to read and display results. The user subroutine is the third major part of the program. This consists of several blank subroutines that are called by the solver module. These subroutines allow the users to incorporate any new physical model, resistance option, fluid, etc. in the model.

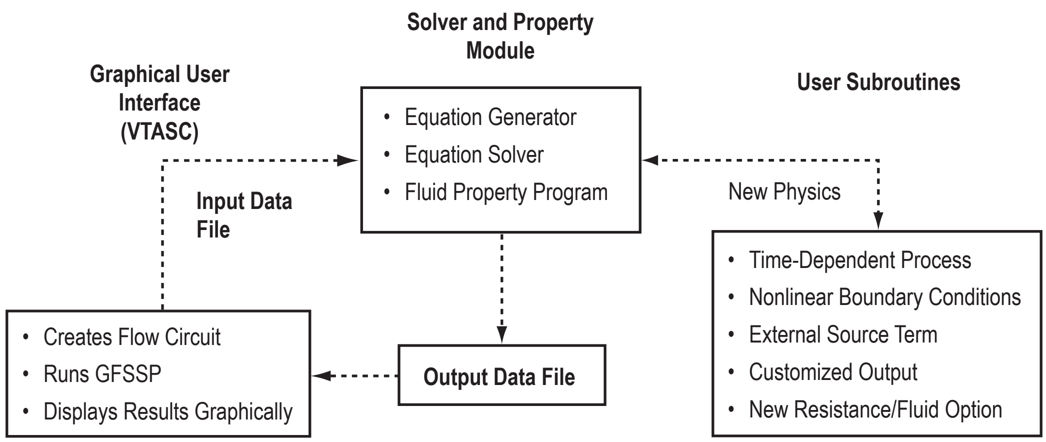

Figure 4. GFSSP's program structure showing the interaction of three major modules.

2.3 Mathematical Formulation and Solution Algorithm

GFSSP solves for conservation equations in internal fluid nodes, branches, and solid nodes to calculate pressure, temperature, and concentrations in fluid nodes, flow rates in branches and temperatures in solid nodes. Table 1 shows the mathematical closure that describes the unknown variables and the available equations to solve the variables. The equations are coupled and nonlinear; therefore, they are solved by an iterative numerical scheme. GFSSP employs a unique numerical scheme known as SASS (simultaneous adjustment with successive substitution), which is a combination of the Newton-Raphson and Successive Substitution methods. The mass and momentum conservation equations and the equation of state are solved by the Newton-Raphson method while the conservation of energy and species are solved by the Successive Substitution method. The user has a choice to solve the energy conservation equation of a solid by either the Successive Substitution or Newton-Raphson method.

Table 1. Mathematical closure.

Unknown Variables	Equations to Solve
Pressure	Mass conservation equation
Flow rate	Momentum conservation equation
Fluid temperature	Energy conservation equation of fluid
Specie concentrations	Conservation equations for mass fraction of species
Mass	Thermodynamic equation of state
Solid temperature	Energy conservation equation of solid

2.4 Property and Resistance Option

Three thermodynamic property programs (GASP,[6] WASP,[7]and GASPAK[8]) are integrated with GFSSP to provide 'real fluid' thermodynamic and thermophysical properties for 35 fluids and ideal gas as shown in table 2. There is also a provision for adding additional fluids with the help of look-up tables.

Table 2. Fluids and ideal gas available in GFSSP.

Index	Fluid/Ideal Gas	Index	Fluid/Ideal Gas
1	Helium	19	Krypton
2	Methane	20	Propane
3	Neon	21	Xenon
4	Nitrogen	22	R-11
5	Carbon monoxide	23	R-12
6	Oxygen	24	R-22
7	Argon	25	R-32
8	Carbon dioxide	26	R-123
9	Parahydrogen	27	R-124
10	Hydrogen	28	R-125
11	Water	29	R-134A
12	RP-1	30	R-152A
13	Isobutane	31	Nitrogen triflouride
14	Butane	32	Ammonia
15	Deuterium	33	Ideal gas
16	Ethane	34	Hydrogen peroxide
17	Ethylene	35	Universal property package
18	Hydrogen sulfide	36	Air

Twenty-one different resistance/source options are provided for modeling momentum sinks or sources in the branches. These options include pipe flow, flow through a restriction, noncircular duct, pipe flow with entrance and/or exit losses, thin sharp orifice, thick orifice, square-edge reduction, square-edge expansion, rotating annular duct, rotating radial duct, labyrinth seal, parallel plates, common fittings and valves, pump characteristics, pump power, valve with a given loss coefficient, Joule-Thompson device, control valve, compressible flow orifice, heat exchanger core, and parallel tubes. The program has the provision of including additional resistance options through user subroutines.

2.5 Code Validation and Verification

GFSSP has gone through extensive validation and verification since the first version was released in 1996. Three methods have been used for code validation: (1) Comparison with classical analytical and numerical solution, (2) comparison with other codes, and (3) comparison with test data. Detailed comparisons with test data and analytical solutions are described in references 3, 4, 9, and 10.

3. DESCRIPTION OF CRYOGENIC PROPELLANT TANKS

3.1 Demonstration Tanks

Two identical 1/15th scale demonstration test tanks were manufactured by PHPK, Inc. for the CESAT test program. Both tanks (fig. 2) were constructed with stainless steel inner and outer spheres. The annular space between the two spheres in each tank can be filled with an insulating material and the pressure can be reduced to vacuum conditions. Both tanks include fill/drain lines, vent lines, support structures, and antirotation systems that could contribute to heat leak. Finally, both tanks are heavily instrumented with identical measurements in identical locations. This section discusses the relevant geometric characteristics and instrumentation for both tanks.

3.1.1 Geometry

Figure 5 shows the dimensions of the two CESAT demonstration tanks. The inner diameter of the inner sphere is ≈1.245 m (≈49 in), which results in a total inner sphere volume of 1,000 L (35.31 ft^3). The outer diameter of the outer sphere is 1.534 m (60.375 in). Both spheres have a wall thickness of 4.7625 mm (0.1875 in). The resulting annular space is 134.938 mm (5.3125 in) wide. A section of the vent line with a length of 1.245 m (49 in) and an inside diameter of 22.911 mm (0.902 in) was included in the CESAT boiloff models. The geometry of the support structures and antirotation system was considered in a separate analysis that is included in appendix A. No other geometries were considered in the CESAT boiloff models discussed here.

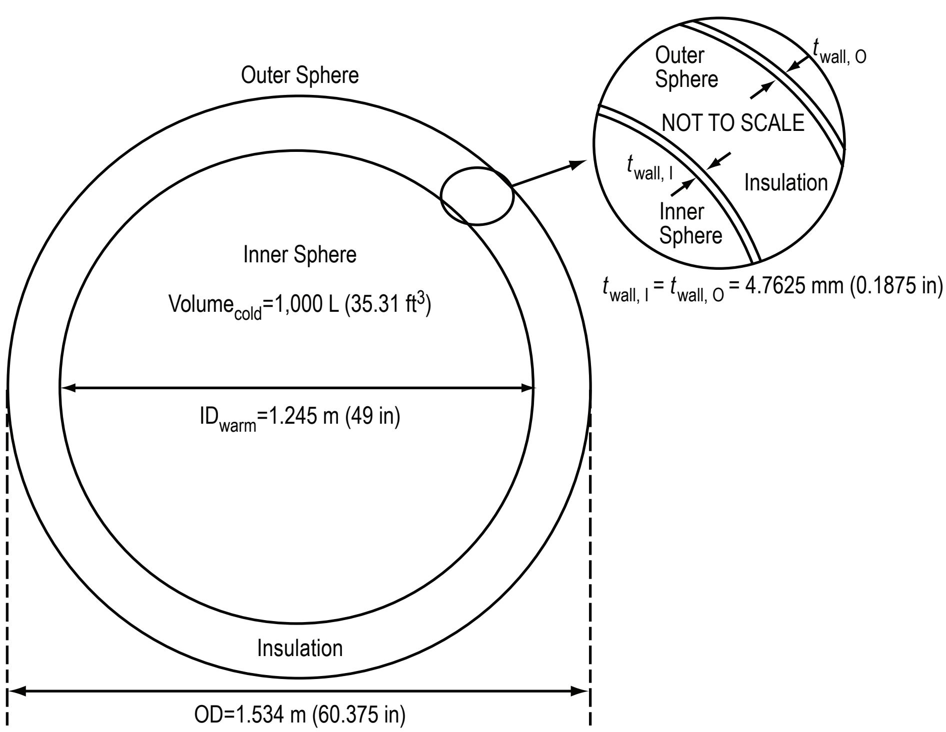

Figure 5. CESAT demonstration tank schematic.

3.1.2 Instrumentation

Both CESAT tanks are heavily instrumented, but not all measurements were used during the boiloff modeling efforts. The relevant instrumentation is discussed here. The primary method for measuring boiloff during CESAT testing was through two flow meters installed on the vent line of each tank (designated F1 and F2), where one flow meter was calibrated for low flow rates while the other was calibrated for high flow rates. Alternately, boiloff could be measured by evaluating the total change in weight of the tank during testing, which was measured by summing three load cells (designated L1 through L3). The other primary parameter of interest was temperature, which was measured at several locations throughout the test tank.

Figure 6 shows the locations of 12 silicone diode instruments that were used to measure the skin temperature of the inner sphere (designated S1A through S6B). Measurements S1A and S1B were useful for comparing ullage temperature predictions with measured data. The other 10 measurements were useful for evaluating liquid temperatures and giving a rough indication of liquid level. Twelve thermocouples were also installed on the outer sphere in corresponding locations radially outward from the inner sphere measurements shown in figure 6 (designated TC11 through TC22). These twelve outer sphere skin temperature measurements were useful for determining the ambient conditions during testing. Finally, two temperature rakes were installed at different locations in the annular space between the inner sphere and outer sphere, where each rake consists of five thermocouples placed at equal intervals throughout the annular space (designated TC1 through TC10). These measurements were useful in determining the temperature profile through the installed insulating material.

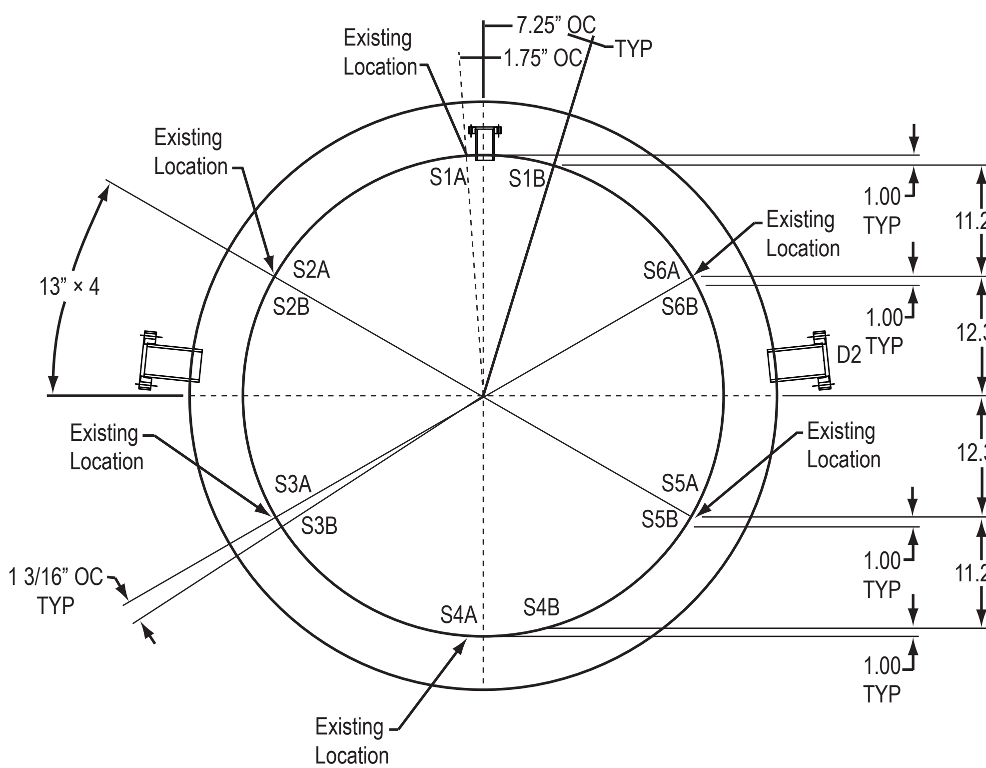

Figure 6. CESAT inner sphere skin temperature measurement locations.

3.2 Full-Scale Tanks

There are two full-scale liquid hydrogen tanks located at KSC LC-39. Both tanks were built in 1965 for the Apollo program and fabricated by Chicago Bridge and Iron, Salt Lake City, Utah. Both tanks (fig. 1) were constructed with austenitic stainless steel inner spheres and carbon steel outer spheres. The annular space between the two spheres in each tank can be filled with an insulating material and the pressure can be reduced to vacuum conditions. Both tanks include fill lines, vent lines, and support structures that could contribute to heat leak. This section discusses the relevant geometric characteristics and instrumentation for both tanks.

3.2.1 Geometry

Figure 7 shows the dimensions of the two full-scale tanks. The inner diameter of the inner sphere is ≍18.715 m (≈61.4 ft), which results in a total inner sphere volume of 3,432,020 L (121,200 ft^3). The outer diameter of the outer sphere is 21.336 m (70 ft). The outer sphere wall thickness is 17.462 mm (0.6875 in) and the inner sphere wall thickness is 15.875 mm (0.625 in). The resulting annular space is 1.277 m (4.19 ft) wide.

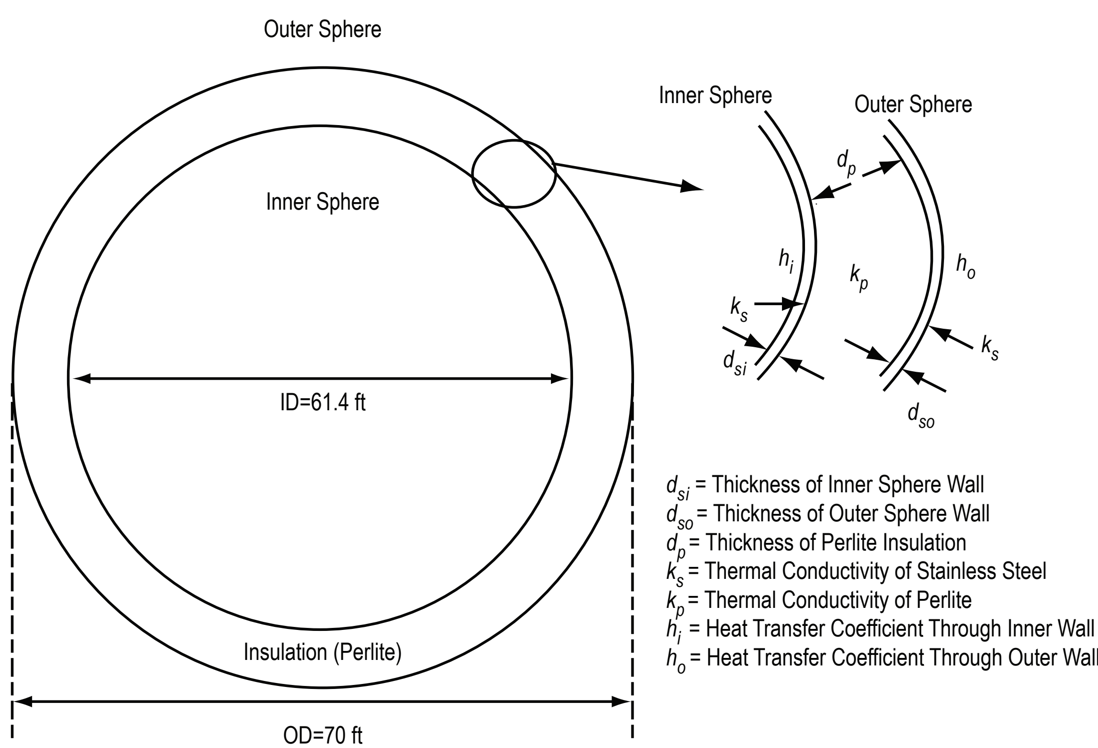

Figure 7. Full-scale tank schematic.

4. NUMERICAL MODEL DEVELOPMENT

4.1 Single Fluid Node Tank Model

Figure 8 shows the earliest GFSSP model that has a single propellant node and a single heat transfer path. Node 2 is a fluid node that represents the fluid volume of the inner sphere. Branch 24 represents the convection heat transfer from the cryogenic fluid to the inner wall of the inner sphere. Branch 45 represents conduction heat transfer through the inner spherical wall. Branches 59, 910, and 106 represent the conduction heat transfer through the insulating material. Branch 67 represents the conduction heat transfer through the outer spherical wall. Branch 78 represents the convection heat transfer from the outside surface of the outer spherical wall to the ambient surroundings.

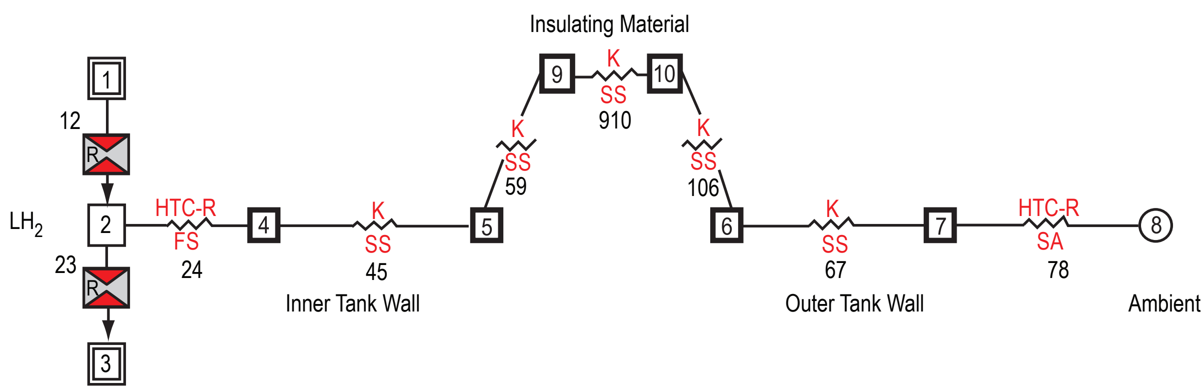

Figure 8. Preliminary GFSSP model with single heat transfer path.

This model evolved into the single fluid node tank model (shown in fig. 9), which accounted for two-dimensional heat flow. Node 2 is a fluid node that represents the fluid volume of the inner sphere. Branches 110 through 117 represents the convection heat transfer from the cryogenic fluid to the inner wall of the inner sphere. Branches 130 through 137 represent conduction heat transfer through the inner spherical wall. Branches 150 through 157, 170 through 177, and 190 through 197 represent the conduction heat transfer through the insulating material. Branches 210 through 217 represent the conduction heat transfer through the outer spherical wall. Branches 230 through 237 represent the forced convection heat transfer from the outside surface of the outer spherical wall to the ambient surroundings. Appendix B discusses the thermal properties and equations that were used for both iterations of this model.

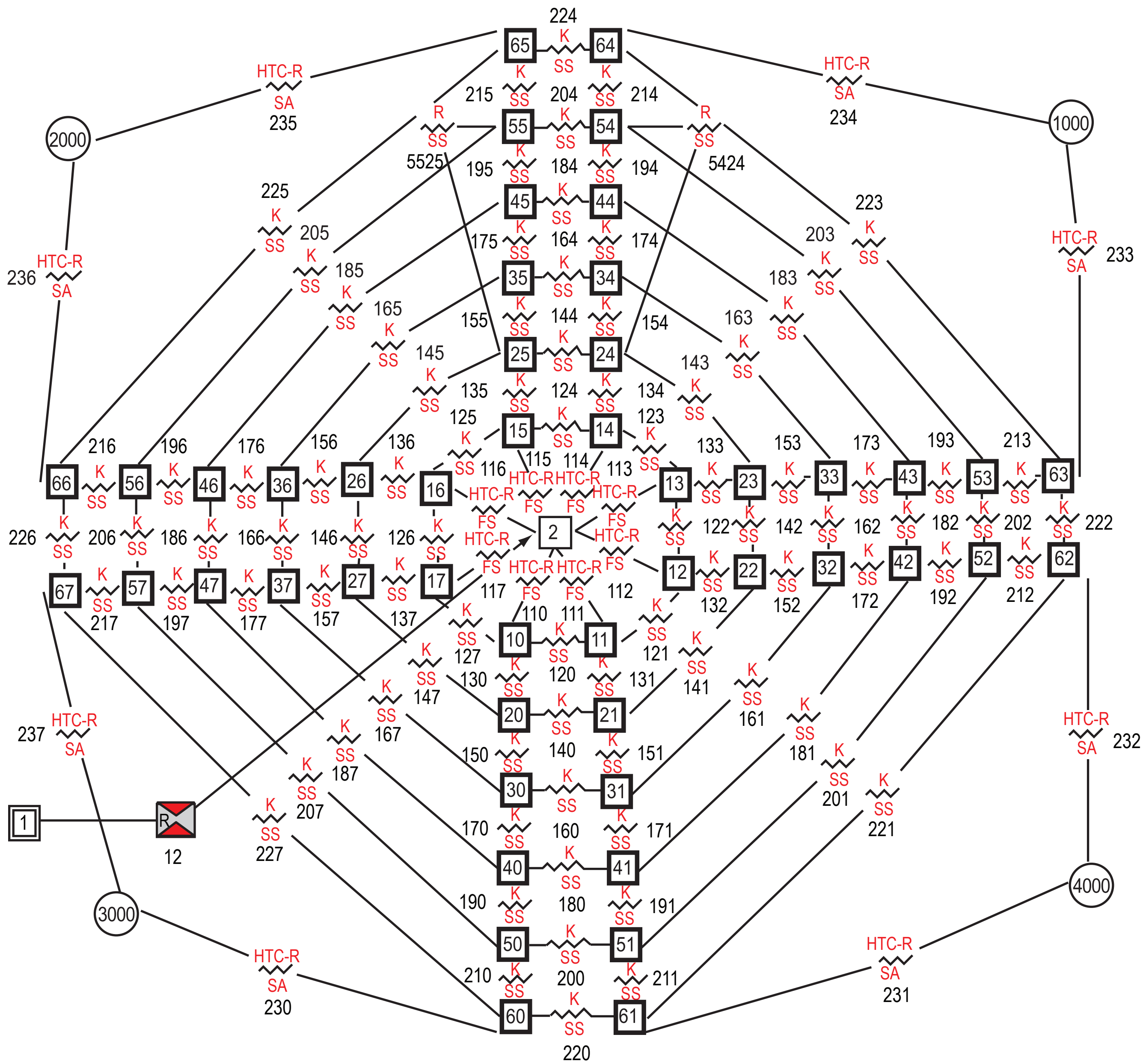

Figure 9. GFSSP single fluid node tank model.

4.2 Ullage and Propellant Node Tank Model

As the CESAT testing effort progressed, KSC expressed interest in modeling boiloff as a function of the tank fill level. Careful consideration and testing of the model discussed in section 4.1 showed that because of the underlying assumption that the ullage and propellant temperature were equal, the model could not consider the change in ullage temperature (and thus heat transfer between the ullage and propellant) that might occur at different fill levels. Therefore, a new model was needed that would allow the ullage temperature to be calculated separately. GFSSP already contains a pressurization option, which considers the interaction between the ullage and liquid in a propellant tank.[4] This pressurization option was adapted to model the fluid portion of the boiloff model by including the capability to calculate spherical geometrical parameters such as volumes, heights, and surface areas. These spherical geometry calculations are discussed in appendix C. Because the pressurization option is a transient option, the model was run in a transient mode of operation, where time step represented an additional iterative step to achieve steady state convergence. The addition of the pressurization option also led to a necessary revision to the heat path modeling technique of the previous model.

Figure 10 shows a schematic that illustrates the technique that was developed for this model. The figure shows that instead of dividing the heat path into eight equal sectors, the heat path from ambient to propellant was broken into an ullage path and a propellant path. The heat transferred through the ullage path into the ullage space ($\dot{Q}_{a\text{-}u}$) is used to calculate the ullage temperature, which GFSSP's pressurization option uses to calculate the heat transfer between the ullage and propellant ($\dot{Q}_{u\text{-}p}$). The heat transferred through the propellant path ($\dot{Q}_{a\text{-}p}$) is calculated independently. The heat transferred through the structure ($\dot{Q}_{s\text{-}p}$) is assumed as a constant value from a separate calculation. $\dot{Q}_{u\text{-}p}$, $\dot{Q}_{a\text{-}u}$, and $\dot{Q}_{s\text{-}p}$ are summed to determine the total heat transferred to the propellant. The total heat transfer is then used to calculate the propellant boiloff rate. Appendix B discusses the thermal properties and equations that were used for this modeling technique.

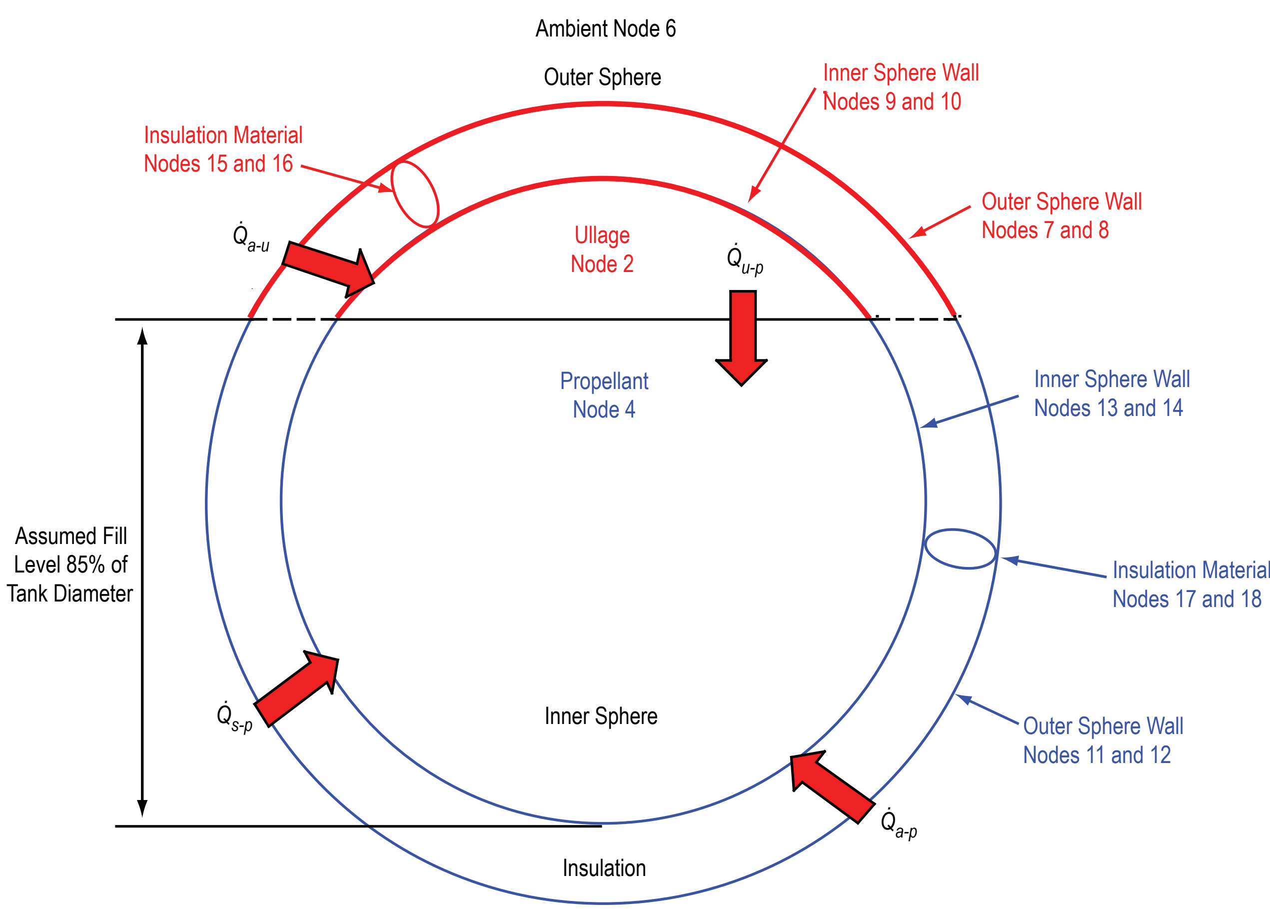

Figure 10. Schematic illustrating boiloff fill level modeling technique.

Figure 11 shows the GFSSP model that was developed based on this modeling technique. The model consists of five fluid nodes connected by three fluid branches, as well as one ambient and twelve solid nodes joined to the fluid and each other by twenty conductors. Node 2 represents the ullage space while node 4 represents the propellant volume. Node 3 is a pseudo-boundary node that allows the ullage and the propellant to interact without mixing through branch 34, which represents the propellant surface. Branch 12 represents the tank vent line leading to the ambient, which is simulated by node 1. Branch 45 represents a fill/drain valve leading to node 5, which is currently simulating ambient conditions. Because no fill/drain operations were simulated, branch 45 was modeled as a closed valve. Conductors 102 and 144 represent the heat transfer between the inner sphere and the fluid. Solid nodes 9, 10, 13, and 14 represent the inner sphere wall. Conductors 910 and 1314 represent the heat transfer through the inner sphere. Conductors 169 and 1813 represent the heat transfer between the inner sphere and insulation. Solid nodes 15–18 represent the insulation material. Conductors 1516 and 1718 represent the heat transfer through the insulation material. Conductors 815 and 1217 represent the heat transfer between the insulation material and the outer sphere. Solid nodes 7, 8, 11, and 12 represent the outer sphere wall. Conductors 78 and 1112 represent the heat transfer through the outer sphere wall. Conductors 67 and 611 represent the heat transfer between the outer sphere wall and ambient conditions. Ambient node 6 represents ambient conditions. Conductors 1014, 913, 1618, 1517, 812, and 711 represent heat transfer between the ullage path and the propellant path.

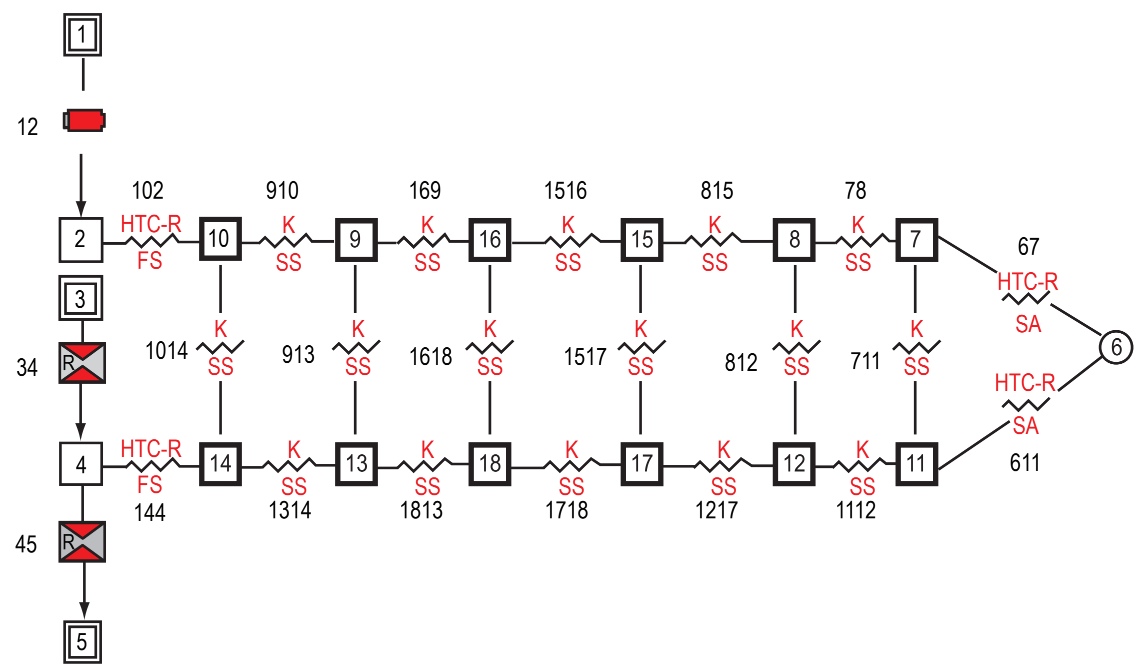

Figure 11. GFSSP ullage and propellant node tank model.

4.3 Stratified Ullage and Propellant Tank Model

While the model discussed in section 4.2 was appropriate for modeling the CESAT demonstration tanks, it was found to be inadequate for modeling the LC-39 cryogenic storage tanks. Because of the difference in scale between the demonstration and full-scale tank ullage spaces, using a single node to represent the ullage space led to unrealistic ullage temperature predictions. Therefore, a decision was made to model the ullage space as several fluid nodes. This would allow GFSSP to more accurately simulate the stratified environment that exists in the ullage space of a cryogenic storage tank. It was necessary to activate GFSSP's gravity option to accurately calculate stratification effects in this model. Initially, the fluid model was modified without changing the heat transfer model. (See fig. 12.) Unfortunately, this configuration had difficulty converging because of the multiple solid to fluid conductors connected to node 10. Figure 13 shows the final stratified ullage and propellant tank model. The final model maintains the modeling technique shown in figure 10 with the thermal properties and equations discussed in appendix B.

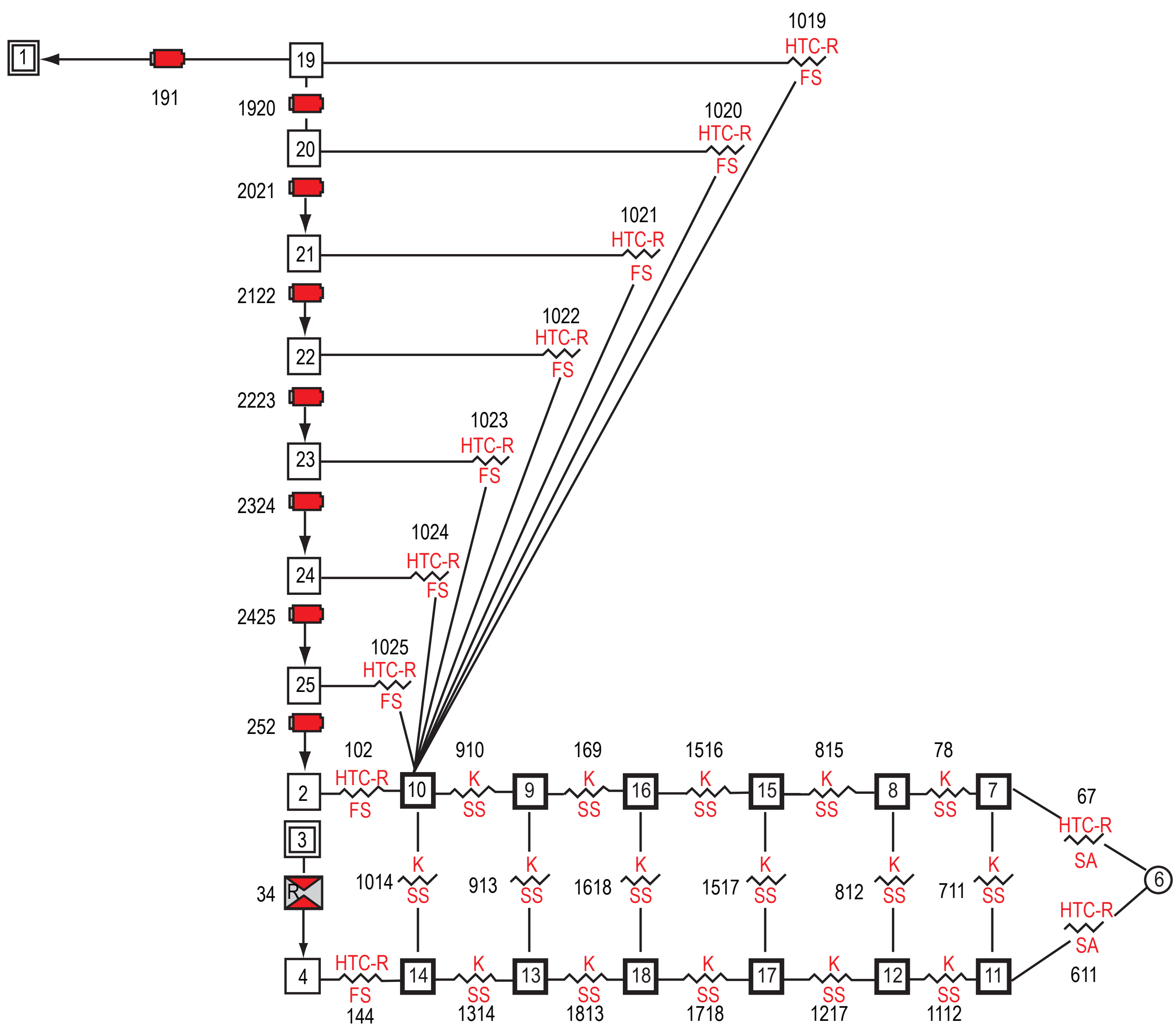

Figure 12. Initial GFSSP stratified ullage and propellant tank model.

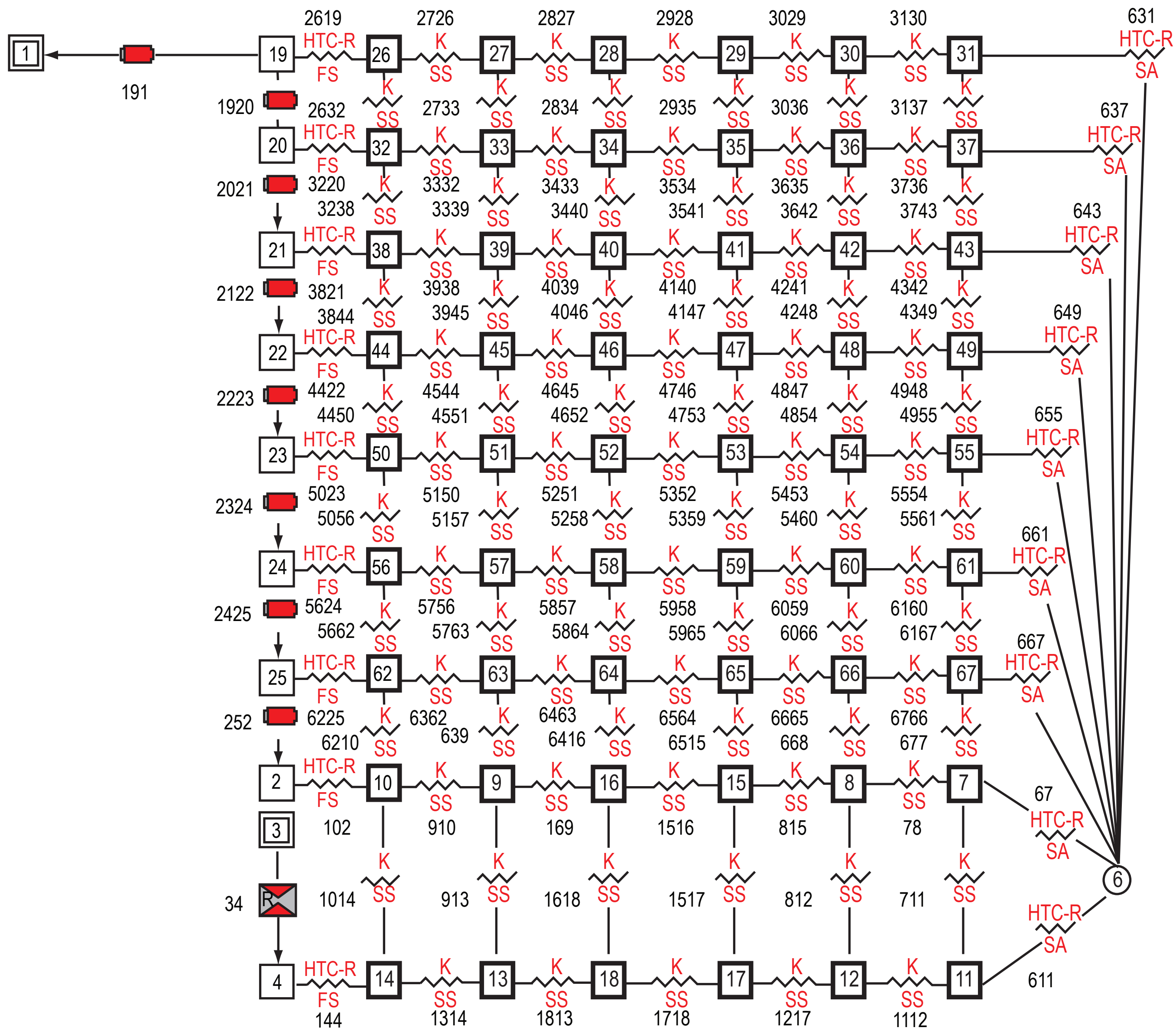

Figure 13. Final GFSSP stratified ullage and propellant tank model.

The fluid portion of the GFSSP model shown in figure 13 consists of 11 nodes connected by 9 branches. The ullage space is divided into nodes 19 through 25 and 2, which each represent one-eighth of the total ullage volume. The choice to use eight divisions to represent the ullage space was made based on balancing the need for more fidelity with the additional numerical complexity of using a larger number of model elements. Branches 1920, 2021, 2122, 2223, 2324, 2425, and 252 connect the eight ullage nodes together and allow ullage gas of different densities to flow from one node to another to model the stratified ullage. Physically, they represent the approximate height and diameter of each ullage volume section. Node 4 represents the propellant volume. Node 3 is a pseudo-boundary node that allows the ullage and the propellant to interact without mixing through branch 34, which represents the propellant surface. Branch 191 represents the tank vent line leading to the ambient, which is simulated by node 1.

Conductors 2619, 3220, 3821, 4422, 5023, 5624, 6225, and 102 represent the heat transfer between the inner sphere and the fluid for each ullage volume section. Conductor 144 represents the heat transfer between the inner sphere and the fluid for the propellant. Solid nodes 26, 27, 32, 33, 38, 39, 44, 45, 50, 51, 56, 57, 62, 63, 9, and 10 represent the inner sphere wall for each ullage volume section. Solid nodes 13 and 14 represent the inner sphere wall for the propellant. Conductors 2726, 3332, 3938, 4544, 5150, 5756, 6362, and 910 represent the heat transfer through the inner sphere for each ullage volume section. Conductor 1314 represents the heat transfer through the inner sphere for the propellant.

Conductors 2827, 3433, 4039, 4645, 5251, 5857, 6463, and 169 represent the heat transfer between the inner sphere and insulation for each ullage volume section. Conductor 1813 represents the heat transfer between the inner sphere and insulation for the propellant. Solid nodes 28, 29, 34, 35, 40, 41, 46, 47, 52, 53, 58, 59, 64, 65, 15, and 16 represent the insulation material for each ullage volume section. Solid nodes 17 and 18 represent the insulation material for the propellant. Conductors 2928, 3534, 4140, 4746, 5352, 5958, 6564, and 1516 represent the heat transfer through the insulation material for each ullage volume section. Conductor 1718 represents the heat transfer through the insulation material for the propellant.

Conductors 3029, 3635, 4241, 4847, 5453, 6059, 6665, and 815 represent the heat transfer between the insulation material and the outer sphere for each ullage volume section. Conductor 1217 represents the heat transfer between the insulation material and the outer sphere for the propellant. Solid nodes 30, 31, 36, 37, 42, 43, 48, 49, 54, 55, 60, 61, 66, 67, 7, and 8 represent the outer sphere wall for each ullage volume section. Solid nodes 11 and 12 represent the outer sphere wall for the propellant. Conductors 3130, 3736, 4342, 4948, 5554, 6160, 6766, and 78 represent the heat transfer through the outer sphere wall for each ullage volume section. Conductor 1112 represents the heat transfer through the outer sphere wall for the propellant. Conductors 631, 637, 643, 649, 655, 661, 667, and 67 represent the heat transfer between the outer sphere wall and ambient conditions for each ullage volume section. Conductor 611 represents the heat transfer between the outer sphere wall and ambient conditions for the propellant. Ambient node 6 represents ambient conditions.

Conductors 2632, 2733, 2834, 2935, 3036, and 3137 represent the heat transfer between the first and second ullage volume sections. Conductors 3238, 3339, 3440, 3541, 3642, and 3743 represent the heat transfer between the second and third ullage volume sections. Conductors 3844, 3945, 4046, 4147, 4248, and 4349 represent the heat transfer between the third and fourth ullage volume sections. Conductors 4450, 4551, 4652, 4753, 4854, and 4955 represent the heat transfer between the fourth and fifth ullage volume sections. Conductors 5056, 5157, 5258, 5359, 5460, and 5561 represent the heat transfer between the fifth and sixth ullage volume sections. Conductors 5662, 5763, 5864, 5965, 6066, and 6167 represent the heat transfer between the sixth and seventh ullage volume sections. Conductors 6210, 639, 6416, 6515, 668, and 667 represent the heat transfer between the seventh and eighth ullage volume sections. Finally, conductors 1014, 913, 1618, 1517, 812, and 711 represent heat transfer between the ullage path and the propellant path.

5. NUMERICAL MODEL RESULTS

5.1 Radiation Gap Analysis Using Single Fluid Node Model

All 28 cases assumed a liquid hydrogen temperature of 20.37 K. A baseline case (case 52) was run whereby the following were used: thermal conductivity of perlite, the calculated value of h_i, the ambient temperature of 302.6 K, and the calculated value of h_o assuming an 8.05 km/hr (5 mph) wind. Subsequent cases varied the radiation gap through the insulating material. The 28 cases are presented in table 3 and further illustrated in figure 14.

Table 3. Parametric cases.

Case Number	Insulating Material	Radiation Gap (deg)	Surface Area for Radiation Gap (%)	Outer Sphere Surface Area Exposed to Radiation (in^2)
1	Perlite	0	0	0
2	Perlite	0.25	0.07	7.76
3	Perlite	0.5	0.14	15.52
4	Perlite	1	0.28	31.02
5	Perlite	5	1.39	155.12
6	Perlite	15	4.17	465.36
7	Perlite	89	24.72	2761.18
8	Glass microspheres	0	0	0
9	Glass microspheres	0.25	0.07	7.76
10	Glass microspheres	0.5	0.14	15.52
11	Glass microspheres	1	0.28	31.02
12	Glass microspheres	5	1.39	155.12
13	Glass microspheres	15	4.17	465.36
14	Glass microspheres	89	24.72	2761.18
15	Passive aerogel beads	0	0	0
16	Passive aerogel beads	0.25	0.07	7.76
17	Passive aerogel beads	0.5	0.14	15.52
18	Passive aerogel beads	1	0.28	31.02
19	Passive aerogel beads	5	1.39	155.12
20	Passive aerogel beads	15	4.17	465.36
21	Passive aerogel beads	89	24.72	2761.18
22	Translucent white aerogel beads	0	0	0
23	Translucent white aerogel beads	0.25	0.07	7.76
24	Translucent white aerogel beads	0.5	0.14	15.52
25	Translucent white aerogel beads	1	0.28	31.02
26	Translucent white aerogel beads	5	1.39	155.12
27	Translucent white aerogel beads	15	4.17	465.36
28	Translucent white aerogel beads	89	24.72	2761.18

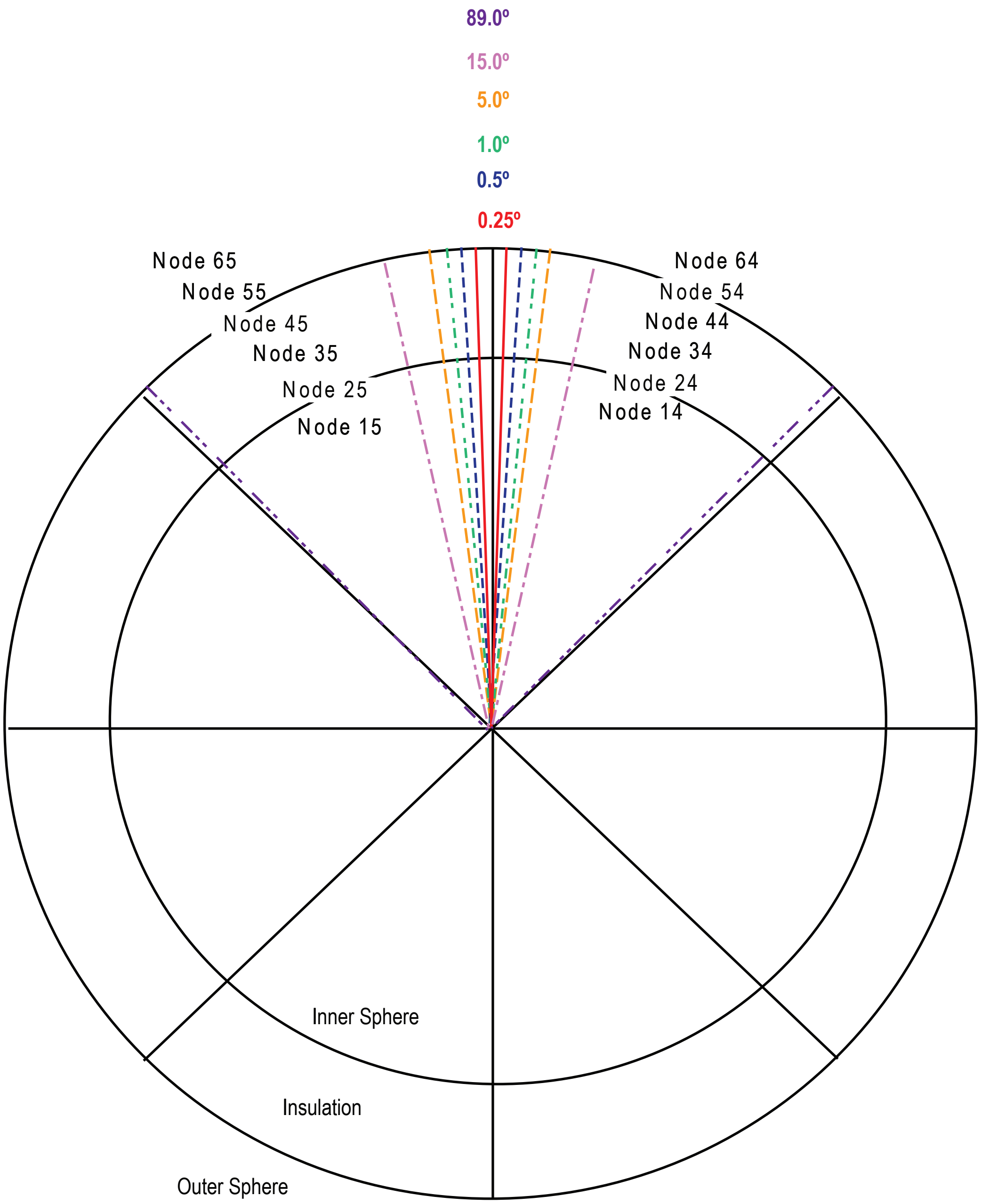

Figure 14. Radiation gap parametric cases.

As the radiation gap grew larger, the mass of insulating material displaced was distributed evenly among the remaining nodes. The results of varying the radiation gap are shown in table 4. Figure 15 shows the effects of varying the radiation gap.

Table 4. Model parametric study results.

Case Number	Insulating Material	Radiation Gap (deg)	Surface Area for Radiation Gap (%)	Outer Sphere Surface Area Exposed to Radiation (in^2)	Boiloff Rate (gal/day)
1	Perlite	0	0	0	16.42
2	Perlite	0.25	0.07	7.76	16.42
3	Perlite	0.5	0.14	15.52	16.42
4	Perlite	1	0.28	31.02	16.42
5	Perlite	5	1.39	155.12	20.72
6	Perlite	15	4.17	465.36	32.83
7	Perlite	89	24.72	2761.18	116.44
8	Glass microspheres	0	0	0	9.5
9	Glass microspheres	0.25	0.07	7.76	9.5
10	Glass microspheres	0.5	0.14	15.52	9.5
11	Glass microspheres	1	0.28	31.02	9.5
12	Glass microspheres	5	1.39	155.12	9.5
13	Glass microspheres	15	4.17	465.36	19.08
14	Glass microspheres	89	24.72	2761.18	102.23
15	Passive aerogel beads	0	0	0	14.14
16	Passive aerogel beads	0.25	0.07	7.76	14.14
17	Passive aerogel beads	0.5	0.14	15.52	14.14
18	Passive aerogel beads	1	0.28	31.02	14.14
19	Passive aerogel beads	5	1.39	155.12	18.31
20	Passive aerogel beads	15	4.17	465.36	30.45
21	Passive aerogel beads	89	24.72	2761.18	111.56
22	Translucent white aerogel beads	0	0	0	21.06
23	Translucent white aerogel beads	0.25	0.07	7.76	21.06
24	Translucent white aerogel beads	0.5	0.14	15.52	21.06
25	Translucent white aerogel beads	1	0.28	31.02	21.06
26	Translucent white aerogel beads	5	1.39	155.12	25.41
27	Translucent white aerogel beads	15	4.17	465.36	37.67
28	Translucent white aerogel beads	89	24.72	2761.18	120.25

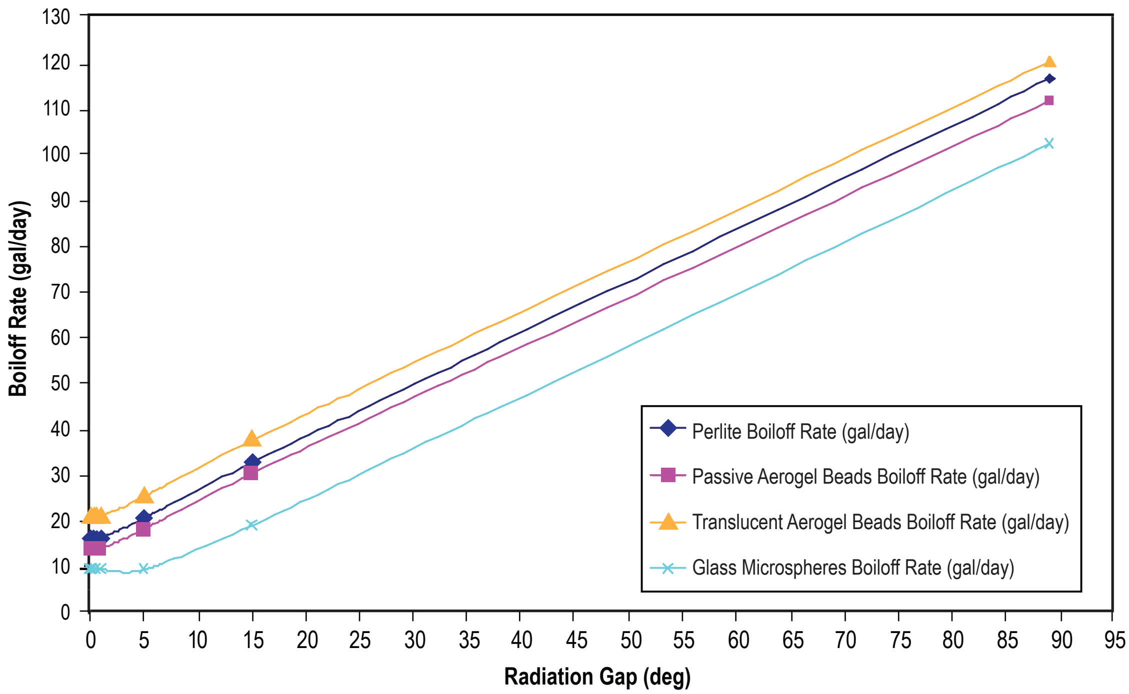

Figure 15. Insulating material gas analysis—effects of varying the radiation gap.

5.2 Ullage and Propellant Node Tank Model Results

The ullage and propellant node tank model was used for two types of predictions. First, the model was used to perform a parametric study of boiloff as a function of height. These predictions were performed before the model had been anchored to CESAT test data, and so they do not include some of the modifications that were made during the test data validation portion of model development. The results are included and discussed here mainly to provide historical insight into the model's development and usage. Second, the model was used to provide predictions for CESAT tests involving liquid nitrogen or liquid hydrogen with either perlite or glass bubbles insulating material. These predictions were compared to CESAT test data as it became available and discrepancies were investigated to improve the model's predictive accuracy.

5.2.1 Fill Level Boiloff Predictions

Three different fill level prediction cases were run using the GFSSP fill level model. Predictions were made at fill levels of 25%, 75%, and 85% of the total height of the tank (corresponding to 15.6%, 84.38%, and 93.92% of the total volume of the tank). All three cases use the following boundary conditions:

- The fluid is nitrogen at 1 atm and 76 K.
- Ambient conditions are 1 atm and 302.6 K.
- The structural heat leak is 1.302333 W as calculated by PHPK[12].
- The insulation material is perlite with a thermal conductivity of 1 mW/m–K. There are no gaps in the insulation.

Figure 16 shows the GFSSP model's predictions for the three fill level cases. GFSSP's predictions show that the total boiloff rate does show some effect due to fill level, but the changes are not large. At the higher fill levels, the ullage has a small effect on the overall heat transfer, which is dominated by the heat transfer between the propellant and the tank wall. As the fill level decreases, the ullage-propellant heat transfer begins to become more significant with very little change in the wall-propellant heat transfer, which leads to a boiloff peak at the 75% prediction. As the fill level further decreases, wall-propellant heat transfer begins to decrease while ullage-propellant heat transfer exerts more influence on the overall heat transfer. The total heat transfer rate (the sum of ullage-propellant, wall-propellant, and structural heat transfer), however, changes very little (<1 W) for all three predictions, resulting in small changes in boiloff rate (<200 sccm).

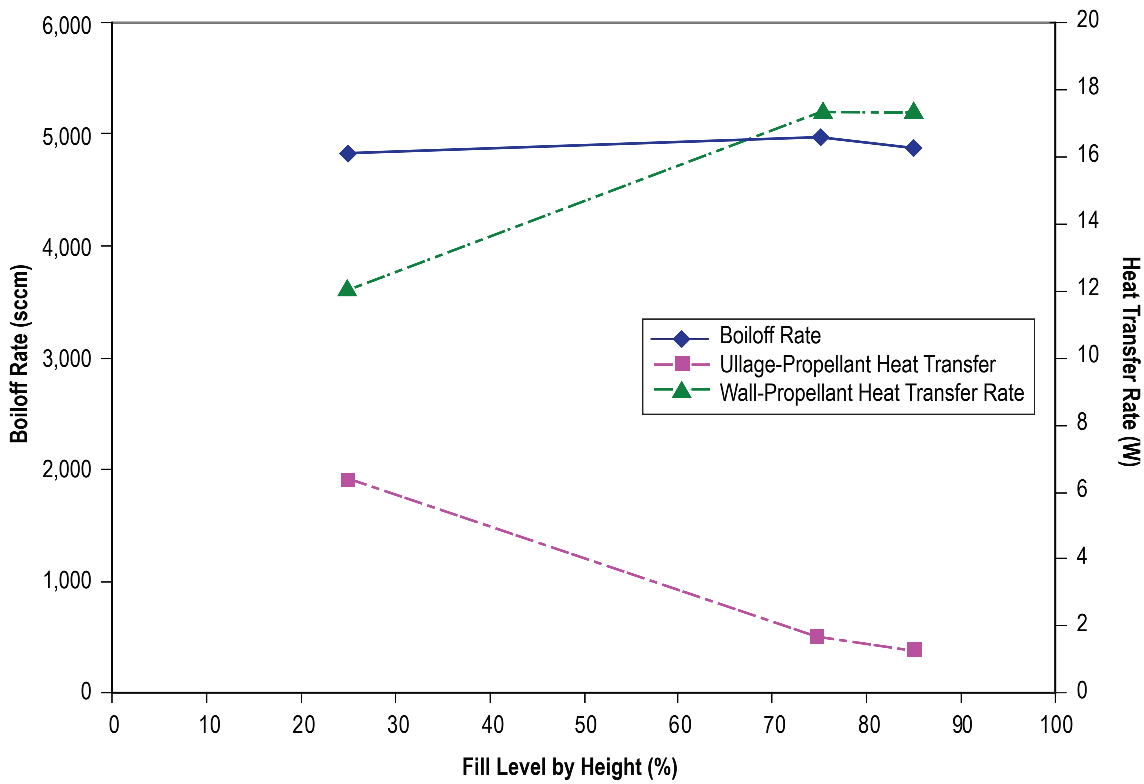

Figure 16. GFSSP predicted CESAT boiloff versus tank height fill level.

5.2.2 CESAT Test Data Comparisons

When discussing test data comparison, it should be noted that the GFSSP model node locations (see sec. 4.2) are not designed to match the instrumentation locations exactly. Figure 17 shows the differences in the radial direction between GFSSP's predictions and the relevant CESAT instrumentation. These differences are not considered significant for the comparisons discussed in this TM.

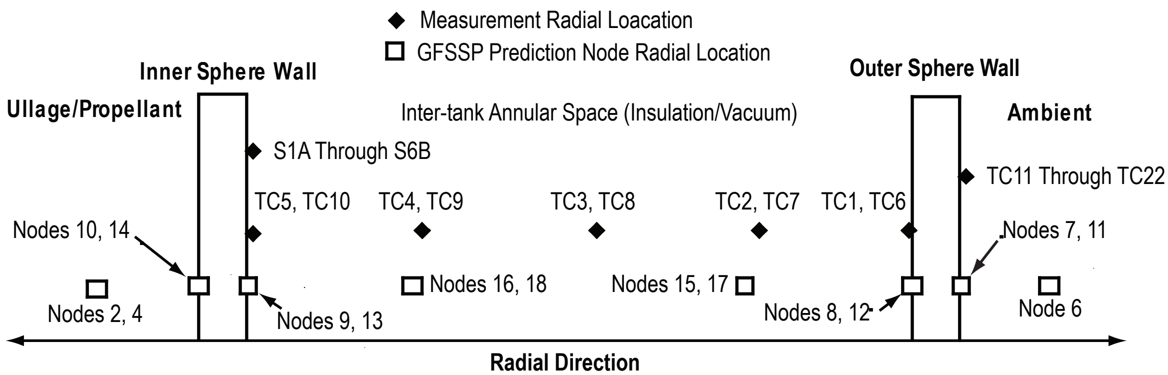

Figure 17. Comparison of GFSSP prediction versus test instrumentation radial location.

A moment should also be taken to discuss exactly how the test data comparison was performed. Due to the time constraints involved in building models to simulate different fill levels, all GFSSP predictions were performed at a fill level of 85% of the tank height (roughly 94% of the total tank volume). Based on discussions with KSC personnel concerning tanking practices, this was a reasonable assumption for a 'full' storage tank. All predictions were first made as pretest predictions. When testing was complete for a particular test series, KSC personnel would process the data and provide it for comparisons. Each test data set received from KSC consisted of multiple boiloff tests, so each boiloff test in a data set was examined to determine which boiloff test had initial conditions (ambient conditions and fill level) closest to the GFSSP predictions. The outer sphere skin temperature measurements (TC1 through TC10) were examined first. In some cases, predictions were updated to more closely match the average measured ambient temperature. Next, the total weight for each boiloff test in a data set was examined. Using the tank dry weights and fluid densities, the initial fill level for each test could be calculated, and the test with the fill level closest to the 85% GFSSP predicted fill level was chosen for comparison. Figure 18 shows how the time interval for a boiloff test was determined using the total weight.

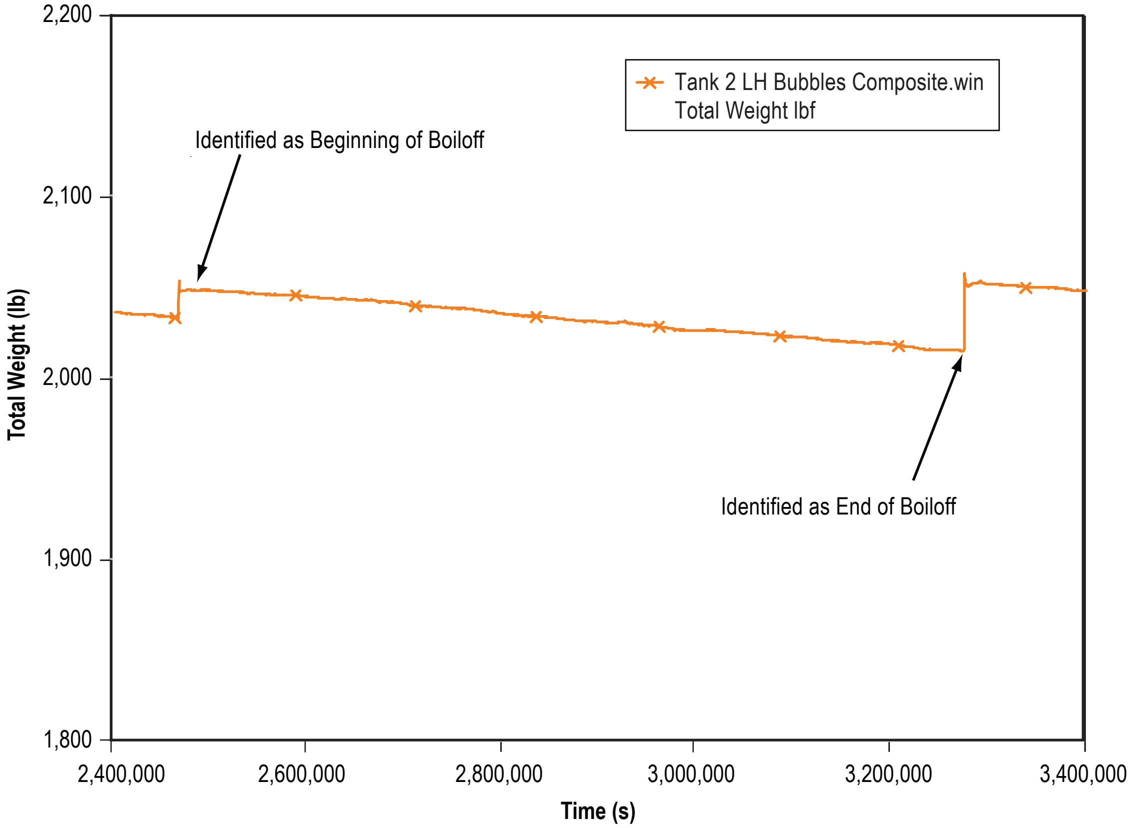

Figure 18. Example of using total weight to identify a boiloff test.

Once a particular boiloff test was identified, the parameters of interest (boiloff rate, liquid temperature, and ullage temperature) were extracted from the test data set. Because the GFSSP predictions using this model are steady state predictions, steady state approximations were made for boiloff and ullage temperature. The average mass flow rates indicated by F1 and/or F2 over the desired time interval were taken as one indicator of boiloff rate. Boiloff rate was also evaluated by calculating the change in total weight over the desired time interval. (See fig. 18.) The measured liquid temperature was determined by calculating the average value of inner sphere skin temperature measurement S4A over the desired time interval. The measured ullage temperature was determined by calculating the average value of inner sphere skin temperature measurement S1B over the desired time interval. If measurement S1B was unavailable, the average value of measurement S1A over the desired time interval was used.

Some modifications were made to the GFSSP model used in section 5.2.1 based on initial comparisons with CESAT test data and other analyses. First, an independent structural heat leak calculation produced a lower heat leak value of 1.010586 W. This heat leak consists of PHPK's heat leak values of 0.229564 W (piping and tube heat leak) and 0.002222 W (gas conduction pipe heat leak)[12] summed with the structural support cables heat leak of 0.7788 W calculated in appendix A. Second, initial test data comparisons revealed a discrepancy in the predicted propellant exposed tank wall temperature and the actual skin temperature measurements. This discrepancy was due to the assumptions made in calculating the heat transfer coefficient for the wall-propellant heat transfer. (See appendix B.) Since the interaction between the propellant and the wall is a static environment, the model was modified to use an infinite heat transfer coefficient for the wall-propellant heat transfer calculations. Also, some changes were made to GFSSP's conjugate heat transfer numerical scheme. Appendix D contains input files, sample output files, and sample output plots for each case that was considered.

Figure 19 compares GFSSP's predicted temperature gradient through the insulated annular space with measured data from the CESAT temperature rakes (TC1 through TC10). The measured test data[13,14] shows that the majority of the temperature gradient is confined to the inch of insulation closest to the inner sphere. Due to the model's coarse insulation grid, GFSSP's prediction is not equipped to capture this behavior. A finer grid in the insulation space would be more suitable for modeling the temperature gradient, but would also impact the numerical complexity of the model. Since the focus of this work was on predicting tank boiloff rates, the grid was not modified for the work discussed here.

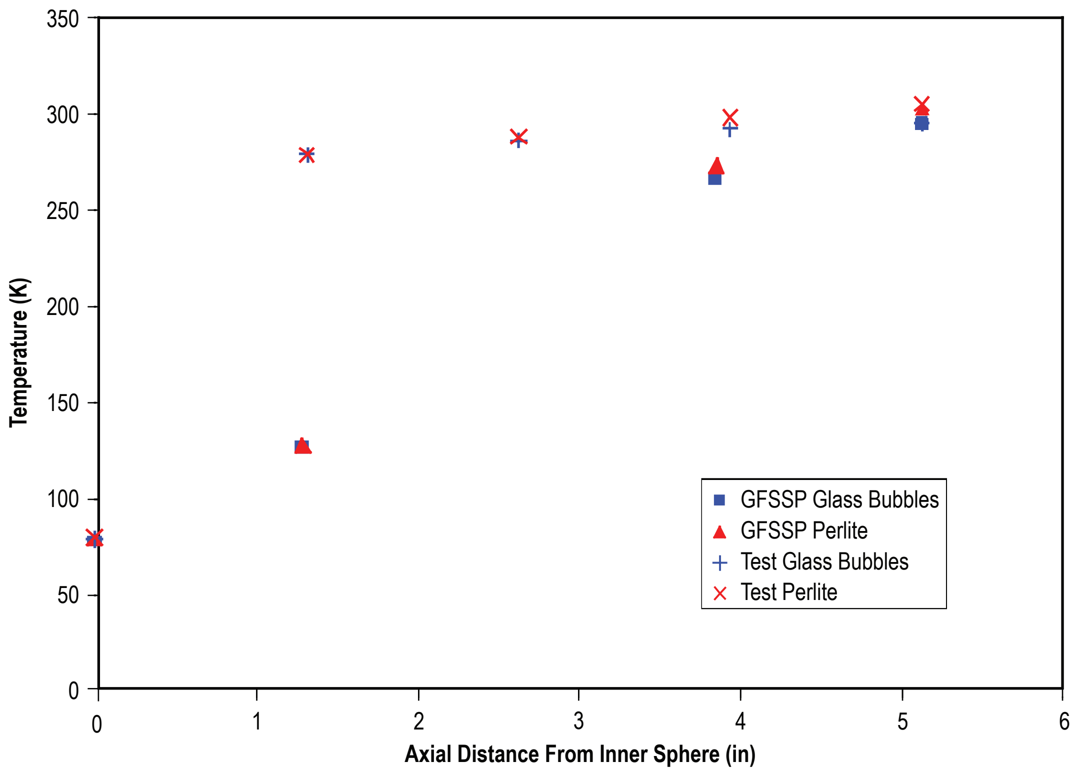

Figure 19. Liquid nitrogen CESAT annular space temperature gradient comparison.

Table 5 shows the comparison between the GFSSP prediction and average test data values for two CESAT tests using liquid nitrogen with perlite insulation.[13,15,16] Table 6 shows the comparison between the GFSSP prediction and average test data values for a CESAT test using liquid nitrogen with glass bubbles insulation.[14] Table 7 shows the comparison between the GFSSP prediction and average test data values for a CESAT test using liquid hydrogen with perlite insulation.[17] Table 8 shows the comparison between the GFSSP prediction and average test data values for a CESAT test using liquid hydrogen with glass bubbles insulation.[18] The first column in each table compares GFSSP's predicted inner tank wall temperature of the ullage space (nodes 9 and 10) with an average value of skin temperature S1B. The second column in each table compares GFSSP's predicted inner tank wall temperature exposed to propellant (nodes 13 and 14) with an average value taken from skin temperature S4A. The third column in each table compares GFSSP's predicted boiloff rate with the test boiloff rates as calculated from both the change in load cell readings (L1–L3) and flow meter data (F1 and F2).

GFSSP predicts a lower ullage space skin temperature than the S1B measurement for all four cases. Due to the fact that S1B is a point temperature measurement, while GFSSP is calculating the average skin temperature for the entire ullage-exposed inner sphere, the differences are believed to be due to the fidelity of the model. For the two liquid nitrogen comparisons, note that GFSSP's liquid skin temperature is 1 K colder than test data. The reason for this difference is that it was necessary to subcool the liquid nitrogen at node 4 (see fig. 11) in the GFSSP model by 1 K to avoid artificially evaporating the liquid. This was not necessary with the liquid hydrogen comparisons.

The predicted boiloff rates for the two liquid nitrogen comparisons are consistently lower than the measured test data. One factor in these discrepancies was uncertainty in the ullage-wall and ullage-propellant heat transfer coefficients, which were not adjusted at all. Another possible factor is that KSC personnel suspect that the antirotation devices for both test tanks may have been in contact during liquid nitrogen testing. Appendix A discusses a calculation that was formed evaluating heat leak due to antirotation contact in the demonstration tanks. The predicted boiloff rates for the two liquid hydrogen comparisons match very well with measured test data. Initially, the liquid hydrogen comparisons were predicting much higher boiloff rates than those seen in testing. It was found that the ullage-propellant heat transfer was disproportionately high for these GFSSP predictions. Because temperature stratification in the ullage of a liquid hydrogen tank is more pronounced than that of a liquid nitrogen tank, the effect of natural convection is negligible in a liquid hydrogen tank. Therefore, it was assumed that $\dot{Q}_{u\text{-}p}$ was governed by conduction heat transfer for the liquid hydrogen predictions. The ratio of heat transfer coefficient between pure conduction and natural convection in ullage was found to be equal to 0.00265. This ratio was applied as an adjustment factor to GFSSP's liquid hydrogen boiloff predictions for both the perlite and glass bubbles insulation, resulting in the predictions shown in tables 7 and 8.

Table 5. Liquid nitrogen with perlite insulation preliminary GFSSP prediction comparison with test data, test tank 2.

	T_{skin}, Exposed to Ullage (K)	T_{skin}, Exposed to Liquid (K)	Boiloff Rate (sccm)
Test 1	92	77	Flow meter = 3,860 Load cells = 4,018
Test 2	89	77	Flow meter = 3,938 Load cells = 4,206
GFSSP	81	76	3,468

Table 6. Liquid nitrogen with glass bubbles insulation preliminary GFSSP prediction comparison with test data, test tank 2.

	T_{skin}, Exposed to Ullage (K)	T_{skin}, Exposed to Liquid (K)	Boiloff Rate (sccm)
Test	92	77	Flow meter = 3,230 Load cells = 3,260
GFSSP	80	76	2,493

Table 7. Liquid hydrogen with perlite insulation preliminary GFSSP prediction comparison with test data, test tank 1.

	T_{skin}, Exposed to Ullage (K)	T_{skin}, Exposed to Liquid (K)	Boiloff Rate (sccm)
Test	34	20	Flow meter = 20,414 Load cells = 19,182
GFSSP	21	20	20,980

Table 8. Liquid hydrogen with glass bubbles insulation preliminary GFSSP prediction comparison with test data, test tank 2.

	T_{skin}, Exposed to Ullage (K)	T_{skin}, Exposed to Liquid (K)	Boiloff Rate (sccm)
Test	31	20	Flow meter = 13,396 Load cells = 13,242
GFSSP	21	20	12,920

5.3 Stratified Ullage and Propellant Tank Model Results

The comparisons between GFSSP predictions and CESAT test measurements discussed in section 5.2 helped to refine and instill confidence in GFSSP's cryogenic storage modeling capability. Based on the results of the CESAT work, a GFSSP model was developed for the LC-39 complex liquid hydrogen storage tanks. As discussed in section 4.3, early modeling attempts made it clear that a single node was not adequate to model the full-scale tanks' ullage space. Therefore, the stratified ullage model in figure 13 was developed. This model was used to provide a baseline boiloff prediction using perlite insulating material to further validate the model. Finally, this model was used to provide a boiloff prediction using glass bubbles insulating material.

The GFSSP model was anchored where possible to the assumptions and practices of the single ullage and propellant node model validated using CESAT test data. The fluid was liquid hydrogen. The tank was assumed to be filled to 85% of the tank height (roughly 94% of the tank volume). The CESAT ullage to propellant heat transfer coefficient adjustment factor of 0.00265 was used in this model. A constant structural heat leak value of 52.308 W (0.04962 Btu/s) was taken from KSC analyses.[19] Appendix E contains input files, sample output files, and sample output plots for the two GFSSP predictions. The full-scale perlite GFSSP model predicts a boiloff of 258 gal/day. This compares to the LC-39A measurement of ≈300 gal/day.[19] The main reason for the discrepancy is uncertainty in the ullage to propellant heat transfer coefficient adjustment factor due to the size differences between CESAT and the full-scale storage tanks. Using this model, GFSSP predicts that a full-scale liquid hydrogen storage tank with glass bubbles insulation would have a boiloff rate of 182 gal/day. Figure 20 shows GFSSP's stratified ullage temperature prediction for the full-scale glass bubbles model. Heights from the propellant surface to the 'top' of each node location are noted in figure 20. GFSSP predicts a 90 K differential between the ullage temperature at the propellant surface and the ullage temperature at the top of the tank.

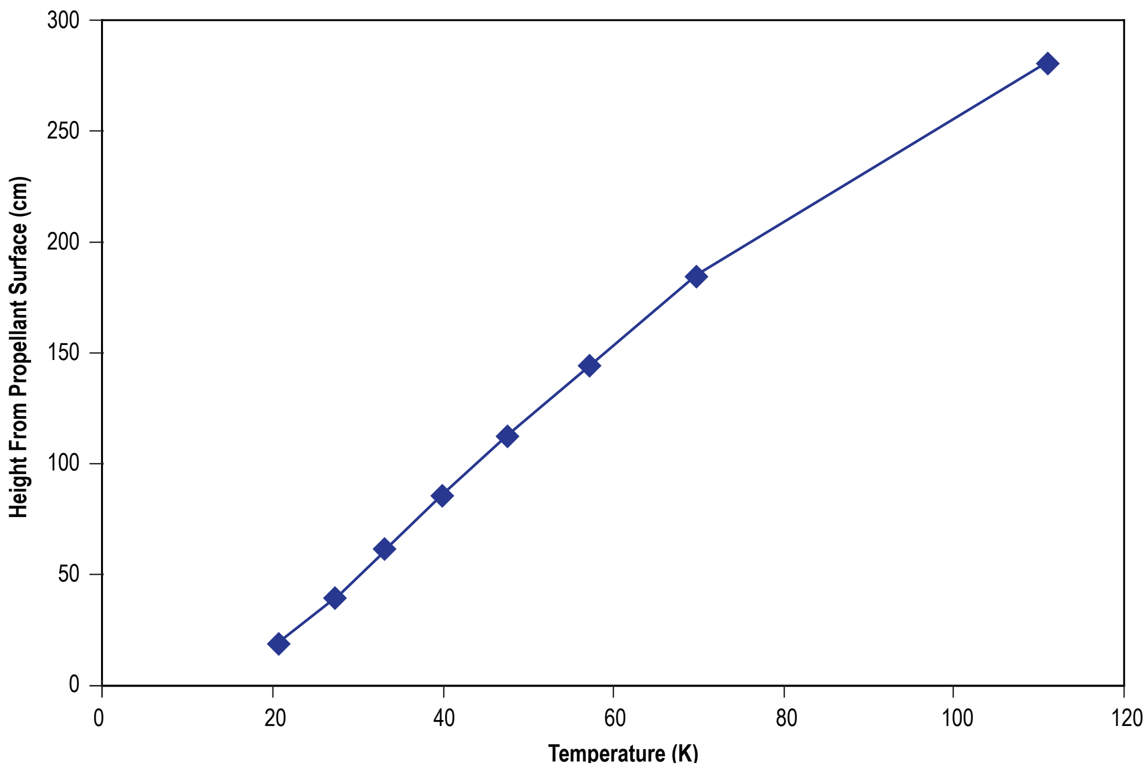

Figure 20. GFSSP stratified ullage temperature prediction for LC-39 with glass bubbles insulation.

6. CONCLUSION

A novel numerical modeling technique has been developed using GFSSP to predict boiloff rate from a spherical cryogenic storage tank. The model recognizes the separation of liquid and the vapor space and appropriately solves for mass, momentum, and energy conservation equations of liquid and vapor volume in the tank in conjunction with heat conduction equations through metallic walls and insulation material. A numerical model has been built for the demonstration tanks developed at KSC. The numerical predictions have compared favorably with test data for liquid nitrogen and liquid hydrogen with perlite and glass bubbles insulation. With the experience gained from the demonstration tank models, a separate numerical model was developed for the liquid hydrogen storage tank at LC-39 at KSC. This model has used multiple nodes in the ullage space to account for the effect of stratification. The numerical model of the full-scale tank was then run using perlite and glass bubbles insulation. The boiloff rate using perlite insulation is in agreement with field data. When using glass bubbles instead of perlite as insulation, the numerical model predicts (1) a 28% reduction in boiloff rate in the liquid nitrogen demonstration tank, (2) a 38% reduction in boiloff rate in liquid hydrogen demonstration tank, and (3) a 30% reduction in boiloff of liquid hydrogen storage tank in LC-39 at KSC.

The numerical model has potential for several extensions and improvements. They are as follows:

- Modeling insulation settling in ullage and propellant node tank model and stratified ullage and propellant tank model.

- Perform modeling at different fill levels to investigate wall temperatures for thermal cycle analysis.

- Modeling boiloff in a cylindrical tank and correlation with test data.

- Improvement of numerical performance of the solver to enhance the computational speed.

APPENDIX A—HEAT LEAK THROUGH SUPPORT STRUCTURE

During CESAT liquid nitrogen testing, it was observed that one of the demonstration tanks consistently predicted higher boiloff rates than the other tank. For an identical design, such a discrepancy may happen due to a difference in heat leak between the two tanks. KSC personnel determined such a possibility may exist if certain portions of G-10 insulating material have physical contact with stainless steel in one of the radial standoffs. In the original design, the radial standoffs are supposed to have an air gap. Conduction analysis was performed to estimate the heat leak caused by radial standoff contact between G-10 and stainless steel.

A.1 Conduction Calculation to Estimate Heat Leak

This section presents a heat transfer calculation in a composite layer to estimate heat leak through cables and a radial support. The objective of this calculation is to (1) compare the calculation results with the PHPK spreadsheet calculation,[11] and (2) analyze the effect of physical contact between G-10 and stainless steel to understand the discrepancy observed in boiloff rates between two tanks.

A.1.1 Cable

Heat leak through the cable was estimated from the heat conduction equation:

$$q = \frac{T_{\text{hot}} - T_{\text{cold}}}{\dfrac{L_1}{K_1 A_1} + \dfrac{L_2}{K_2 A_2} + \dfrac{L_3}{K_3 A_3}} = 0.00123 \text{ Btu/s} = 0.1298 \text{ W} . \quad (1)$$

Total heat leak through six cables = 0.7788 W. It may be noted that the calculated value is significantly less than the PHPK spreadsheet calculation (1.0705 W).

The heat conduction circuit is shown in figure 21.

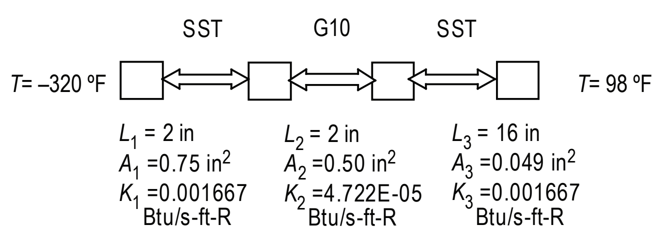

Figure 21. Cable heat conduction circuit.

A.1.2 Radial Support

Heat leak through the radial support was estimated from the heat conduction equation:

$$q = \frac{T_{\text{hot}} - T_{\text{cold}}}{\dfrac{L_1}{K_1 A_1} + \dfrac{L_2}{K_2 A_2} + \dfrac{L_3}{K_3 A_3}} = 0.00573 \text{ Btu/s} = 6.045 \text{ W} . \qquad (2)$$

This calculation assumes one face of G-10 insulation has 100% contact with the stainless steel plate.

The above sets of calculation show heat leak through the radial support could be significantly higher than that of the cable if there is a contact and can explain the discrepancy observed in boiloff rate between the two tanks.

The heat conduction circuit is shown in figure 22.

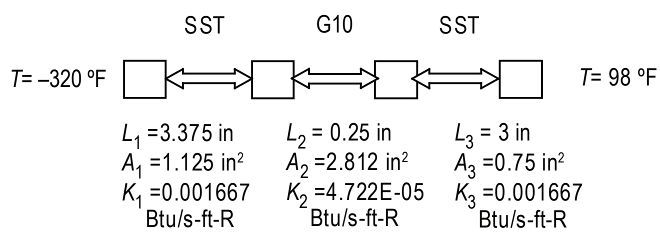

Figure 22. Radial support heat conduction circuit.

APPENDIX B—THERMAL PROPERTIES

B.1 Thermal Conductivity and Specific Heat

Table 9 shows the baseline insulating material physical properties used for the analyses discussed in this TM. One exception to this was that the KSC Cryogenics Test Laboratory recommended a thermal conductivity of 0.6 mW/mK (96×10^{-9} Btu/s-ft-F) be used for glass microspheres at liquid hydrogen temperatures.

Table 9. Insulating material physical properties.

	Perlite	Glass Microspheres	Passive Aerogel Beads	Translucent White Aerogel Beads
Thermal conductivity (Btu/s-ft-F)	1.61×10^{-7}	1.12×10^{-7}	1.93×10^{-7}	3.21×10^{-7}
Specific heat (Btu/lb-F)	0.2	0.19	0.25	0.25
Density (lbm/in^3)	0.00361	0.0045	0.0043	0.0043

B.2 Heat Transfer Coefficient

Manual calculations were performed both to obtain inputs into the GFSSP model and to validate the results from cases run using the GFSSP model. Equation (3) was used to determine the boiloff rate in gallons/day:

$$BR = (\dot{Q}/(h_{fg} * \rho)) * CF \quad , \tag{3}$$

where

BR = boiloff rate (gal/day)
$\dot{Q}$ = heat rate (W)
h_{fg} = enthalpy (Btu/lb)
ρ = density (lb/ft^3)
CF = conversion factor (613 s-Btu-gal/day-J-ft^3).

Equation (4) was used to find $\dot{Q}$ (W):

$$\dot{Q} = U * A * (T_{\text{ambient}} - T_{\text{cryogenic liquid}}) \quad , \tag{4}$$

where

U = overall heat transfer through the system (W/m^2-K)
A = area (m^2).

Equation (5) was used to calculate the overall heat transfer through the system:

$$U = \frac{1}{\frac{1}{h_i} + \frac{\delta_{si}}{k_s} + \frac{\delta_p}{k_p} + \frac{\delta_{so}}{k_s} + \frac{1}{h_o}} , \tag{5}$$

where

δ_{si} = thickness of inner sphere wall (0.004755 m)
δ_{so} = thickness of outer sphere wall (0.004755 m)
δ_p = thickness of insulation material (0.12509 m)
k_s = thermal conductivity of stainless steel (15.5636 W/(m-K))
k_p = thermal conductivity of insulation material (W/(m-K))
h_i = heat transfer coefficient through inner wall (17.361 W/(m^2-K))
h_o = heat transfer coefficient through outer wall (9.068 W/(m^2-K)).

The convection heat transfer coefficient (h_i) was derived using equation (6) (Rayleigh number) and equation (7) (Nusselt number):

$$Ra = \frac{g * \beta * \Delta T * D^3}{\nu * \alpha} , \tag{6}$$

where

Ra = Rayleigh number (dimensionless)
g = acceleration of gravity (39.8067 m/s^2)
β = thermal expansion coefficient (9.5×10^{-6} m/m-K)
ΔT = temperature difference between liquid and wall (assume 0.55K)
D = diameter of inner wall (1.245 m)
ν = kinematic viscosity of fluid (1.96×10^{-7} m^2/s)
α = thermal diffusivity of fluid (1.75×10^{-7} m^2/s).

$$Nu = \frac{h_i * D}{k} = 0.13(Ra)^{1/3} , \tag{7}$$

where

k = thermal conductivity of fluid (0.1164 W/m-K).

The heat transfer coefficient from the outside surface of the outer sphere to ambient conditions (h_o), was derived using equations (8) (Reynolds number) and (9) (Nusselt number):

$$Re = \frac{\rho * v * D}{\mu} , \tag{8}$$

where

ρ = density of air (1.2 kg/m^3)
v = velocity of air (assume 5 mph wind = 2.235 m/s)
D = diameter of the outer tank wall (1.524 m)
μ = viscosity of air (1.86×10^{-5} kg/m-s)
Re = Reynolds number (dimensionless),

and

$$Nu = \frac{h_o * D}{k} = 0.33(Re)^{0.6} , \tag{9}$$

where

k = thermal conductivity of air (26,154 W/m-K).

B.3 Optical Properties

For the gap radiation cases, all surface emmisivities were 0.4.

APPENDIX C—SPHERICAL TANK GEOMETRY

When the first phases of model development began, GFSSP did not have the built-in capability to model a spherical tank. Therefore, a new algorithm was developed to perform the necessary geometrical calculations using spherical tank geometry. This included the ability to calculate the tank diameter, the heights and volumes of the ullage space or propellant, the ullage-propellant interface surface area, the tank surface areas exposed to ullage or propellant, and the conductive surface area between the tank wall sections exposed to ullage and propellant. The algorithm was based on general spherical and circular geometrical equations available in the literature.

Later on, these same equations were adapted and applied to geometrical calculations extending through the annular space, the outer sphere, and even divisions within the ullage space. The equation for the volume of a sphere (eq. (10)) was used to calculate the tank diameter, where V_t is the volume of a spherical tank and D_t is the diameter of a spherical tank. The height (h_x) of either the propellant or ullage space was calculated by iteratively solving equation (11), where x is either the ullage or propellant, and V_x is the corresponding volume. The ullage-propellant interface heat transfer area ($A_{u\text{-}p}$) is calculated from equation (12) (the area of a circle), where the radius ($R_{u\text{-}p}$) is calculated from equation (13) using either the ullage or propellant height. The tank surface areas exposed to ullage or propellant were calculated using equation (14). The conduction area between the tank wall sections exposed to ullage and propellant ($A_{u\text{-}p,cond}$) was calculated using equation (15), which is derived from subtracting $A_{u\text{-}p}$ from a circular area with a radius of $R = R_{u\text{-}p} + t_{\text{wall}}$, where t_{wall} is the wall thickness of the tank:

$$V_t = \frac{4}{3}\pi\left(\frac{D_t}{2}\right)^3 \tag{10}$$

$$V_x = \frac{\pi}{3}h_x^2\left(\frac{3}{2}D_t - h_x\right) \tag{11}$$

$$A_{u\text{-}p} = \pi R_{u\text{-}p}^2 \tag{12}$$

$$R_{u\text{-}p} = \sqrt{h_x\left(D_t - h_x\right)} \tag{13}$$

$$A_{x\text{-}w} = \pi D_t h_x \tag{14}$$

$$A_{u\text{-}p,cond} = \pi\left(2R_{u\text{-}p}t_{\text{wall}} + t_{\text{wall}}^2\right). \tag{15}$$

APPENDIX D—INPUT/OUTPUT FOR DEMONSTRATION TANK MODEL

D.1 CESAT Liquid Nitrogen and Perlite Input Data File

```
GFSSP VERSION
   500
ANALYST
   Todd Steadman
INPUT DATA FILE NAME
   D:\GFSSP\KSC LH2 Tank\New Press Mods\Cesat_LN2.dat
OUTPUT FILE NAME
   Cesat_LN2.out
TITLE
   KSC Liquid Nitrogen Test Tank - 85% Full by Height

USETUP
   F
DENCON     GRAVITY    ENERGY     MIXTURE    THRUST     STEADY     TRANSV     SAVER
   F       F          T          F          F          F          T          F
HEX        HCOEF      REACTING   INERTIA    CONDX      ADDPROP    PRINTI     ROTATION
   F       F          F          F          F          F          F          F
BUOYANCY   HRATE      INVAL      MSORCE     MOVBND     TPA        VARGEO     TVM
   F       T          F          F          F          F          F          F
SHEAR      PRNTIN     PRNTADD    OPVALVE    TRANSQ     CONJUG     RADIAT     WINPLOT
   F       F          F          F          F          T          T          T
PRESS      INSUC      VARROT     CYCLIC     CHKVALS
   T       F          F          F          T
NORMAL     SIMUL      SECONDL    NRSOLVT
   F       T          F          T
NNODES     NINT       NBR        NF
   5       2          3          1
RELAXK     RELAXD     RELAXH     CC         NITER
   1       0.5        0.01       1e-06      500
DTAU       TIMEF      TIMEL      NPSTEP
   1        0         36000      500

NFLUID(I), I = 1, NF
   4
NODE    INDEX    DESCRIPTION
   1    2        "Vent Exit (Ambient)"
   2    1        "LN2 Ullage Space"
   3    2        "LN2 Tank Pseudo Node"
   4    1        "LN2 Propellant Volume"
   5    2        "Transfer Line Exit (Ambient)"

NODE  PRES (PSI)  TEMP (DEGF)  MASS SOURC  HEAT SOURC  THRST AREA  NODE-VOLUME
   2  14.7        -316         0           0           0           3710.4
   4  15.91       -322         0           0           0           57313
ln2prsh1.dat
```

```
ln2prsh3.dat
lc39bhs1.dat
INODE     NUMBR       NAMEBR
  2       1           12
  4       2           34          45
BRANCH    UPNODE      DNNODE      OPTION      DESCRIPTION
  12      1           2           1           «Vent Line»
  34      3           4           2           «Propellant Surface (Pseudo Branch)»
  45      4           5           2           «Transfer Line»
BRANCH    OPTION -1   LENGTH          DIA        EPSD            ANGLE        AREA
  12                  49              0.902      0.00088692      0            0.639
BRANCH    OPTION -2   FLOW COEFF      AREA
  34                  0               956.12
BRANCH    OPTION -2   FLOW COEFF      AREA
  45                  0.6             0.0001
INITIAL FLOWRATES IN BRANCHES FOR UNSTEADY FLOW
  12     0.0001
  34     0.0001
  45     0.0001
NUMBER OF PRESSURIZATION PROPELLANT TANKS IN CIRCUIT
  1
TNKTYPE   NODUL     NODULB     NODPRP     IBRPRP     TNKAR      TNKTH      TNKRHO     TNKCP
  0       2         3          4          34         1124.9     0.1875     467        0.07
TNKCON    ARHC      FCTHC      TNKTM
  0.0017  956.12    1          -322
NSOLID    NAMB      NSSC       NSFC       NSAC       NSSR
  12      1         16         2          2          0

NODESL MATRL SMASS     TS          NUMSS NUMSF NUMSA NUMSSR DESCRIPTION
  7     29   62.28500  85.00000    2     0     1     0      «Outer Half of Ullage Outer Tank Wall»
NAMESS
  78    711
NAMESA
  67
  8     29   62.28500  85.00000    3     0     0     0      «Inner Half of Ullage Outer Tank Wall»
NAMESS
  78    812  815
  9     29   28.97500  -314.00000  3     0     0     0      «Outer Half of Ullage Tank Wall»
NAMESS
  910   913  169
  10    29   28.97500  -314.00000  2     1     0     0      «Inner Half of Ullage Tank Wall»
NAMESS
  910   1014
NAMESF
  102
  11    29   226.05500 85.00000    2     0     1     0      «Outer Half of Propellant Outer Tank Wall»
NAMESS
  1112  711
NAMESA
  611
  12    29   226.05500 85.00000    3     0     0     0      «Inner Half of Propellant Outer TankWall»
NAMESS
  1112  812  1217
  13    29   164.21000 -322.00000  3     0     0     0      «Outer Half of Propellant Tank Wall»
```

```
NAMESS
   1314    913       1813
   14      29        164.21000   -322.00000  2     1      0      0      «Inner Half of Propellant Tank Wall»
NAMESS
   1314    1014
NAMESF
   144
   15      42        17.20500    37.00000    3     0      0      0      «Outer Half of Ullage Insulation»
NAMESS
   815     1516      1517
   16      42        17.20500    -217.00000  3     0      0      0      «Inner Half of Ullage Insulation»
NAMESS
   1516    169       1618
   17      42        74.28000    26.00000    3     0      0      0      «Outer Half of Propellant Insulation»
NAMESS
   1217    1718      1517
   18      42        74.28000    -241.00000  3     0      0      0      «Inner Half of Propellant Insulation»
NAMESS
   1718    1813      1618
NODEAM     TAMB        DESCRIPTION
   6       85.00000    "Ambient Condition"
ICONSS     ICNSI    ICNSJ    ARCSIJ        DISTSIJ      DESCRIPTION
   78      7        8        2458.34000    0.09000      «Ullage Surface Area at Midpoint of Outer Tank Wall»
   910     9        10       1143.67000    0.09000      «Ullage Surface Area at Midpoint of Tank Wall»
   1112    11       12       8922.19000    0.09000      «Propellant Surface Area at Midpoint of Outer Tank Wall»
   1314    13       14       6410.84000    0.09000      «Propellant Surface Area at Midpoint of Tank Wall»
   1014    10       14       14.41000      76.88000     «Inner Half Inner Sphere Ull-Prp Cond»
   913     9        13       14.47000      77.18000     «Outer Half Inner Sphere Ull-Prp Cond»
   812     8        12       17.69000      94.40000     «Inner Half Outer Sphere Ull-Prp Cond»
   711     7        11       17.76000      94.70000     «Outer Half Outer Sphere Ull-Prp Cond»
   815     8        15       2433.01000    1.39000      «Ullage Outer Sphere-Insulation Interface Area»
   1516    15       16       1752.24000    2.70000      «Ullage Surface Area at Midpoint of Insulation»
   169     16       9        1162.54000    1.39000      «Ullage Inner Sphere-Insulation Interface Area»
   1217    12       17       8876.72000    1.39000      «Propellant Outer Sphere-Insulation Interface Area»
   1718    17       18       7618.50000    2.70000      «Propellant Surface Area at Midpoint of Insulation»
   1813    18       13       6449.86000    1.39000      «Propellant Inner Sphere-Insulation Interface Area»
   1517    15       17       485.02000     90.02000     «Outer Half Insulation Ull-Prp Cond»
   1618    16       18       439.59000     81.56000     «Inner Half Insulation Ull-Prp Cond»

ICONSF  ICS  ICF  MODEL  ARSF          HCSF          EMSFS         EMSFF         DESCRIPTION
   102  10   2    0      1.12491e+03   0.00000e+00   0.00000e+00   0.00000e+00   «Ullage-Tank Wall Surface Area»
   144  14   4    0      6.37194e+03   0.00000e+00   0.00000e+00   0.00000e+00   «Propellant-Tank Wall Surface Area»

ICONSA  ICSAS  ICSAA  ARSA          HCSA          EMSAS         EMSAA         DESCRIPTION
   67   7      6      2.48330e+03   4.44000e-04   7.00000e-01   7.00000e-01   «Ullage Space Outer Surface of Outer Tank»
   611  11     6      8.96825e+03   4.44000e-04   7.00000e-01   7.00000e-01   «Propellant Space Outer Surface of Outer Tank»
```

D.2 CESAT Liquid Nitrogen and Perlite Sample Output Data File

```
ISTEP =****     TAU = 0.36000E+05
BOUNDARY NODES
NODE    P (PSI)        TF (F)         Z (COMP)       RHO            QUALITY
                                                     (LBM/FT^3)
   1    0.1470E+02     0.8500E+02     0.0000E+00     0.7047E-01     0.1000E+01
```

3	0.1591E+02	-0.3220E+03	0.0000E+00	0.5044E+02	0.0000E+00
5	0.1470E+02	0.8500E+02	0.0000E+00	0.7047E-01	0.1000E+01

SOLUTION

INTERNAL NODES

NODE	P (PSI)	TF (F)	Z (COMP)	RHO (LBM/FT^3)	EM (LBM)	QUALITY
2	0.1470E+02	-0.3160E+03	0.9587E+00	0.2787E+00	0.6035E+00	0.1000E+01
4	0.1591E+02	-0.3220E+03	0.5986E-02	0.5044E+02	0.1673E+04	0.0000E+00

BRANCHES

BRANCH	KFACTOR (LBF-S^2/ (LBM-FT)^2)	DELP (PSI)	FLOW RATE (LBM/SEC)	VELOCITY (FT/SEC)	REYN. NO.	MACH NO.	ENTROPY GEN. BTU/(R-SEC)	LOST WORK LBF-FT/SEC
12	0.260E+10	0.000E+00	0.107E-07	0.343E-04	0.149E-01	0.295E-07	0.108E-18	0.456E-13
34	0.000E+00	0.000E+00	-0.306E-04	-0.915E-07	0.118E+00	0.135E-09	0.000E+00	0.000E+00
45	0.177E+10	0.121E+01	0.588E-05	0.168E+00	0.702E+02	0.248E-03	0.668E-13	0.715E-08

SOLID NODES

NODESL	CPSLD BTU/LB F	TS F
7	0.109E+00	0.848E+02
8	0.109E+00	0.848E+02
9	0.693E-01	-0.314E+03
10	0.693E-01	-0.314E+03
11	0.109E+00	0.848E+02
12	0.109E+00	0.848E+02
13	0.690E-01	-0.322E+03
14	0.690E-01	-0.322E+03
15	0.200E+00	0.370E+02
16	0.200E+00	-0.217E+03
17	0.200E+00	0.260E+02
18	0.200E+00	-0.241E+03

SOLID TO SOLID CONDUCTOR

ICONSS	CONDKIJ BTU/S FT F	QDOTSS BTU/S
78	0.262E-02	0.218E-02
910	0.167E-02	0.199E-02
1112	0.262E-02	0.924E-02
1314	0.167E-02	0.103E-01
1014	0.167E-02	0.205E-03
913	0.167E-02	0.206E-03
812	0.262E-02	0.171E-05
711	0.262E-02	0.171E-05
815	0.322E-06	0.225E-02
1516	0.161E-06	0.221E-02
169	0.322E-06	0.218E-02
1217	0.322E-06	0.101E-01
1718	0.161E-06	0.101E-01
1813	0.322E-06	0.101E-01
1517	0.161E-06	0.795E-06
1618	0.161E-06	0.175E-05

SOLID TO FLUID CONDUCTOR

ICONSF	QDOTSF	HCSF	HCSFR
	BTU/S	BTU/S FT**2 F	BTU/S FT**2 F
102	-0.180E-02	0.125E-03	0.000E+00
144	-0.135E-01	0.100E+02	0.000E+00

SOLID TO AMBIENT CONDUCTOR

ICONSA	QDOTSA	HCSA	HCSAR
	BTU/S	BTU/SFT**2 F	BTU/S FT**2 F
67	0.185E-02	0.444E-03	0.166E-03
611	0.825E-02	0.444E-03	0.166E-03

NUMBER OF PRESSURIZATION SYSTEMS = 1

NODUL	NODPRP	QULPRP	QULWAL	QCOND	TNKTM	VOLPROP	VOLULG
2	4	0.0025	0.0000	0.0000	137.6000	33.1672	2.1653

D.2.1 CESAT Liquid Nitrogen and Perlite Sample Output Plots

CESAT liquid nitrogen and perlite solid node temperature predictions, ulllage and propellant path heat transfer rates, and boiloff rate output plots are shown in figures 23–25, respectively.

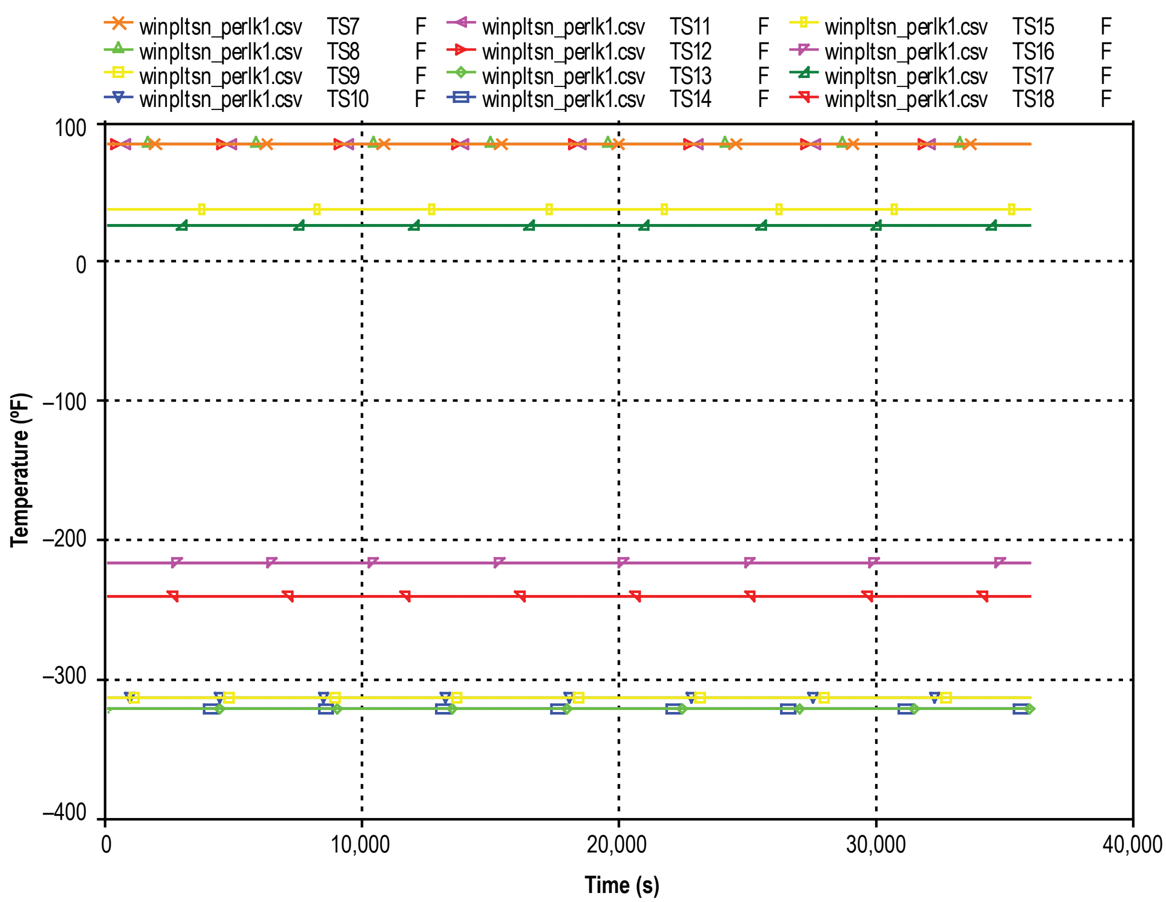

Figure 23. CESAT liquid nitrogen and perlite solid node temperature predictions.

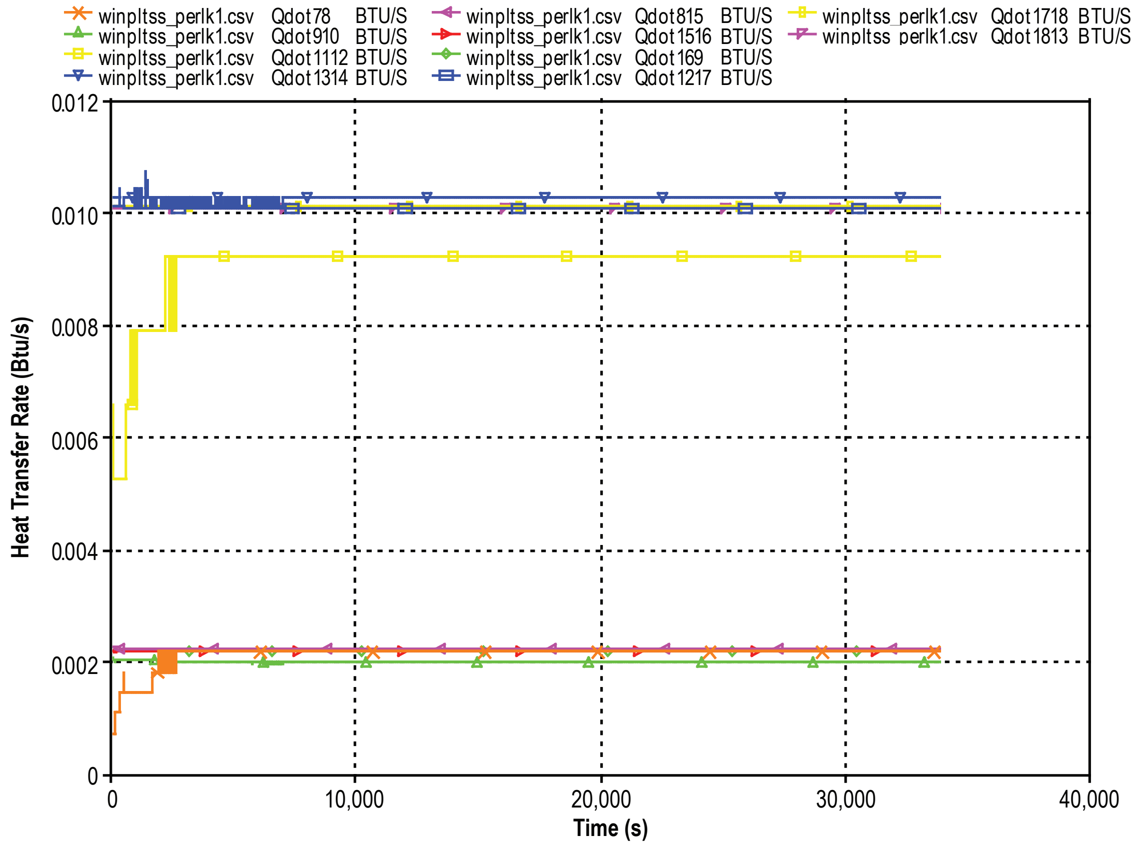

Figure 24. CESAT liquid nitrogen and perlite ullage and propellant path heat transfer rates.

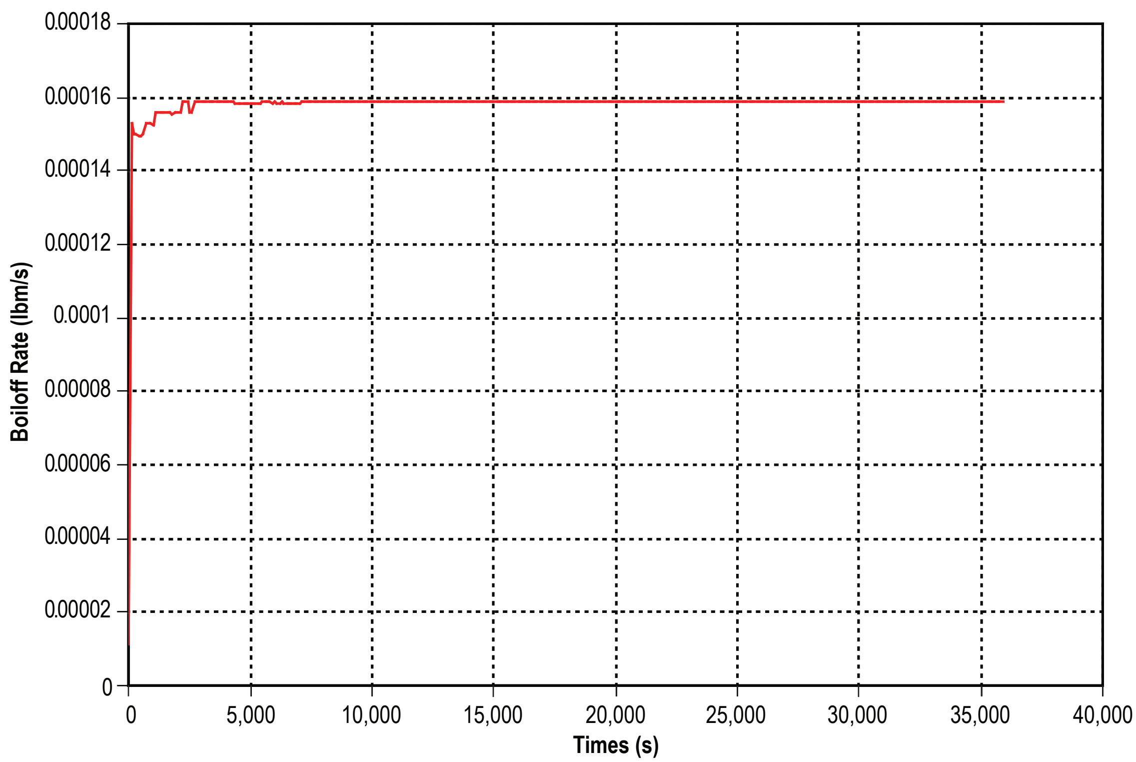

Figure 25. CESAT liquid nitrogen and perlite boiloff rates.

D.3 CESAT Liquid Nitrogen and Glass Bubbles Input Data File

```
GFSSP VERSION
   500
GFSSP INSTALLATION PATH
ANALYST
   Todd Steadman
INPUT DATA FILE NAME
   D:\GFSSP\KSC LH2 Tank\New Press Mods\Cesat_LN2_glas07.dat
OUTPUT FILE NAME
   Cesat_LN2_glas07.out
TITLE
   KSC Liquid Nitrogen Test Tank - 85% Full by Height, Glass Bubbles k=0.7 mW/m-K

USETUP
   F
DENCON      GRAVITY     ENERGY      MIXTURE     THRUST      STEADY      TRANSV      SAVER
   F        F           T           F           F           F           T           F
HEX         HCOEF       REACTING    INERTIA     CONDX       ADDPROP     PRINTI      ROTATION
   F        F           F           F           F           F           F           F
BUOYANCY    HRATE       INVAL       MSORCE      MOVBND      TPA         VARGEO      TVM
   F        T           F           F           F           F           F           F
SHEAR       PRNTIN      PRNTADD     OPVALVE     TRANSQ      CONJUG      RADIAT      WINPLOT
   F        F           F           F           F           T           T           T
PRESS       INSUC       VARROT      CYCLIC      CHKVAL
   T        F           F           F           T
NORMAL      SIMUL       SECONDL     NRSOLV
   F        T           F           T
NNODES      NINT        NBR         NF
   5        2           3           1
RELAXK      RELAXD      RELAXH      CC          NITER
   1        0.5         0.01        1e-06       500
DTAU        TIMEF       TIMEL       NPSTEP
   1        0           36000       500
NFLUID(I), I = 1, NF
   4
NODE    INDEX    DESCRIPTION
   1      2        "Vent Exit (Ambient)"
   2      1        "LN2 Ullage Space"
   3      2        "LN2 Tank Pseudo Node"
   4      1        "LN2 Propellant Volume"
   5      2        "Transfer Line Exit (Ambient)"

NODE  PRES (PSI)  TEMP (DEGF)  MASS SOURC  HEAT SOURC  THRST AREA  NODE-VOLUME
   2   14.7        -317         0           0           0           3710.4
   4   15.91       -322         0           0           0           57313
ln2ph1gb.dat
ln2prsh3.dat
ln2ph1gb.dat
INODE       NUMBR       NAMEBR
   2        1           12
   4        2           34          45
BRANCH      UPNODE      DNNODE      OPTION      DESCRIPTION
   12       1           2           1           «Vent Line»
```

```
   34        3          4            2          «Propellant Surface (Pseudo Branch)»
   45        4          5            2          «Transfer Line»
BRANCH    OPTION -1     LENGTH       DIA        EPSD          ANGLE        AREA
   12                   49           0.902      0.00088692    0            0.639
BRANCH    OPTION -2     FLOW COEFF   AREA
   34                   0            956.12
BRANCH    OPTION -2     FLOW COEFF   AREA
   45                   0.6          0.0001
INITIAL FLOWRATES IN BRANCHES FOR UNSTEADY FLOW
   12         0.0001
   34         0.0001
   45         0.0001
NUMBER OF PRESSURIZATION PROPELLANT TANKS IN CIRCUIT
   1
TNKTYPE   NODUL   NODULB   NODPRP   IBRPRP   TNKAR    TNKTH    TNKRHO   TNKCP   TNKCON
   0      2       3        4        34       1124.9   0.1875   467      0.07    0.0017
ARHC      FCTHC   TNKTM
   956.12 1       -322
NSOLID   NAMB   NSSC   NSFC   NSAC   NSSR
   12    1      16     2      2      0

NODESL  MATRL  SMASS       TS           NUMSS  NUMSF  NUMSA  NUMSSR     DESCRIPTION
   7    29     62.28500    74.00000     2      0      1      0      "Outer Half of Ullage Outer Tank Wall"
NAMESS
   78   711
NAMESA
   67
   8    29     62.28500    74.00000     3      0      0      0      "Inner Half of Ullage Outer Tank Wall"
NAMESS
   78   812    815
   9    29     28.97500    -316.00000   3      0      0      0      "Outer Half of Ullage Tank Wall"
NAMESS
   910  913    169
   10   29     28.97500    -316.00000   2      1      0      0      "Inner half of Ullage Tank Wall"
NAMESS
   910  1014
NAMESF
   102
   11   29     226.05500   74.00000     2      0      1      0      "Outer Half of Propellant Outer Tank Wall"
NAMESS
   1112  711
NAMESA
   611
   12   29     226.05500   74.00000     3      0      0      0      "Inner Half of Propellant Outer Tank Wall"
NAMES
   1112 812    1217
   13   29     164.21000   -322.00000   3      0      0      0      "Outer Half of Propellant Tank Wall"
NAMESS
   1314 913    1813
   14   29     164.21000   -322.00000   2      1      0      0      "Inner Half of Propellant Tank Wall"
NAMESS
   1314 1014
NAMESF
   144
```

15 43 11.01000 28.00000 3 0 0 0 “Outer Half of Ullage Insulation”
NAMESS
815 1516 1517
16 43 11.01000 -219.00000 3 0 0 0 “Inner Half of Ullage Insulation”
NAMESS
1516 169 1618
17 43 47.53000 17.00000 3 0 0 0 “Outer Half of Propellant Insulation”
NAMESS
1217 1718 1517
18 43 47.53000 -242.00000 3 0 0 0 “Inner Half of Propellant Insulation”
NAMESS
1718 1813 1618

NODEAM	TAMB	DESCRIPTION
6	74.00000	“Ambient Condition”

ICONSS	ICNSI	ICNSJ	ARCSIJ	DISTSIJ	DESCRIPTION
78	7	8	2458.34000	0.09000	«Ullage Surface Area at Midpoint of Outer Tank Wall»
910	9	10	1143.67000	0.09000	«Ullage Surface Area at Midpoint of Tank Wall»
1112	11	12	8922.19000	0.09000	«Propellant Surface Area at Midpoint of outer Tank Wall»
1314	13	14	6410.84000	0.09000	«Propellant Surface Area at Midpoint of Tank Wall»
1014	10	14	14.41000	76.88000	«Inner Half Inner Sphere Ull-Prp Cond»
913	9	13	14.47000	77.18000	«Outer Half Inner Sphere Ull-Prp Cond»
812	8	12	17.69000	94.40000	«Inner Half Outer Sphere Ull-Prp Cond»
711	7	11	17.76000	94.70000	«Outer Half Outer Sphere Ull-Prp Cond»
815	8	15	2433.01000	1.39000	«Ullage Outer Sphere-Insulation Interface Area»
1516	15	16	1752.24000	2.70000	«Ullage Surface Area at Midpoint of Insulation»
169	16	9	1162.54000	1.39000	«Ullage Inner Sphere-Insulation Interface Area»
1217	12	17	8876.72000	1.39000	«Propellant Outer Sphere-Insulation Interface Area»
1718	17	18	7618.50000	2.70000	«Propellant Surface Area at Midpoint of Insulation»
1813	18	13	6449.86000	1.39000	«Propellant Inner Sphere-Insulation Interface Area»
1517	15	17	485.02000	90.02000	«Outer Half Insulation Ull-Prp Cond»
1618	16	18	439.59000	81.56000	«Inner Half Insulation Ull-Prp Cond»

ICONSF	ICS	ICF	MODEL	ARSF	HCSF	EMSFS	EMSFF	DESCRIPTION
102	10	2	0	1.12491e+03	0.00000e+00	0.00000e+00	0.00000e+00	«Ullage-Tank Wall Surface Area»
144	14	4	0	6.37194e+03	0.00000e+00	0.00000e+00	0.00000e+00	«Propellant-Tank Wall Surface Area»

ICONSA	ICSAS	ICSAA	ARSA	HCSA	EMSAS	EMSAA	DESCRIPTION
67	7	6	2.48330e+03	4.44000e-04	7.00000e-01	7.00000e-01	«Ullage Space Outer Surface of Outer Tank»
611	11	6	8.96825e+03	4.44000e-04	7.00000e-01	7.00000e-01	«Propellant Space Outer Surface of Outer Tank»

D.4 CESAT Liquid Nitrogen and Glass Bubbles Sample Output Data File

ISTEP =**** TAU = 0.36000E+05
BOUNDARY NODES

NODE	P (PSI)	TF (F)	Z (COMP)	RHO (LBM/FT^3)	QUALITY
1	0.1470E+02	0.7400E+02	0.0000E+00	0.7193E-01	0.1000E+01
3	0.1591E+02	-0.3220E+03	0.0000E+00	0.5044E+02	0.0000E+00
5	0.1470E+02	0.7400E+02	0.0000E+00	0.7193E-01	0.1000E+01

SOLUTION

INTERNAL NODES

NODE	P (PSI)	TF (F)	Z (COMP)	RHO (LBM/FT^3)	EM (LBM)	QUALITY
2	0.1470E+02	-0.3173E+03	0.9574E+00	0.2816E+00	0.6098E+00	0.1000E+01
4	0.1591E+02	-0.3220E+03	0.5986E-02	0.5044E+02	0.1673E+04	0.0000E+00

BRANCHES

BRANCH	KFACTOR (LBF-S^2/ (LBM-FT)^2)	DELP (PSI)	FLOW RATE (LBM/SEC)	VELOCITY (FT/SEC)	REYN. NO.	MACH NO.	ENTROPY GEN. BTU/(R-SEC)	LOST WORK LBF-FT/SEC
12	0.747E+10	0.000E+00	0.361E-08	0.113E-04	0.511E-02	0.982E-08	0.118E-19	0.489E-14
34	0.000E+00	0.000E+00	0.146E-04	0.436E-07	0.564E-01	0.643E-10	0.000E+00	0.000E+00
45	0.177E+10	0.121E+01	0.588E-05	0.168E+00	0.702E+02	0.248E-03	0.667E-13	0.715E-08

SOLID NODES

NODESL	CPSLD BTU/LB F	TS F
7	0.109E+00	0.739E+02
8	0.109E+00	0.739E+02
9	0.692E-01	-0.316E+03
10	0.692E-01	-0.316E+03
11	0.109E+00	0.739E+02
12	0.109E+00	0.739E+02
13	0.690E-01	-0.322E+03
14	0.690E-01	-0.322E+03
15	0.190E+00	0.280E+02
16	0.190E+00	-0.219E+03
17	0.190E+00	0.170E+02
18	0.190E+00	-0.242E+03

SOLID TO SOLID CONDUCTOR

ICONSS	CONDKIJ BTU/S FT F	QDOTSS BTU/S
78	0.260E-02	0.145E-02
910	0.167E-02	0.135E-02
1112	0.260E-02	0.656E-02
1314	0.167E-02	0.710E-02
1014	0.167E-02	0.158E-03
913	0.167E-02	0.158E-03
812	0.260E-02	0.145E-05
711	0.260E-02	0.145E-05
815	0.224E-06	0.150E-02
1516	0.112E-06	0.150E-02
169	0.224E-06	0.151E-02
1217	0.224E-06	0.678E-02
1718	0.112E-06	0.683E-02
1813	0.224E-06	0.690E-02
1517	0.112E-06	0.553E-06
1618	0.112E-06	0.117E-05

SOLID TO FLUID CONDUCTOR

ICONSF	QDOTSF	HCSF	HCSFR
	BTU/S	BTU/S FT**2 F	BTU/S FT**2 F
102	-0.117E-02	0.113E-03	0.000E+00
144	-0.675E-02	0.100E+02	0.000E+00

SOLID TO AMBIENT CONDUCTOR

ICONSA	QDOTSA	HCSA	HCSAR
	BTU/S	BTU/S FT**2 F	BTU/S FT**2 F
67	0.111E-02	0.444E-03	0.156E-03
611	0.533E-02	0.444E-03	0.156E-03

NUMBER OF PRESSURIZATION SYSTEMS = 1

NODUL	NODPRP	QULPRP	QULWAL	QCOND	TNKTM	VOLPROP	VOLULG
2	4	0.0019	0.0000	0.0000	137.6000	33.1672	2.1653

D.4.1 CESAT Liquid Nitrogen and Glass Bubbles Sample Output Plots

CESAT liquid nitrogen and glass bubbles solid node temperature predictions, ulllage and propellant path heat transfer rates, and boiloff rate output plots are shown in figures 26–28, respectively.

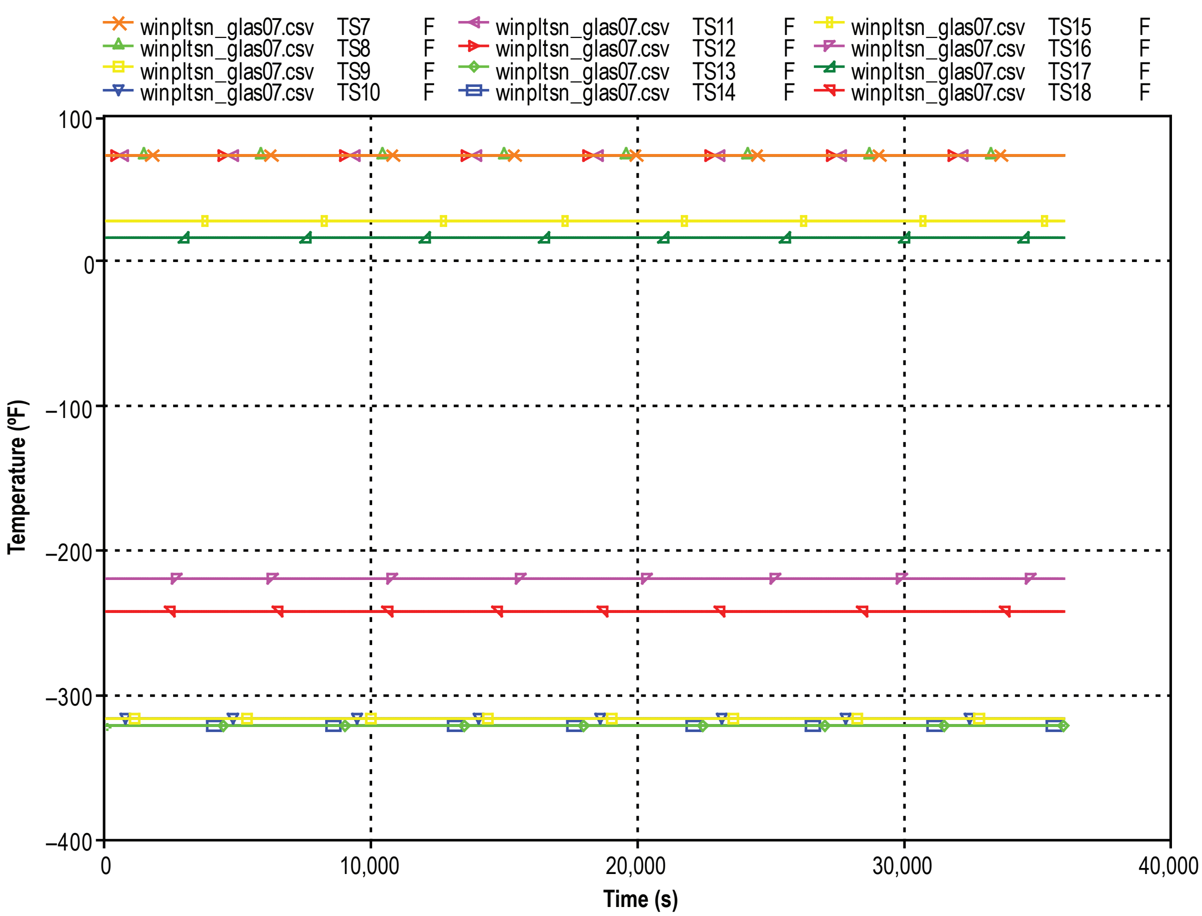

Figure 26. CESAT liquid nitrogen and glass bubbles solid node temperature predictions.

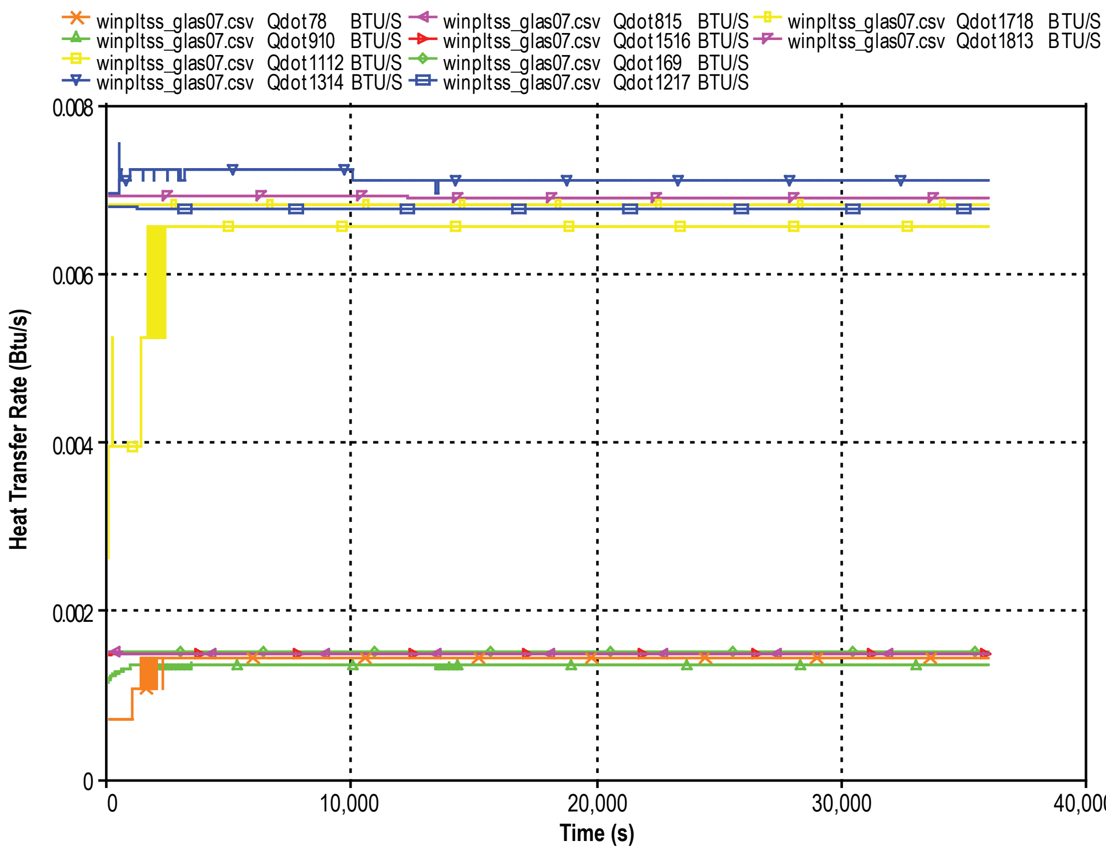

Figure 27. CESAT liquid nitrogen and glass bubbles ulllage and propellant path heat transfer rates.

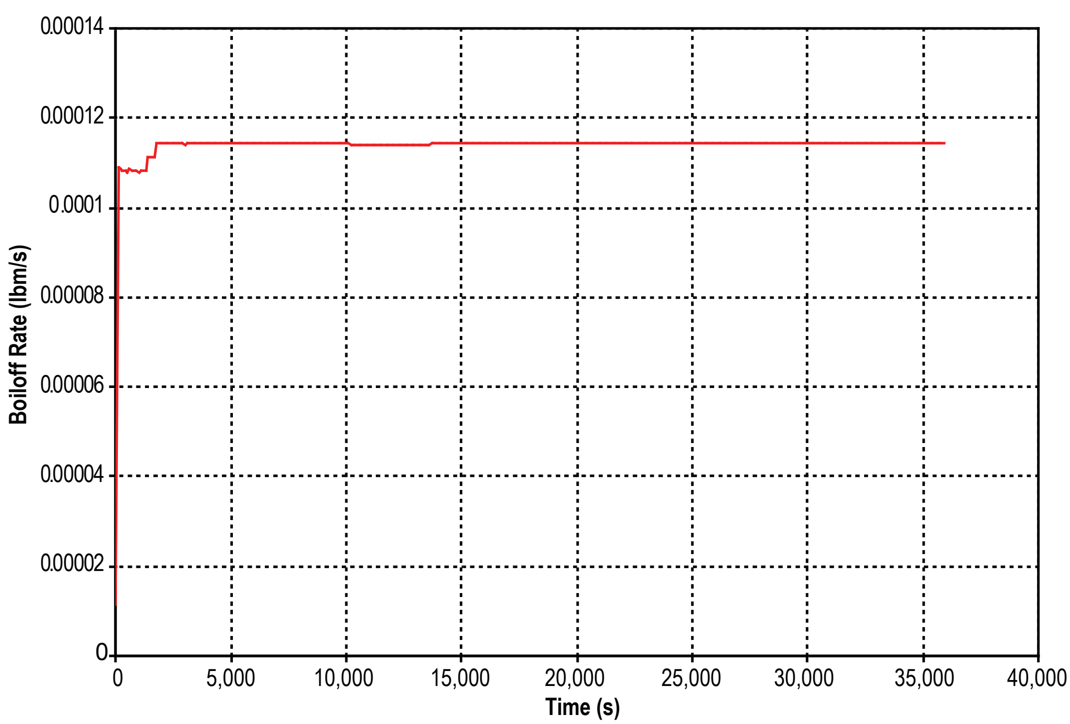

Figure 28. CESAT liquid nitrogen and glass bubbles boiloff rates.

D.5 CESAT Liquid Hydrogen and Perlite Input Data File

```
GFSSP VERSION
  500
GFSSP INSTALLATION PATH
  C:\Program Files\GFSSP\
ANALYST
  Todd Steadman
INPUT DATA FILE NAME
  D:\KSC_Cryotank\CESAT_LH2Bubble\Cesat_LH2_perlk1.dat
OUTPUT FILE NAME
  Cesat_LH2_perlk1.out
TITLE
  KSC Liquid Hydrogen Test Tank - 85% Full by Height

USETUP
  F
DENCON      GRAVITY     ENERGY      MIXTURE     THRUST      STEADY      TRANSV      SAVER
  F         F           T           F           F           F           T           T
HEX         HCOEF       REACTING    INERTIA     CONDX       ADDPROP     PRINTI      ROTATION
  F         F           F           F           F           F           F           F
BUOYANCY    HRATE       INVAL       MSORCE      MOVBND      TPA         VARGEO      TVM
  F         T           T           F           F           F           F           F
SHEAR       PRNTIN      PRNTADD     OPVALVE     TRANSQ      CONJUG      RADIAT      WINPLOT
  F         F           F           F           F           T           T           T
PRESS       INSUC       VARROT      CYCLIC      CHKVALS
  T         F           F           F           T
NORMAL      SIMUL       SECONDL     NRSOLVT
  F         F           F           T
NNODES      NINT        NBR         NF
  5         2           3           1
RELAXK      RELAXD      RELAXH      CC          NITER
  1         0.5         0.01        1e-06       500
DTAU        TIMEF       TIMEL       NPSTEP
  0.4       15000       30000       300
NFLUID(I), I = 1, NF
  10

NODE    INDEX    DESCRIPTION
  1     2        “Vent Exit (Ambient)”
  2     1        «LH2 Ullage Space»
  3     2        «LH2 Tank Pseudo Node»
  4     1        «LH2 Propellant Volume»
  5     2        «Transfer Line Exit (Ambient)»

NODE  PRES (PSI)  TEMP (DEGF)  MASS SOURC  HEAT SOURC  THRST AREA  NODE-VOLUME
  2   14.7        -421         0           0           0           3710.4
  4   14.81       -423.6       0           0           0           57313
ln2prsh1.dat
lh2prsh3.dat
lc39bhs1.dat
INODE    NUMBR    NAMEBR
  2      1        12
  4      2        34       45
```

```
BRANCH    UPNODE      DNNODE     OPTION      DESCRIPTION
  12      1           2          1           «Vent Line»
  34      3           4          2           «Propellant Surface (Pseudo Branch)»
  45      4           5          2           «Transfer Line»
BRANCH    OPTION -1   LENGTH     DIA         EPSD        ANGLE AREA
  12                   49            0.902      0.00088692        0              0.639
BRANCH    OPTION -2   FLOW COEFF    AREA
  34                  0             1e-05
BRANCH    OPTION -2   FLOW COEFF    AREA
  45                  0.6           0.0001
INITIAL FLOWRATES IN BRANCHES FOR UNSTEADY FLOW
  12      0.0001
  34      0.0001
  45      0.0001
NUMBER OF PRESSURIZATION PROPELLANT TANKS IN CIRCUIT = 1
TNKTYPE   NODUL    NODULB    NODPRP    IBRPRP    TNKAR     TNKTH     TNKRHO    TNKCP
  0       2        3         4         34        1124.9    0.1875    467       0.07
TNKCON    ARHC     FCTHC     TNKTM
  0.0017  956.12   0.00265   -423.6
RESTART NODE INFORMATION FILE
 FNODE.DAT
RESTART BRANCH INFORMATION FILE
 FBRANCH.DAT
NSOLID    NAMB     NSSC      NSFC      NSAC      NSSR
  12      1        16        2         2         0
NODESL  MATRL  SMASS      TS          NUMSS  NUMSF  NUMSA  NUMSSR  DESCRIPTION
  7     29     62.28500   85.00000    2      0      1      0       «Outer Half of Ullage Outer Tank Wall»
NAMESS
  78    711
NAMESA
  67
  8     29     62.28500   85.00000    3      0      0      0       «Inner Half of Ullage Outer Tank Wall»
NAMESS
  78    812    815
  9     29     28.97500   -420.00000  3      0      0      0       «Outer Half of Ullage Tank Wall»
NAMESS
  910   913    169
  10    29     28.97500   -420.00000  2      1      0      0       «Inner Half of Ullage Tank Wall»
NAMESS
  910   1014
NAMESF
  102
  11    29     226.05500  85.00000    2      0      1      0       «Outer Half of Propellant Outer Tank Wall»
NAMESS
  1112  711
NAMESA
  611
  12    29     226.05500  85.00000    3      0      0      0       «Inner Half of Propellant Outer Tank Wall»
NAMESS
  1112  812    1217
  13    29     164.21000  -423.60000  3      0      0      0       «Outer Half of Propellant Tank Wall»
NAMESS
  1314  913    1813
  14    29     164.21000  -423.60000  2      1      0      0       «Inner Half of Propellant Tank Wall»
```

NAMESS
1314 1014
NAMESF
144
15 42 17.20500 32.00000 3 0 0 0 «Outer Half of Ullage Insulation»
NAMESS
815 1516 1517
16 42 17.20500 -280.00000 3 0 0 0 «Inner Half of Ullage Insulation»
NAMESS
1516 169 1618
17 42 74.28000 28.00000 3 0 0 0 «Outer Half of Propellant Insulation»
NAMESS
1217 1718 1517
18 42 74.28000 -310.00000 3 0 0 0 «Inner Half of Propellant Insulation»
NAMESS
1718 1813 1618

NODEAM	TAMB	DESCRIPTION
6	85.00000	"Ambient Condition"

ICONSS	ICNSI	ICNSJ	ARCSIJ	DISTSIJ	DESCRIPTION
78	7	8	2458.34000	0.09000	«Ullage Surface Area at Midpoint of Outer Tank Wall»
910	9	10	1143.67000	0.09000	«Ullage Surface Area at Midpoint of Tank Wall»
1112	11	12	8922.19000	0.09000	«Propellant Surface Area at Midpoint of Outer Tank Wall»
1314	13	14	6410.84000	0.09000	«Propellant Surface Area at Midpoint of Tank Wall»
1014	10	14	14.41000	76.88000	«Inner Half Inner Sphere Ull-Prp Cond»
913	9	13	14.47000	77.18000	«Outer Half Inner Sphere Ull-Prp Cond»
812	8	12	17.69000	94.40000	«Inner Half Outer Sphere Ull-Prp Cond»
711	7	11	17.76000	94.70000	«Outer Half Outer Sphere Ull-Prp Cond»
815	8	15	2433.01000	1.39000	«Ullage Outer Sphere-Insulation Interface Area»
1516	15	16	1752.24000	2.70000	«Ullage Surface Area at Midpoint of Insulation»
169	16	9	1162.54000	1.39000	«Ullage Inner Sphere-Insulation Interface Area»
1217	12	17	8876.72000	1.39000	«Propellant Outer Sphere-Insulation Interface Area»
1718	17	18	7618.50000	2.70000	«Propellant Surface Area at Midpoint of Insulation»
1813	18	13	6449.86000	1.39000	«Propellant Inner Sphere-Insulation Interface Area»
1517	15	17	485.02000	90.02000	«Outer Half Insulation Ull-Prp Cond»
1618	16	18	439.59000	81.56000	«Inner Half Insulation Ull-Prp Cond»

ICONSF	ICS	ICF	MODEL	ARSF	HCSF	EMSFS	EMSFF	DESCRIPTION
102	10	2	0	1.12491e+03	0.00000e+00	0.00000e+00	0.00000e+00	«Ullage-Tank Wall Surface Area»
144	14	4	0	6.37194e+03	0.00000e+00	0.00000e+00	0.00000e+00	«Propellant-Tank Wall Surface Area»

ICONSA	ICSAS	ICSAA	ARSA	HCSA	EMSAS	EMSAA	DESCRIPTION
67	7	6	2.48330e+03	4.44000e-04	7.00000e-01	7.00000e-01	«Ullage Space Outer Surface of Outer Tank»
611	11	6	8.96825e+03	4.44000e-04	7.00000e-01	7.00000e-01	«Propellant Space Outer Surface of Outer Tank»

D.6 CESAT Liquid Hydrogen and Perlite Sample Output Data File

ISTEP =**** TAU = 0.30000E+05
BOUNDARY NODES

NODE	P (PSI)	TF (F)	Z (COMP)	RHO (LBM/FT^3)	QUALITY
1	0.1470E+02	0.8500E+02	0.0000E+00	0.5065E-02	0.1000E+01

3	0.1481E+02	-0.4236E+03	0.0000E+00	0.4437E+01	0.0000E+00
5	0.1470E+02	0.8500E+02	0.0000E+00	0.5065E-02	0.1000E+01

SOLUTION

INTERNAL NODES

NODE	P (PSI)	TF (F)	Z (COMP)	RHO (LBM/FT^3)	EM (LBM)	QUALITY
2	0.1470E+02	-0.4231E+03	0.7275E+00	0.1040E+00	0.2253E+00	0.7999E+00
4	0.1351E+02	-0.4236E+03	0.1590E-01	0.4437E+01	0.1472E+03	0.0000E+00

BRANCHES

BRANCH	KFACTOR (LBF-S^2/ (LBM-FT)^2)	DELP (PSI)	FLOW RATE (LBM/SEC)	VELOCITY (FT/SEC)	REYN. NO.	MACH NO.	ENTROPY GEN. BTU/(R-SEC)	LOST WORK LBF-FT/SEC
12	0.209E+05	-0.694E-06	-0.691E-04	-0.150E+00	0.126E+04	0.347E-04	0.234E-11	0.663E-07
34	0.000E+00	0.129E+01	0.522E-07	0.169E+00	0.244E+02	0.138E-03	0.000E+00	0.000E+00
45	0.177E+14	-0.119E+01	-0.545E-08	-0.155E+01	0.124E+01	0.126E-02	0.133E-14	0.566E-09

SOLID NODES

NODESL	CPSLD BTU/LB F	TS F
7	0.130E+00	0.848E+02
8	0.130E+00	0.848E+02
9	0.107E+00	-0.422E+03
10	0.107E+00	-0.422E+03
11	0.130E+00	0.847E+02
12	0.130E+00	0.847E+02
13	0.107E+00	-0.423E+03
14	0.107E+00	-0.423E+03
15	0.200E+00	0.302E+02
16	0.200E+00	-0.284E+03
17	0.200E+00	0.229E+02
18	0.200E+00	-0.312E+03

SOLID TO SOLID CONDUCTOR

ICONSS	CONDKIJ BTU/S FT F	QDOTSS BTU/S
78	0.312E-02	0.256E-02
910	0.255E-02	0.305E-02
1112	0.312E-02	0.106E-01
1314	0.255E-02	0.139E-01
1014	0.255E-02	0.598E-04
913	0.255E-02	0.598E-04
812	0.312E-02	0.168E-05
711	0.312E-02	0.168E-05
815	0.322E-06	0.256E-02
1516	0.161E-06	0.273E-02
169	0.322E-06	0.311E-02
1217	0.322E-06	0.106E-01
1718	0.161E-06	0.127E-01
1813	0.322E-06	0.138E-01
1517	0.161E-06	0.534E-06
1618	0.161E-06	0.209E-05

SOLID TO FLUID CONDUCTOR

ICONSF	QDOTSF	HCSF	HCSFR
	BTU/S	BTU/S FT**2 F	BTU/S FT**2 F
102	-0.300E-02	0.332E-03	0.000E+00
144	-0.139E-01	0.192E-02	0.000E+00

SOLID TO AMBIENT CONDUCTOR

ICONSA	QDOTSA	HCSA	HCSAR
	BTU/S	BTU/S FT**2 F	BTU/S FT**2 F
67	0.256E-02	0.444E-03	0.166E-03
611	0.106E-01	0.444E-03	0.166E-03

NUMBER OF PRESSURIZATION SYSTEMS = 1

NODUL	NODPRP	QULPRP	QULWAL	QCOND	TNKTM	VOLPROP	VOLULG
2	4	0.0000	0.0000	0.0000	36.0000	33.1673	2.1653

D.6.1 CESAT Liquid Hydrogen and Perlite Sample Output Plots

CESAT liquid hydrogen and perlite solid node temperature predictions, ulllage and propellant path heat transfer rates, and boiloff rate output plots are shown in figures 29–31, respectively.

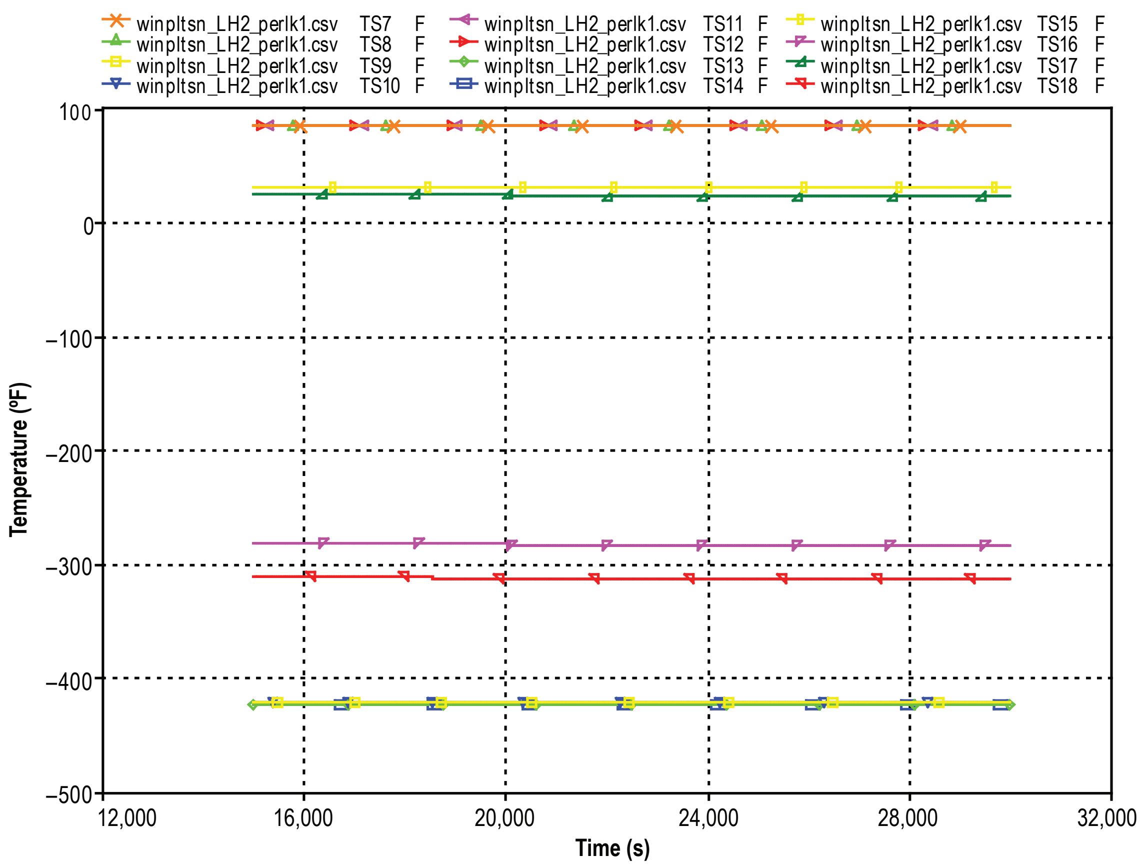

Figure 29. CESAT liquid hydrogen and perlite solid node temperature predictions.

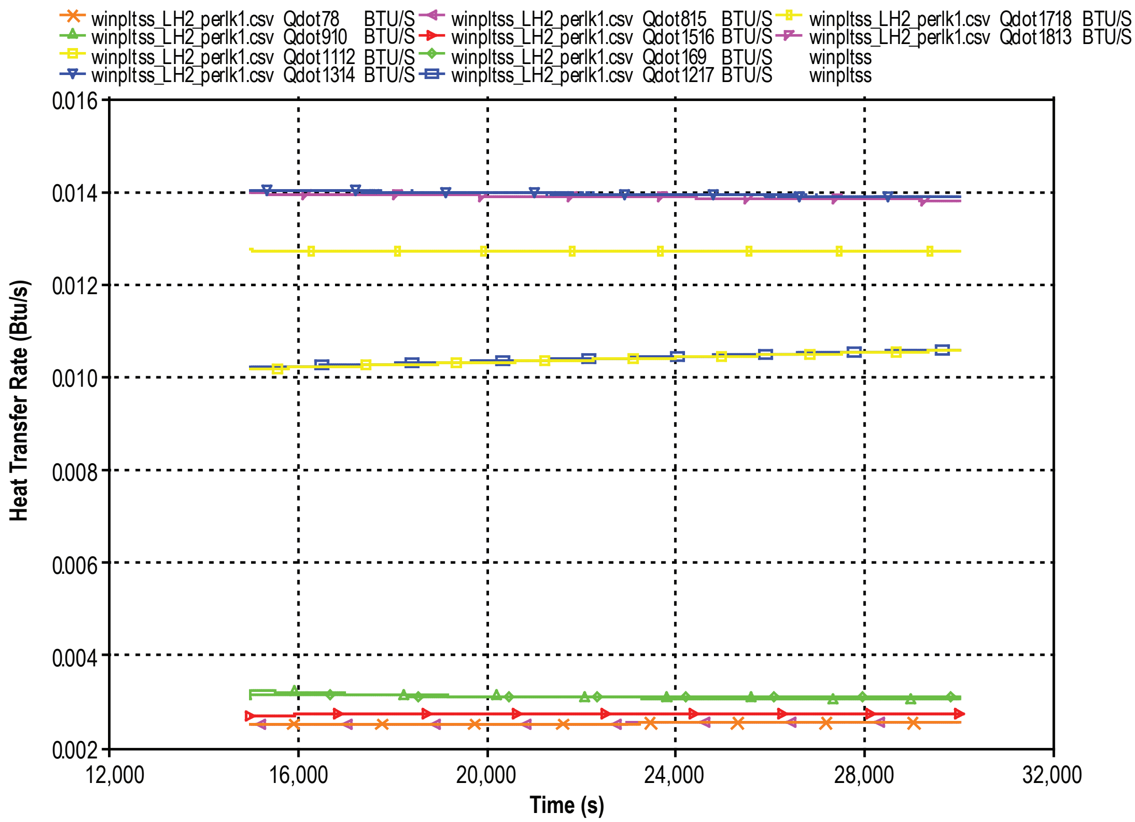

Figure 30. CESAT liquid hydrogen and perlite ullage and propellant path heat transfer rates.

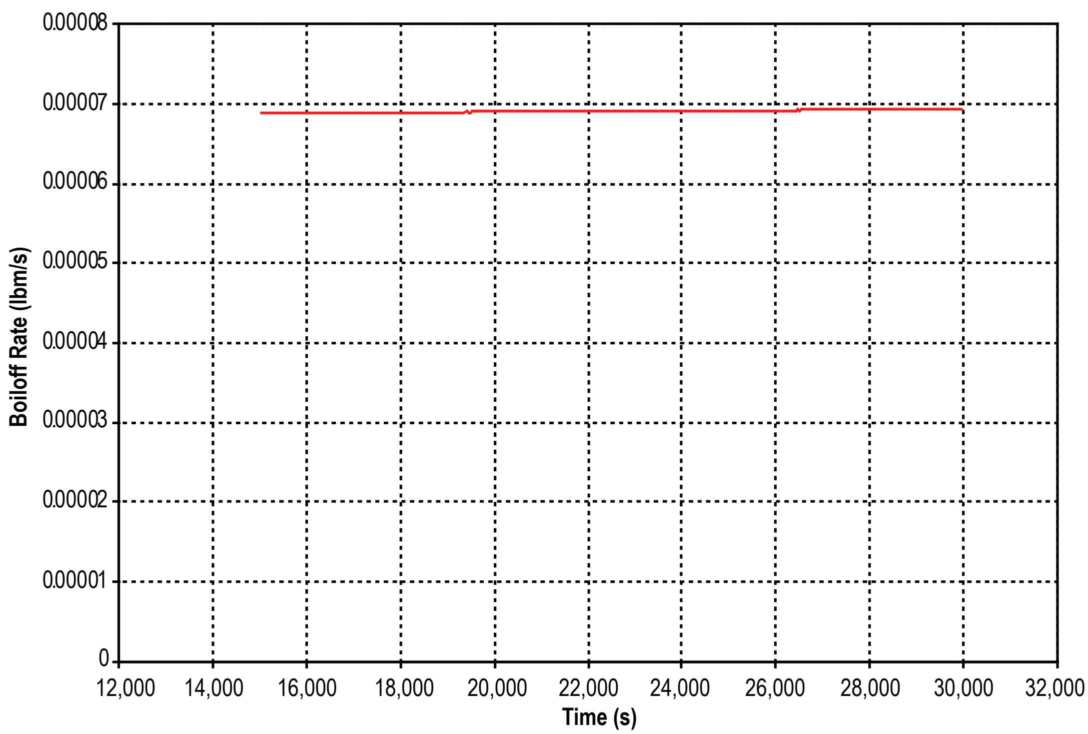

Figure 31. CESAT liquid hydrogen and perlite boiloff rates.

D.7 CESAT Liquid Hydrogen and Glass Bubbles Input Data File

```
GFSSP VERSION
  500
GFSSP INSTALLATION PATH
ANALYST
  Todd Steadman
INPUT DATA FILE NAME
  D:\GFSSP\KSC LH2 Tank\New Press Mods\Cesat_LH2_glas07.dat
OUTPUT FILE NAME
  Cesat_LH2_glas07.out
TITLE
  KSC Liquid Hydrogen Test Tank - 85% Full by Height

USETUP
  F
DENCON      GRAVITY   ENERGY    MIXTURE   THRUST    STEADY    TRANSV    SAVER
  F         F         T         F         F         F         T         F
HEX         HCOEF     REACTING  INERTIA   CONDX     ADDPROP   PRINTI    ROTATION
  F         F         F         F         F         F         F         F
BUOYANCY    HRATE     INVAL      MSORCE   MOVBND    TPA       VARGEO    TVM
  F         T         T         F         F         F         F         F
SHEAR       PRNTIN    PRNTADD   OPVALVE   TRANSQ    CONJUG    RADIAT    WINPLOT
  F         F         F         F         F         T         T         T
PRESS       INSUC     VARROT    CYCLIC    CHKVALS
  T         F         F         F         T
NORMAL      SIMUL     SECONDL   NRSOLVT
  F         F         F         T
NNODES      NINT      NBR       NF
  5         2         3         1
RELAXK      RELAXD    RELAXH    CC        NITER
  1         0.5       0.01      1e-06     500
DTAU        TIMEF     TIMEL     NPSTEP
  1         0         36000     300
NFLUID(I), I = 1, NF
  10

NODE      INDEX     DESCRIPTION
   1        2       « Vent Exit (Ambient)»
   2        1       « LH2 Ullage Space»
   3        2       « LH2 Tank Pseudo Node»
   4        1       «LH2 Propellant Volume»
   5        2       «Transfer Line Exit (Ambient)»

NODE   PRES (PSI)   TEMP (DEGF)   MASS SOURC   HEAT SOURC   THRST AREA   NODE-VOLUME
  2    14.7         -421          0            0            0            3710.4
  4    14.81        -425.1        0            0            0            57313
ln2prsh1.dat
lh2prsh3.dat
lc39bhs1.dat
INODE     NUMBR     NAMEBR
  2       1         12
  4       2         34        45
BRANCH    UPNODE    DNNODE    OPTION    DESCRIPTION
  12      1         2         1         «Vent Line»
```

```
   34          3              4              2              «Propellant Surface (Pseudo Branch)»
   45          4              5              2              «Transfer Line»
BRANCH     OPTION -1     LENGTH        DIA            EPSD           ANGLE       AREA
   12                         49            0.902          0.00088692     0           0.639
BRANCH     OPTION -2     FLOW COEFF      AREA
   34                          0               956.12
BRANCH     OPTION -2     FLOW COEFF      AREA
   45                          0.6             0.0001
INITIAL FLOWRATES IN BRANCHES FOR UNSTEADY FLOW
   12      0.0001
   34      0.0001
   45      0.0001
NUMBER OF PRESSURIZATION PROPELLANT TANKS IN CIRCUIT
   1
TNKTYPE     NODUL      NODULB      NODPRP      IBRPRP      TNKAR      TNKTH      TNKRHO
   0           2          3           4           34          1124.9     0.1875     467
TNKCP        TNKCON      ARHC        FCTHC      TNKTM
0.07         0.0017      956.12      1          -425.1
RESTART NODE INFORMATION FI
   FNDLH2GL.DAT
RESTART BRANCH INFORMATION FILE
   FBRLH2GL.DAT
NSOLID  NAMB    NSSC      NSFC     NSAC       NSSR
   12      1       16        2        2          0

NODESL  MATRL  SMASS     TS           NUMSS NUMSF  NUMSA  NUMSSR  DESCRIPTION
   7       29     62.28500  85.00000      2       0       1        0      «Outer Half of Ullage Outer Tank Wall»
NAMESS
   78      711
NAMESA
   67
   8       29     62.28500  85.00000     3       0       0       0       «Inner Half of Ullage Outer Tank Wall»
NAMESS
   78      812     815
   9       29     28.97500  -420.00000 3       0       0       0       «Outer Half of Ullage Tank Wall»
NAMESS
   910     913     169
   10      29     28.97500  -420.00000 2       1       0       0       «Inner Half of Ullage Tank Wall»
NAMESS
   910     1014
NAMESF
   102
   11      29     226.05500 85.00000     2       0       1       0       «Outer Half of Propellant Outer Tank Wall»
NAMESS
   1112  711
NAMESA
   611
   12      29     226.05500 85.00000      3       0       0       0       «Inner Half of Propellant Outer Tank Wall»
NAMESS
   1112    812     1217
   13      29     164.21000 -425.10000 3       0       0       0       «Outer Half of Propellant Tank Wall»
NAMESS
   1314    913     1813
   14      29     164.21000 -425.10000 2       1       0       0       «Inner Half of Propellant Tank Wall»
```

NAMESS
1314 1014
NAMESF
144

15	43	11.01000	32.00000	3	0	0	0	«Outer Half of Ullage Insulation»

NAMESS
815 1516 1517

16	43	11.01000	-280.00000	3	0	0	0	«Inner Half of Ullage Insulation»

NAMESS
1516 169 1618

17	43	47.53000	28.00000	3	0	0	0	«Outer Half of Propellant Insulation»

NAMESS
1217 1718 1517

18	43	47.53000	-310.00000	3	0	0	0	«Inner Half of Propellant Insulation»

NAMESS
1718 1813 1618

NODEAM	TAMB	DESCRIPTION
6	85.00000	"Ambient Condition"

ICONSS	ICNSI	ICNSJ	ARCSIJ	DISTSIJ	DESCRIPTION
78	7	8	2458.34000	0.09000	«Ullage Surface Area at Midpoint of Outer Tank Wall»
910	9	10	1143.67000	0.09000	«Ullage Surface Area at Midpoint of Tank Wall»
1112	11	12	8922.19000	0.09000	«Propellant Surface Area at Midpoint of Outer Tank Wall»
1314	13	14	6410.84000	0.09000	«Propellant Surface Area at Midpoint of Tank Wall»
1014	10	14	14.41000	76.88000	«Inner Half Inner Sphere Ull-Prp Cond»
913	9	13	14.47000	77.18000	«Outer Half Inner Sphere Ull-Prp Cond»
812	8	12	17.69000	94.40000	«Inner Half Outer Sphere Ull-Prp Cond»
711	7	11	17.76000	94.70000	«Outer Half Outer Sphere Ull-Prp Cond»
815	8	15	2433.01000	1.39000	«Ullage Outer Sphere-Insulation Interface Area»
1516	15	16	1752.24000	2.70000	«Ullage Surface Area at Midpoint of Insulation»
169	16	9	1162.54000	1.39000	«Ullage Inner Sphere-Insulation Interface Area»
1217	12	17	8876.72000	2.70000	«Propellant Surface Area at Midpoint of Insulation»
1813	18	13	6449.86000	1.39000	«Propellant Inner Sphere-Insulation Interface Area»
1517	15	17	485.02000	90.02000	«Outer Half Insulation Ull-Prp Cond»
1618	16	18	439.59000	81.56000	«Inner Half Insulation Ull-Prp Cond»

ICONSF	ICS	ICF	MODEL	ARSF	HCSF	EMSFS	EMSFF	DESCRIPTION
102	10	2	0	1.12491e+03	0.00000e+00	0.00000e+00	0.00000e+00	«Ullage-Tank Wall Surface Area»
144	14	4	0	6.37194e+03	0.00000e+00	0.00000e+00	0.00000e+00	«Propellant-Tank Wall Surface Area»

ICONSA	ICSAS	ICSAA	ARSA	HCSA	EMSAS	EMSAA	DESCRIPTION
67	7	6	2.48330e+03	4.44000e-04	7.00000e-01	7.00000e-01	«Ullage Space Outer Surface of Outer Tank»
611	11	6	8.96825e+03	4.44000e-04	7.00000e-01	7.00000e-01	«Propellant Space Outer Surface of Outer Tank»

D.8 CESAT Liquid Hydrogen and Glass Bubbles Sample Output Data File

ISTEP =**** TAU = 0.56800E+05
BOUNDARY NODES

NODE	P (PSI)	TF (F)	Z (COMP)	RHO (LBM/FT^3)	QUALITY
1	0.1470E+02	0.8500E+02	0.0000E+00	0.5065E-02	0.1000E+01

3	0.1481E+02	-0.4236E+03	0.0000E+00	0.4437E+01	0.0000E+00
5	0.1470E+02	0.8500E+02	0.0000E+00	0.5065E-02	0.1000E+01

SOLUTION

INTERNAL NODES

NODE	P (PSI)	TF (F)	Z (COMP)	RHO (LBM/FT^3)	EM (LBM)	QUALITY
2	0.1470E+02	-0.4231E+03	0.9053E+00	0.8361E-01	01810E+00	0.1000E+01
4	0.1350E+02	-0.4236E+03	0.1589E-01	0.4437E+01	0.1472E+03	0.6021E-06

BRANCHES

BRANCH	KFACTOR (LBF-S^2/ (LBM-FT)^2)	DELP (PSI)	FLOW RATE (LBM/SEC)	VELOCITY (FT/SEC)	REYN. NO.	MACH NO.	ENTROPY GEN. BTU/(R-SEC)	LOST WORK LBF-FT/SEC
12	0.344E+05	-0.432E-06	-0.427E-04	-0.115E+00	0.953E+03	0.267E-04	0.113E-11	0.320E-07
34	0.000E+00	0.131E+01	0.124E-06	0.404E+00	0.581E+02	0.329E-03	0.000E+00	0.000E+00
45	0.177E+14	-0.120E+01	-0.130E-07	-0.370E+01	0.297E+01	0.302E-02	0.182E-13	0.772E-08

SOLID NODES

NODESL	CPSLD BTU/LB F	TS F
7	0.130E+00	0.699E+02
8	0.130E+00	0.699E+02
9	0.107E+00	-0.422E+03
10	0.107E+00	-0.422E+03
11	0.130E+00	0.698E+02
12	0.130E+00	0.698E+02
13	0.107E+00	-0.424E+03
14	0.107E+00	-0.424E+03
15	0.190E+00	0.157E+02
16	0.190E+00	-0.296E+03
17	0.190E+00	0.264E+01
18	0.190E+00	-0.323E+03

SOLID TO SOLID CONDUCTOR

ICONSS	CONDKIJ BTU/S FT F	QDOTSS BTU/S
78	0.310E-02	0.152E-02
910	0.255E-02	0.163E-02
1112	0.310E-02	0.686E-02
1314	0.255E-02	0.753E-02
1014	0.255E-02	0.589E-04
913	0.255E-02	0.590E-04
812	0.310E-02	0.179E-05
711	0.310E-02	0.178E-05
815	0.192E-06	0.152E-02
1516	0.960E-07	0.162E-02
169	0.192E-06	0.168E-02
1217	0.192E-06	0.686E-02
1718	0.960E-07	0.735E-02
1813	0.192E-06	0.747E-02
1517	0.960E-07	0.563E-06
1618	0.960E-07	0.114E-05

SOLID TO FLUID CONDUCTOR

ICONSF	QDOTSF	HCSF	HCSFR
	BTU/S	BTU/S FT**2 F	BTU/S FT**2 F
102	-0.158E-02	0.189E-03	0.000E+00
144	-0.759E-02	0.166E-02	0.000E+00

SOLID TO AMBIENT CONDUCTOR

ICONSA	QDOTSA	HCSA	HCSAR
	BTU/S	BTU/S FT**2 F	BTU/S FT**2 F
67	0.152E-02	0.444E-03	0.152E-03
611	0.685E-02	0.444E-03	0.152E-03

NUMBER OF PRESSURIZATION SYSTEMS = 1

NODUL	NODPRP	QULPRP	QULWAL	QCOND	TNKTM	VOLPROP	VOLULG
2	4	0.0000	0.0000	0.0000	36.0000	33.1673	2.1652

D.8.1 CESAT Liquid Hydrogen and Glass Bubbles Sample Output Plots

CESAT liquid hydrogen and glass bubbles solid node temperature predictions, ulllage and propellant path heat transfer rates, and boiloff rate output plots are shown in figures 32–34, respectively.

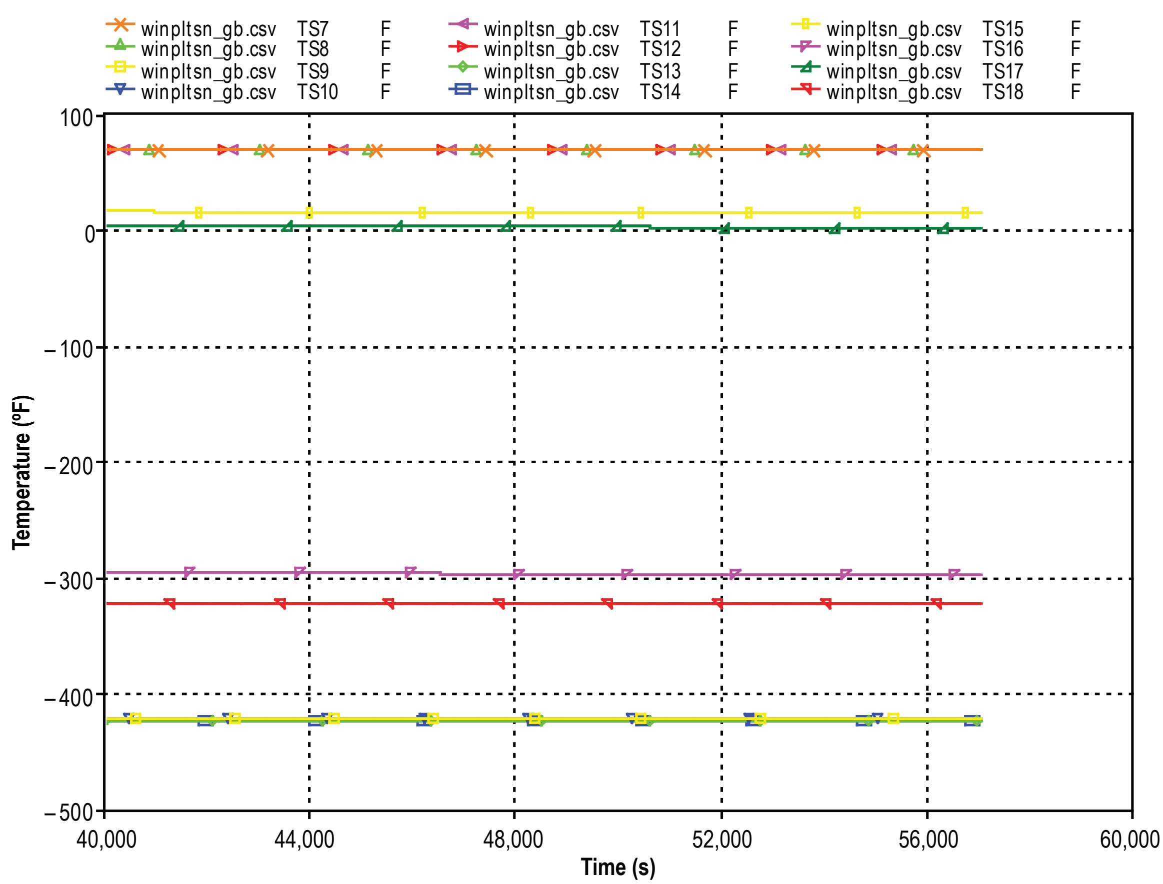

Figure 32. CESAT liquid hydrogen and glass bubbles solid node temperature predictions.

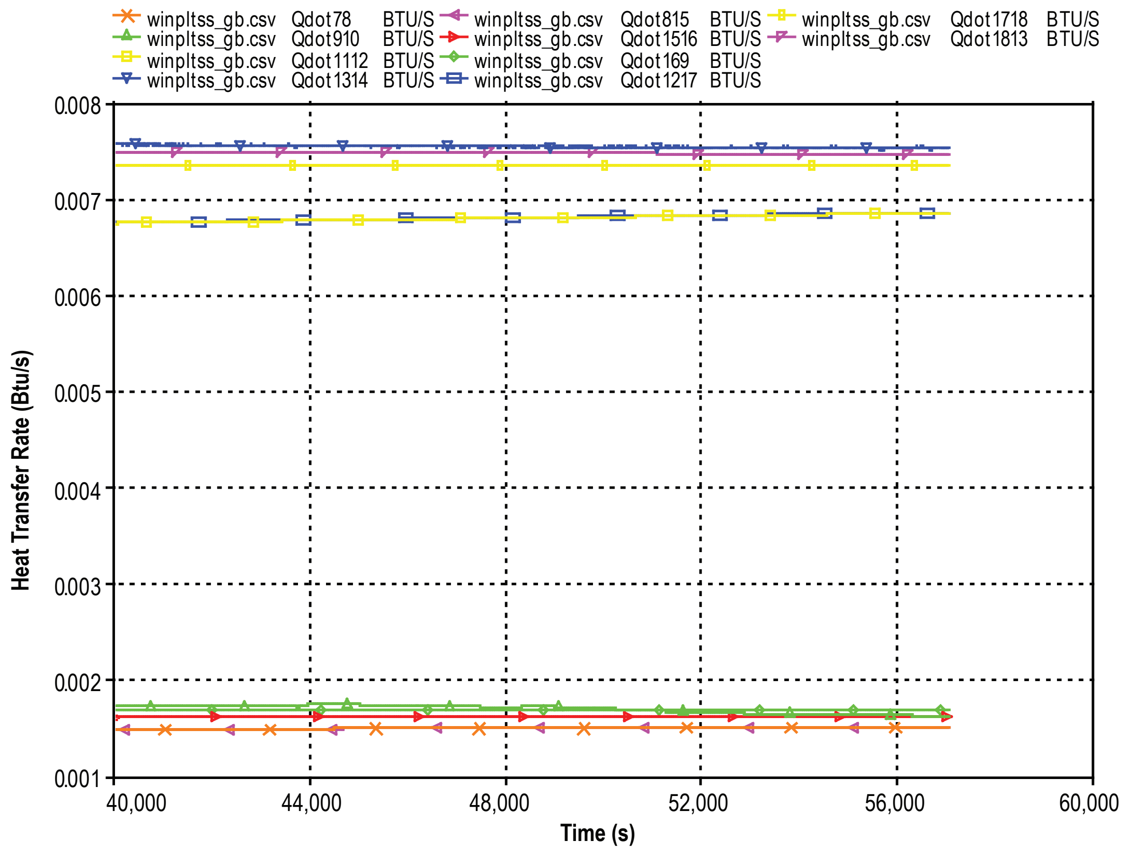

Figure 33. CESAT liquid hydrogen and glass bubbles ullage and propellant path heat transfer rates.

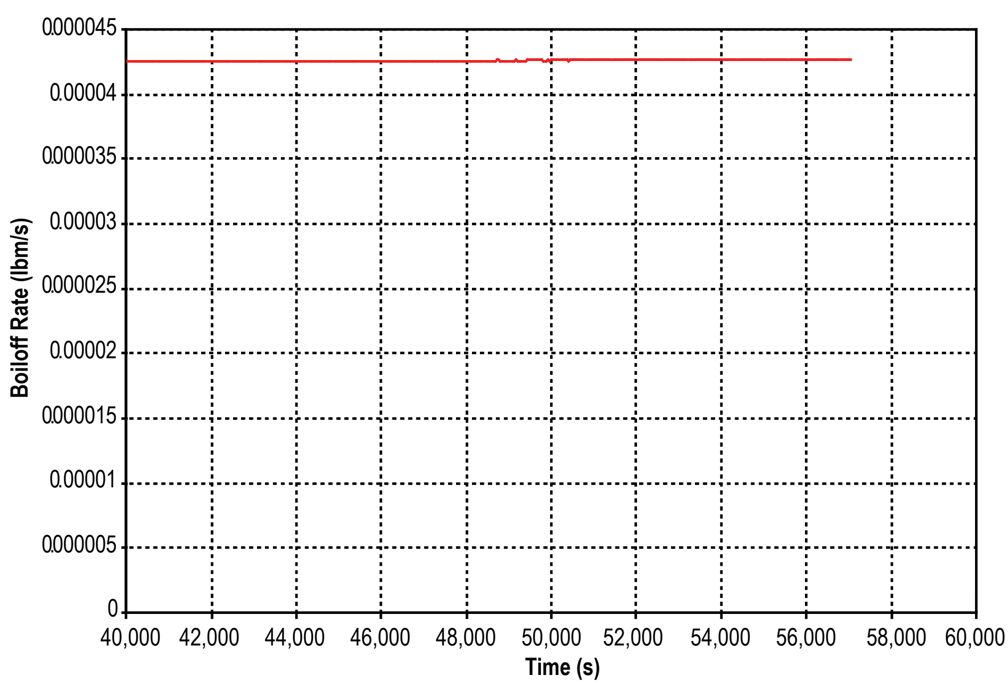

Figure 34 CESAT liquid hydrogen and glass bubbles boiloff rates.

APPENDIX E—INPUT/OUTPUT FOR FULL-SCALE TANK MODEL

E.1 LC-39 Perlite Input Data File

```
GFSSP VERSION
   500
GFSSP INSTALLATION PATH
ANALYST
   Todd Steadman
INPUT DATA FILE NAME
   D:\GFSSP\KSC LH2 Tank\New Press Mods\LC39B_LH2_perlk1c.dat
OUTPUT FILE NAME
   LC39B_LH2_perlk1c.out
TITLE
   LC-39B Liquid Hydrogen Tank - 85% Full by Height

USETUP
   F
DENCON       GRAVITY     ENERGY      MIXTURE     THRUST      STEADY      TRANSV      SAVER
   F         T           T           F           F           F           T           T
HEX          HCOEF       REACTING    INERTIA     CONDX       ADDPROP     PRINTI      ROTATION
   F         F           F           F           F           F           F           F
BUOYANCY     HRATE       INVAL       MSORCE      MOVBND      TPA         VARGEO      TVM
   T         T           T           F           F           F           F           F
SHEAR        PRNTIN      PRNTADD     OPVALVE     TRANSQ      CONJUG      RADIAT      WINPLOT
   F         F           T           F           F           T           T           T
PRESS        INSUC       VARROT      CYCLIC      CHKVALS
   T         F           F           F           T
NORMAL       SIMUL       SECONDL     NRSOLVT
   F         F           F           T
NNODES       NINT        NBR         NF
   11        9           9           1
RELAXK       RELAXD      RELAXH      CC          NITER
   1         0.5         0.01        1e-06       500
DTAU         TIMEF       TIMEL       NPSTEP
   10        0           36000       300
NFLUID(I), I = 1, NF
   10

NODE         INDEX       DESCRIPTION
   1         2           “Vent Exit (Ambient)”
   2         1           “Ullage Node 8”
   3         2           “LH2 Tank Pseudo Node”
   4         1           “LH2 Propellant Volume”
   19        1           “Ullage Node 1”
   20        1           “Ullage Node 2”
   21        1           “Ullage Node 3”
   22        1           “Ullage Node 4”
   23        1           “Ullage Node 5”
```

24	1	“Ullage Node 6”
25	1	«Ullage Node 7»

REFERENCE NODE FOR DENSITY

19

NODE	PRES (PSI)	TEMP (DEGF)	MASS SOURC	HEAT SOURC	THRST AREA	NODE-VOLUME
2	14.7	-421	0	0	0	1.5982e+06
4	16.3	-423.6	0	0	0	1.9767e+08
19	14.7	-421	0	0	0	1.5982e+06
20	14.7	-421	0	0	0	1.5982e+06
21	14.7	-421	0	0	0	1.5982e+06
22	14.7	-421	0	0	0	1.5982e+06
23	14.7	-421	0	0	0	1.5982e+06
24	14.7	-421	0	0	0	1.5982e+06
25	14.7	-421	0	0	0	1.5982e+06

ln2prsh1.dat

lh2prsh3.dat

INODE	NUMBR	NAMEBR	
2	1	252	
4	1	34	
19	2	1920	191
20	2	2021	1920
21	2	2122	2021
22	2	2223	2122
23	2	2324	2223
24	2	2425	2324
25	2	252	2425

BRANCH	UPNODE	DNNODE	OPTION	DESCRIPTION
34	3	4	2	“Propellant Surface (Pseudo Branch)”
252	25	2	1	“Pipe 252”
2425	24	25	1	“Pipe 2425”
2324	23	24	1	“Pipe 2324”
2223	22	23	1	“Pipe 2223”
2122	21	22	1	“Pipe 2122”
2021	20	21	1	«Pipe 2021»
1920	19	20	1	«Pipe 1920»
191	19	1	1	«Vent Line»

BRANCH	OPTION -2	FLOW COEFF	AREA
34		0	1e-05

BRANCH	OPTION -1	LENGTH	DIA	EPSD	ANGLE	AREA
252		7.79	511.82	0	0	2.0574e+05
BRANCH	OPTION -1	LENGTH	DIA	EPSD	ANGLE	AREA
2425		8.34	494.59	0	0	1.9212e+05
BRANCH	OPTION -1	LENGTH	DIA	EPSD	ANGLE	AREA
2324		9.07	474.71	0	0	1.7699e+05
BRANCH	OPTION -1	LENGTH	DIA	EPSD	ANGLE	AREA
2223		10.07	451.17	0	0	1.5987e+05
BRANCH	OPTION -1	LENGTH	DIA	EPSD	ANGLE	AREA
2122		11.57	422.14	0	0	1.3996e+05
BRANCH	OPTION -1	LENGTH	DIA	EPSD	ANGLE	AREA
2021		14.27	383.83	0	0	1.1571e+05
BRANCH	OPTION -1	LENGTH	DIA	EPSD	ANGLE	AREA

```
   1920                    45.81         325.3        0              0             83109
BRANCH       OPTION -1     LENGTH        DIA          EPSD           ANGLE         AREA
   191                     897           12.39        6.4568e-05     90            120.57

INITIAL FLOWRATES IN BRANCHES FOR UNSTEADY FLOW
         34      0.0001
         252     0
         2425    0
         2324    0
         2223    0
         2122    0
         2021    0
         1920    0
         191     0.0001

NUMBER OF PRESSURIZATION PROPELLANT TANKS IN CIRCUIT
   1
TNKTYPE    NODUL    NODULB    NODPRP    IBRPRP    TNKAR         TNKTH     TNKRHO    TNKCP
   0       2        3         4         34        2.5666e+05    0.625     467       0.07
TNKCON     ARHC          FCTHC      TNKTM
0.0017     2.1816e+05    0.00265    -423.6
RESTART NODE INFORMATION FILE
   FNDLC39B.DAT
RESTART BRANCH INFORMATION FILE
   FBRLC39B.DAT
NSOLID    NAMB      NSSC      NSFC      NSAC      NSSR
   54     1         93        9         9         0

NODESL  MATRL SMASS        TS            NUMSS    NUMSF   NUMSA   NUMSSR  DESCRIPTION
   7      44    1933.78000   85.00000        3        0       1        0       «Sec 8 OS Outer»
NAMESS
   78     711     677
NAMESA
   67
   8      44    1933.78000   85.00000        4        0       0        0       «Sec 7 OS Inner»
NAMESS
   78     812     815      668
   9      29    1477.42000   -417.00000      4        0       0        0       «Sec 8 IS Outer»
NAMESS
   910    913     169      639
   10     29    1477.42000   -418.00000      3        1       0        0       «Sec 8 IS Inner»
NAMESS
   910    1014    6210
NAMESF
   102
   11     44    173893.00000      85.00000   2        0       1        0       «Outer Half of Propellant
                                                                                   Outer Tank Wall
NAMESS
   1112   711
NAMESA
   611
   12     44    173893.00000   85.00000      3        0       0        0       «Inner Half of  Propellant
                                                                                   Outer Tank Wall»
```

```
NAMESS
   1112     812      1217
   13       29       122995.00000   -423.60000  3      0      0      0      «Outer Half of Propellant
                                                                                TankWall»
NAMESS
   1314     913      1813
   14       29       122995.00000   -423.60000  2      1      0      0      «Inner Half of Propellant
                                                                                Tank Wall»
NAMESS
   1314     1014
NAMESF
   144
   15       42       1677.20000     28.00000    4      0      0      0      «Sec 8 Ins Outer»
NAMESS
   815      1516     1517           6515
   16       42       1677.20000     -294.00000  4      0      0      0      «Sec 8 Ins Inner»
NAMESS
   1516     169      1618           6416
   17       42       145333.00000   14.00000    3      0      0      0      «Outer Half of Propellant
                                                                                Insulation»
NAMESS
   1217     1718     1517
   18       42       145333.00000   -324.00000  3      0      0      0      «Inner Half of Propellant
                                                                                Insulation»
NAMESS
   1718     1813     1618
   26       29       7195.20000     -408.00000  2      1      0      0      «Sec 1 IS Inner»
NAMESS
   2726     2632
NAMESF
   2619
   27       29       7195.20000     -408.00000  3      0      0      0      «Sec 1 IS Outer»
NAMESS
   2726     2827     2733
   28       42       14186.60000    -294.00000  3      0      0      0      «Sec 1 Ins Inner»
NAMESS
   2827     2928     2834
   29       42       14186.60000    28.00000    3      0      0      0      «Sec 1 Ins Outer»
NAMESS
   2928     3029     2935
   30       44       22683.70000    85.00000    3      0      0      0      «Sec 1 OS Inner»
NAMESS
   3029     3130     3036
   31       44       22683.70000    85.00000    2      0      1      0      «Sec 1 OS Outer»
NAMESS
   3130     3137
NAMESA
   631
   32       29       3146.34000     -409.00000  3      1      0      0      «Sec 2 IS Inner»
NAMESS
   3332     2632     3238
NAMESF
   3220
   33       29       3146.34000     -409.00000  4      0      0      0      «Sec 2 IS Outer»
```

```
NAMESS
   3332    3433    2733           3339
   34      42      3571.61000     -294.00000  4    0    0    0    «Sec 2 Ins Inner»
NAMESS
   3433    3534    2834           3440
   35      42      3571.61000     28.00000    4    0    0    0    «Sec 2 Ins Outer»
NAMESS
   3534    3635    2935           3541
   36      44      4117.99000     85.00000    4    0    0    0    «Sec 2 OS Inner»
NAMESS
   3635    3736    3036           3642
   37      44      4117.99000     85.00000    3    0    1    0    «Sec 2 OS Outer»
NAMESS
   3736    3137    3743
NAMESA
   637
  38       29      2448.33000     -410.00000  3    1    0    0    «Sec 3 IS Inner»
NAMESS
   3938    3238    3844
NAMESF
   3821
   39      29      2448.33000     -410.00000  4    0    0    0    «Sec 3 IS Outer»
NAMESS
   3938    4039    3339           3945
   40      42      2779.40000     -294.00000  4    0    0    0    «Sec 3 Ins Inner»
NAMESS
   4039    4140    3440           4046
   41      42      2779.40000     28.00000    4    0    0    0    «Sec 3 Ins Outer»
NAMESS
   4140    4241    3541           4147
   42      44      3204.60000     85.00000    4    0    0    0    «Sec 3 OS Inner»
NAMESS
   4241    4342    3642           4248
   43      44      3204.60000     85.00000    3    0    1    0    «Sec 3 OS Outer»
NAMESS
   4342    3743    4349
NAMESA
   643
   44      29      2088.37000     -411.00000  3    1    0    0    «Sec 4 IS Inner»
NAMESS
   4544    3844    4450
NAMESF
   4422
   45      29      2088.37000     -411.00000  4    0    0    0    «Sec 4 IS Outer»
   4544    4645    3945           4551
   46      42      2370.63000     -294.00000  4    0    0    0    «Sec 4 Ins Inner»
NAMESS
   4645    4746    4046           4652
   47      42      2370.63000     28.00000    4    0    0    0    «Sec 4 Ins Outer»
NAMESS
   4746    4847    4147           4753
   48      44      2733.29000     85.00000    4    0    0    0    «Sec 4 OS Inner»
NAMESS
   4847    4948    4248           4854
```

49	44	2733.29000	85.00000	3	0	1	0	«Sec 4 OS Outer»
NAMESS								
4948	4349	4955						
NAMESA								
649								
50	29	1859.02000	-412.00000	3	1	0	0	«Sec 5 IS Inner»
NAMESS								
5150	4450	5056						
NAMESF								
5023								
51	29	1859.02000	-412.00000	4	0	0	0	«Sec 5 IS Outer»
NAMESS								
5150	5251	4551	5157					
52	42	2110.28000	-294.00000	4	0	0	0	«Sec 5 Ins Inner»
NAMESS								
5251	5352	4652	5258					
53	42	2110.28000	28.00000	4	0	0	0	«Sec 5 Ins Outer»
NAMESS								
5352	5453	4753	5359					
54	44	2433.11000	85.00000	4	0	0	0	«Sec 5 OS Inner»
NAMESS								
5453	5554	4854	5460					
55	44	2433.11000	85.00000	3	0	1	0	«Sec 5 OS Outer»
NAMESS								
5554	4955	5561						
NAMESA								
655								
56	29	1696.69000	-413.00000	3	1	0	0	«Sec 6 IS Inner»
NAMESS								
5756	5056	5662						
NAMESF								
5624								
57	29	1696.69000	-413.00000	4	0	0	0	«Sec 6 IS Outer»
NAMESS								
5756	5857	5157	5763					
58	42	1926.00000	-294.00000	4	0	0	0	«Sec 6 Ins Inner»
NAMESS								
5857	5958	5258	5864					
59	42	1926.00000	28.00000	4	0	0	0	«Sec 6 Ins Outer»
NAMESS								
5958	6059	5359	5965					
60	44	2220.64000	85.00000	4	0	0	0	«Sec 6 OS Inner»
NAMESS								
6059	6160	5460	6066					
61	44	2220.64000	85.00000	3	0	1	0	«Sec 6 OS Outer»
NAMESS								
6160	5561	6167						
NAMESA								
661								
62	29	1574.14000	-414.00000	3	1	0	0	«Sec 7 IS Inner»
NAMESS								
6362	5662	6210						
NAMESF								
6225								

63	29	1574.14000	-414.00000	4	0	0	0	«Sec 7 IS Outer»
NAMESS								
6362	6463	5763	639					
64	42	1786.89000	-294.00000	4	0	0	0	«Sec 7 Ins Inner»
NAMESS								
6463	6564	5864	6416					
65	42	1786.89000	28.00000	4	0	0	0	«Sec 7 Ins Outer»
NAMESS								
6564	6665	5965	6515					
66	44	2060.25000	85.00000	4	0	0	0	«Sec 7 OS Inner»
NAMESS								
6665	6766	6066	668					
67	44	2060.25000	85.00000	3	0	1	0	«Sec 7 OS Outer»
NAMESS								
6766	6167	677						
NAMESA								
667								

NODEAM	TAMB	DESCRIPTION
6	85.00000	«Ambient Condition»

ICONSS	ICNSI	ICNSJ	ARCSIJ	DISTSIJ	DESCRIPTION
78	7	8	19879.20000	0.34000	«Sec 8 OS In-Out Conduction»
910	9	10	17494.40000	0.31000	«Sec 8 IS In-Out Conduction»
1112	11	12	1787620.00000	0.34000	«Propellant Surface Area at Midpoint of Outer Tank Wall»
1314	13	14	1456350.00000	0.31000	«Propellant Surface Area at Midpoint of Tank Wall»
1014	10	14	724.84000	5.34857	«Sec 8-Prp IS Inner»
913	9	13	725.45000	5.35309	«Sec 8-Prp IS Outer»
812	8	12	906.02100	6.07775	«Sec 8-Prp OS Inner»
711	7	11	906.76400	6.08273	«Sec 8-Prp OS Outer»
815	8	15	19862.90000	12.59000	«Sec 8 Ins-OS Conduction»
1516	15	16	18686.10000	24.84000	«Sec 8 Ins In-Out Conduction»
169	16	9	17509.20000	12.58000	«Sec 8 IS-Ins Conduction»
1217	12	17	1785250.00000	12.59000	«Propellant Outer Sphere-Insulation Interface Area»
1718	17	18	1617900.00000	24.84000	«Propellant Surface Area at Midpoint of Insulation»
1813	18	13	1458310.00000	12.58000	«Propellant Inner Sphere-Insulation Interface Area»
1517	15	17	63514.80000	5.89529	«Sec 8-Prp Ins Outer»
1618	16	18	59636.70000	5.53533	«Sec 8-Prp Ins Inner»
2726	27	26	88392.50000	0.31000	«Sec 1 IS In-Out Conduction»
2827	28	27	89193.00000	12.58000	«Sec 1 IS-Ins Conduction»
2928	29	28	156764.00000	24.84000	«Sec 1 Ins In-Out Conduction»
3029	30	29	232091.00000	12.59000	«Sec 1 Ins-OS Conduction»
3130	31	30	233187.00000	0.34000	«Sec 1 OS In-Out Conduction»
3332	33	32	37254.40000	0.31000	«Sec 2 IS In-Out Conduction»
3433	34	33	37286.00000	12.58000	«Sec 2 IS-Ins Conduction»
3534	35	34	39792.10000	24.84000	«Sec 2 Ins In-Out Conduction»
3635	36	35	42298.20000	12.59000	«Sec 2 Ins-OS Conduction»
3736	37	36	42332.90000	0.34000	«Sec 2 OS In-Out Conduction»
3938	39	38	28991.20000	0.31000	«Sec 3 IS In-Out Conduction»
4039	40	39	29015.70000	12.58000	«Sec 3 IS-Ins Conduction»
4140	41	40	30966.00000	24.84000	«Sec 3 Ins In-Out Conduction»
4241	42	41	32916.20000	12.59000	«Sec 3 Ins-OS Conduction»
4342	43	42	32943.20000	0.34000	«Sec 3 OS In-Out Conduction»
4544	45	44	24727.40000	0.31000	«Sec 4 IS In-Out Conduction»

4645	46	45	24748.30000	12.58000	«Sec 4 IS-Ins Conduction»
4746	47	46	26411.80000	24.84000	«Sec 4 Ins In-Out Conduction»
4847	48	47	28075.20000	12.59000	«Sec 4 Ins-OS Conduction»
4948	49	48	28098.20000	0.34000	«Sec 4 OS In-Out Conduction»
5150	51	50	22011.70000	0.31000	«Sec 5 IS In-Out Conduction»
5251	52	51	22030.40000	12.58000	«Sec 5 IS-Ins Conduction»
5352	53	52	23511.10000	24.84000	«Sec 5 Ins In-Out Conduction»
5453	54	53	24991.80000	12.59000	«Sec 5 Ins-OS Conduction»
5554	55	54	25012.30000	0.34000	«Sec 5 OS In-Out Conduction»
5756	57	56	20089.60000	0.31000	«Sec 6 IS In-Out Conduction»
5857	58	57	20106.60000	12.58000	«Sec 6 IS-Ins Conduction»
5958	59	58	21458.00000	24.84000	«Sec 6 Ins In-Out Conduction»
6059	60	59	22809.50000	12.59000	«Sec 6 Ins-OS Conduction»
6160	61	60	22828.20000	0.34000	«Sec 6 OS In-Out Conduction»
6362	63	62	18638.60000	0.31000	«Sec 7 IS In-Out Conduction»
6463	64	63	18654.40000	12.58000	«Sec 7 IS-Ins Conduction»
6564	65	64	19908.20000	24.84000	«Sec 7 Ins In-Out Conduction»
6665	66	65	21162.00000	12.59000	«Sec 7 Ins-OS Conduction»
6766	67	66	21179.40000	0.34000	«Sec 7 OS In-Out Conduction»
2632	26	32	724.83700	185.78600	«Sec 1-2 IS Inner»
3238	32	38	724.83700	28.05150	«Sec 2-3 IS Inner»
3844	38	44	724.83700	20.39420	«Sec 3-4 IS Inner»
4450	44	50	724.83700	16.53240	«Sec 4-5 IS Inner»
5056	50	56	724.83700	14.12770	«Sec 5-6 IS Inner»
5662	56	62	724.83700	12.46210	«Sec 6-7 IS Inner»
6210	62	10	724.83700	11.22990	«Sec 7-8 IS Inner»
2733	27	33	725.45000	185.94300	«Sec 1-2 IS Outer»
3339	33	39	725.45000	28.07530	«Sec 2-3 IS Outer»
3945	39	45	725.45000	20.41150	«Sec 3-4 IS Outer»
4551	45	51	725.45000	16.54640	«Sec 4-5 IS Outer»
5157	51	57	725.45000	14.13970	«Sec 5-6 IS Outer»
5763	57	63	725.45000	12.47270	«Sec 6-7 IS Outer»
639	63	9	725.45000	11.23940	«Sec 7-8 IS Outer»
2834	28	34	59636.70000	192.27400	«Sec 1-2 Ins Inner»
3440	34	40	59636.70000	29.03110	«Sec 2-3 Ins Inner»
4046	40	46	59636.70000	21.10640	«Sec 3-4 Ins Inner»
4652	46	52	59636.70000	17.10970	«Sec 4-5 Ins Inner»
5258	52	58	59636.70000	14.62110	«Sec 5-6 Ins Inner»
5864	58	64	59636.70000	12.89730	«Sec 6-7 Ins Inner»
6416	64	16	59636.70000	11.62200	“Sec 7-8 Ins Inner”
2935	29	35	63514.80000	204.77700	“Sec 1-2 Ins Outer”
3541	35	41	63514.80000	30.91890	«Sec 2-3 Ins Outer»
4147	41	47	63514.80000	22.47890	«Sec 3-4 Ins Outer»
4753	47	53	63514.80000	18.22230	«Sec 4-5 Ins Outer»
5359	53	59	63514.80000	15.57180	«Sec 5-6 Ins Outer»
5965	59	65	63514.80000	13.73600	«Sec 6-7 Ins Outer»
6515	65	15	63514.80000	12.37780	«Sec 7-8 Ins Outer»
3036	30	36	906.02100	211.11500	«Sec 1-2 OS Inner»
3642	36	42	906.02100	31.87590	«Sec 2-3 OS Inner»
4248	42	48	906.02100	23.17460	«Sec 3-4 OS Inner»
4854	48	54	906.02100	18.78630	«Sec 4-5 OS Inner»
5460	54	60	906.02100	16.05380	«Sec 5-6 OS Inner»
6066	60	66	906.02100	14.16110	«Sec 6-7 OS Inner»
668	66	8	906.02100	12.76090	«Sec 7-8 OS Inner»

3137	31	37	906.76400	211.28800	«Sec 1-2 OS Outer»
3743	37	43	906.76400	31.90200	«Sec 2-3 OS Outer»
4349	43	49	906.76400	23.19360	«Sec 3-4 OS Outer»
4955	49	55	906.76400	18.80170	"Sec 4-5 OS Outer"
5561	55	61	906.76400	16.06700	"Sec 5-6 OS Outer"
6167	61	67	906.76400	14.17270	"Sec 6-7 OS Outer"
677	67	7	906.76400	12.77140	"Sec 7-8 OS Outer"

ICONSF	ICS	ICF	MODEL	ARSF	HCSF	EMSFS	EMSFF	DESCRIPTION
102	10	2	0	1.74796e+04	1.00000e+00	0.00000e+00	0.00000e+00	«Sec 8 IS Ullage Wall»
144	14	4	0	1.45439e+06	0.00000e+00	0.00000e+00	0.00000e+00	«Propellant-Tank Wall Surface Area»
2619	26	19	0	8.75930e+04	1.00000e+00	0.00000e+00	0.00000e+00	«Sec 1 IS Ullage Wall»
3220	32	20	0	3.72229e+04	1.00000e+00	0.00000e+00	0.00000e+00	«Sec 2 IS Ullage Wall»
3821	38	21	0	2.89667e+04	1.00000e+00	0.00000e+00	0.00000e+00	«Sec 3 IS Ullage Wall»
4422	44	22	0	2.47065e+04	1.00000e+00	0.00000e+00	0.00000e+00	«Sec 4 IS Ullage Wall»
5023	50	23	0	2.19931e+04	1.00000e+00	0.00000e+00	0.00000e+00	«Sec 5 IS Ullage Wall»
5624	56	24	0	2.00726e+04	1.00000e+00	0.00000e+00	0.00000e+00	«Sec 6 IS Ullage Wall»
6225	62	25	0	1.86228e+04	1.00000e+00	0.00000e+00	0.00000e+00	«Sec 7 IS Ullage Wall»

ICONSA	ICSAS	ICSAA	ARSA	HCSA	EMSAS	EMSAA	DESCRIPTION
67	7	6	1.98955e+04	4.44000e-04	7.00000e-01	7.00000e-01	"Sec 8 OS-Amb Convection"
611	11	6	1.78999e+06	4.44000e-04	7.00000e-01	7.00000e-01	"Propellant Space Outer Surface of Outer Tank"
631	31	6	2.34285e+05	4.44000e-04	7.00000e-01	7.00000e-01	"Sec 1 OS-Amb Convection"
637	37	6	4.23676e+04	4.44000e-04	7.00000e-01	7.00000e-01	"Sec 2 OS-Amb Convection"
643	43	6	3.29702e+04	4.44000e-04	7.00000e-01	7.00000e-01	"Sec 3 OS-Amb Convection"
649	49	6	2.81212e+04	4.44000e-04	7.00000e-01	7.00000e-01	"Sec 4 OS-Amb Convection"
655	55	6	2.50328e+04	0.44000e-04	7.00000e-01	7.00000e-01	"Sec 5 OS-Amb Convection"
661	61	6	2.28469e+04	4.44000e-04	7.00000e-01	7.00000e-01	"Sec 6 OS-Amb Convection"
667	67	6	2.11967e+04	4.44000e-04	7.00000e-01	7.00000e-01	"Sec 7 OS-Amb Convection"

E.2 LC-39 Perlite Sample Output Data File

ISTEP =1800 TAU = 0.18000E+05

BOUNDARY NODES

NODE	P (PSI)	TF (F)	Z (COMP)	RHO (LBM/FT^3)	QUALITY
1	0.1470E+02	0.8500E+02	0.0000E+00	0.5065E-02	0.1000E+01
3	0.1631E+02	-0.4236E+03	0.0000E+00	0.4437E+01	0.0000E+00

SOLUTION

INTERNAL NODES

NODE	P (PSI)	TF (F)	Z (COMP)	RHO (LBM/FT^3)	EM (LBM)	QUALITY
2	0.1470E+02	-0.4231E+03	0.5835E+00	0.1297E+00	0.1200E+03	0.6378E+00
4	0.1344E+02	-0.4237E+03	0.1583E-01	0.4439E+01	0.5077E+06	0.6524E-07
19	0.1470E+02	-0.3259E+03	0.9988E+00	0.2068E-01	0.1913E+02	0.1000E+01
20	0.1470E+02	-0.3742E+03	0.9913E+00	0.3262E-01	0.3017E+02	0.1000E+01
21	0.1470E+02	-0.3856E+03	0.9863E+00	0.3782E-01	0.3498E+02	0.1000E+01
22	0.1470E+02	-0.3956E+03	0.9791E+00	0.4409E-01	0.4078E+02	0.1000E+01
23	0.1470E+02	-0.4049E+03	0.9677E+00	0.5216E-01	0.4824E+02	0.1000E+01
24	0.1470E+02	-0.4136E+03	0.9487E+00	0.6323E-01	0.5848E+02	0.1000E+01
25	0.1470E+02	-0.4231E+03	0.9056E+00	0.8349E-01	0.7721E+02	0.1000E+01

NODE	H	ENTROPY	EMU	COND	CP	GAMA
	BTU/LB	BTU/LB-R	LBM/FT-SEC	BTU/FT-S-R	BTU/LB-R	
2	0.1277E+02	0.7340E+01	0.1135E-05	0.7419E-05	0.2606E+01	0.1821E+01
4	-0.1106E+03	0.1907E+01	0.9181E-05	0.1579E-04	0.2250E+01	0.1698E+01
19	0.3333E+03	0.7340E+01	0.2280E-05	0.8964E-05	0.2734E+01	0.1576E+01
20	0.2085E+03	0.7340E+01	0.1610E-05	0.5781E-05	0.2505E+01	0.1691E+01
21	0.1799E+03	0.7340E+01	0.1431E-05	0.5075E-05	0.2529E+01	0.1698E+01
22	0.1544E+03	0.7340E+01	0.1264E-05	0.4449E-05	0.2549E+01	0.1714E+01
23	0.1306E+03	0.7340E+01	0.1103E-05	0.3877E-05	0.2586E+01	0.1736E+01
24	0.1080E+03	0.7340E+01	0.9434E-06	0.3280E-05	0.2647E+01	0.1776E+01
25	0.8222E+02	0.7340E+01	0.7594E-06	0.2617E-05	0.2791E+01	0.1874E+01

BRANCHES

BRANCH	KFACTOR	DELP	LOW RATE	VELOCITY	REYN. NO.	MACH NO.	ENTROPY GEN.	LOST WORK
	(LBF-S^2/ (LBM-FT)^2)	(PSI)	(LBM/SEC)	(FT/SEC)			BTU/(R-SEC)	LBF-FT/SEC
34	0.000E+00	0.287E+01	0.173E-10	0.561E-04	0.807E-02	0.457E-07	0.000E+00	0.000E+00
252	0.000E+00	0.410E-03	-0.172E-02	-0.929E-05	0.453E+02	0.715E-08	0.000E+00	0.000E+00
2425	0.000E+00	0.272E-03	-0.167E-02	-0.150E-04	0.679E+02	0.106E-07	0.000E+00	0.000E+00
2324	0.000E+00	0.211E-03	-0.164E-02	-0.211E-04	0.560E+02	0.138E-07	0.000E+00	0.000E+00
2223	0.000E+00	0.177E-03	-0.161E-02	-0.279E-04	0.495E+02	0.169E-07	0.000E+00	0.000E+00
2122	0.000E+00	0.155E-03	-0.159E-02	-0.370E-04	0.454E+02	0.210E-07	0.000E+00	0.000E+00
2021	0.000E+00	0.145E-03	-0.156E-02	-0.514E-04	0.434E+02	0.272E-07	0.000E+00	0.000E+00
1920	0.000E+00	0.220E-03	-0.154E-02	-0.815E-04	0.448E+02	0.358E-07	0.000E+00	0.000E+00
191	0.609E+01	-0.110E-05	0.151E-02	0.871E-01	0.816E+03	0.382E-04	0.971E-11	0.101E-05

SOLID NODES

NODESL	CPSLD	TS
	BTU/LB F	F
7	0.110E+00	0.850E+02
8	0.110E+00	0.850E+02
9	0.690E-01	-0.423E+03
10	0.690E-01	-0.423E+03
11	0.110E+00	0.850E+02
12	0.110E+00	0.850E+02
13	0.690E-01	-0.424E+03
14	0.690E-01	-0.424E+03
15	0.200E+00	0.257E+02
16	0.200E+00	-0.299E+03
17	0.200E+00	0.138E+02
18	0.200E+00	-0.324E+03
26	0.690E-01	-0.323E+03
27	0.690E-01	-0.323E+03
28	0.200E+00	-0.291E+03
29	0.200E+00	0.281E+02
30	0.110E+00	0.850E+02
31	0.110E+00	0.850E+02
32	0.690E-01	-0.374E+03
33	0.690E-01	-0.374E+03
34	0.200E+00	-0.293E+03
35	0.200E+00	0.273E+02
36	0.110E+00	0.850E+02
37	0.110E+00	0.850E+02
38	0.690E-01	-0.385E+03

39	0.690E-01	-0.385E+03
40	0.200E+00	-0.294E+03
41	0.200E+00	0.273E+02
42	0.110E+00	0.850E+02
43	0.110E+00	0.850E+02
44	0.690E-01	-0.395E+03
45	0.690E-01	-0.395E+03
46	0.200E+00	-0.294E+03
47	0.200E+00	0.273E+02
48	0.110E+00	0.850E+02
49	0.110E+00	0.850E+02
50	0.690E-01	-0.405E+03
51	0.690E-01	-0.405E+03
52	0.200E+00	-0.295E+03
53	0.200E+00	0.273E+02
54	0.110E+00	0.850E+02
55	0.110E+00	0.850E+02
56	0.690E-01	-0.413E+03
57	0.690E-01	-0.413E+03
58	0.200E+00	-0.295E+03
59	0.200E+00	0.273E+02
60	0.110E+00	0.850E+02
61	0.110E+00	0.850E+02
62	0.690E-01	-0.420E+03
63	0.690E-01	-0.420E+03
64	0.200E+00	-0.295E+03
65	0.200E+00	0.272E+02
67	0.110E+00	0.850E+02

SOLID TO SOLID CONDUCTOR

ICONSS	CONDKIJ BTU/S FT F	QDOTSS BTU/S
78	0.750E-02	0.265E-02
910	0.167E-02	0.919E-02
1112	0.750E-02	0.271E+00
1314	0.167E-02	0.326E+00
1014	0.167E-02	0.165E-01
913	0.167E-02	0.165E-01
812	0.750E-02	0.247E-03
711	0.750E-02	0.246E-03
815	0.322E-06	0.251E-02
1516	0.161E-06	0.327E-02
169	0.322E-06	0.463E-02
1217	0.322E-06	0.271E+00
1718	0.161E-06	0.295E+00
1813	0.322E-06	0.310E+00
1517	0.161E-06	0.172E-02
1618	0.161E-06	0.367E-02
2726	0.167E-02	0.797E-01
2827	0.322E-06	0.610E-02
2928	0.161E-06	0.270E-01
3029	0.322E-06	0.281E-01
3130	0.750E-02	0.281E-01
3332	0.167E-02	0.873E-02

3433	0.322E-06	0.638E-02
3534	0.161E-06	0.689E-02
3635	0.322E-06	0.520E-02
3736	0.750E-02	0.520E-02
3938	0.167E-02	0.635E-02
4039	0.322E-06	0.564E-02
4140	0.161E-06	0.537E-02
4241	0.322E-06	0.405E-02
4342	0.750E-02	0.405E-02
4544	0.167E-02	0.518E-02
4645	0.322E-06	0.533E-02
4746	0.161E-06	0.459E-02
4847	0.322E-06	0.345E-02
4948	0.750E-02	0.346E-02
5150	0.167E-02	0.525E-02
5251	0.322E-06	0.516E-02
5352	0.161E-06	0.409E-02
5453	0.322E-06	0.307E-02
5554	0.750E-02	0.308E-02
5756	0.167E-02	0.775E-02
5857	0.322E-06	0.506E-02
5958	0.161E-06	0.373E-02
6059	0.322E-06	0.281E-02
6160	0.750E-02	0.283E-02
6362	0.167E-02	0.460E-01
6463	0.322E-06	0.498E-02
6564	0.161E-06	0.347E-02
6665	0.322E-06	0.260E-02
6766	0.750E-02	0.267E-02
2632	0.167E-02	0.272E-01
3238	0.167E-02	0.413E-01
3844	0.167E-02	0.501E-01
4450	0.167E-02	0.563E-01
5056	0.167E-02	0.603E-01
5662	0.167E-02	0.602E-01
6210	0.167E-02	0.207E-01
2733	0.167E-02	0.272E-01
3339	0.167E-02	0.413E-01
3945	0.167E-02	0.501E-01
4551	0.167E-02	0.563E-01
5157	0.167E-02	0.603E-01
5763	0.167E-02	0.602E-01
639	0.167E-02	0.208E-01
2834	0.161E-06	0.866E-05
3440	0.161E-06	0.138E-04
4046	0.161E-06	0.149E-04
4652	0.161E-06	0.151E-04
5258	0.161E-06	0.157E-04
5864	0.161E-06	0.220E-04
6416	0.161E-06	0.238E-03
3541	0.161E-06	0.861E-07
4147	0.161E-06	0.676E-07
4753	0.161E-06	0.651E-07
5359	0.161E-06	0.106E-06

5965	0.161E-06	0.289E-05
6515	0.161E-06	0.107E-03
3036	0.750E-02	0.166E-05
4248	0.750E-02	0.394E-05
5460	0.750E-02	0.134E-04
6066	0.750E-02	0.405E-04
668	0.750E-02	0.110E-03
3137	0.750E-02	0.166E-05
3743	0.750E-02	0.421E-06
4349	0.750E-02	0.101E-05
4955	0.750E-02	0.393E-05
5561	0.750E-02	0.134E-04
6167	0.750E-02	0.404E-04
677	0.750E-02	0.110E-03

SOLID TO FLUID CONDUCTOR

ICONSF	QDOTSF	HCSF	HCSFR
	BTU/S	BTU/S FT**2 F	BTU/S FT**2 F
102	-0.137E-01	0.307E-03	0.000E+00
2619	-0.153E+00	0.102E-03	0.000E+00
3220	-0.111E-01	0.788E-04	0.000E+00
3821	-0.705E-02	0.808E-04	0.000E+00
4422	-0.503E-02	0.836E-04	0.000E+00
5023	-0.533E-02	0.956E-04	0.000E+00
5624	-0.870E-01	0.255E-03	0.000E+00

SOLID TO AMBIENT CONDUCTOR

ICONSA	QDOTSA	HCSA	HCSAR
	BTU/S	BTU/S FT**2 F	BTU/S FT**2 F
67	0.278E-02	0.444E-03	0.166E-03
611	0.270E+00	0.444E-03	0.166E-03
631	0.281E-01	0.444E-03	0.166E-03
637	0.520E-02	0.444E-03	0.166E-03
643	0.405E-02	0.444E-03	0.166E-03
649	0.346E-02	0.444E-03	0.166E-03
655	0.309E-02	0.444E-03	0.166E-03
661	0.286E-02	0.444E-03	0.166E-03
667	-0.461E-01	0.444E-03	0.166E-03

NUMBER OF PRESSURIZATION SYSTEMS = 1

NODUL	NODPRP	QULPRP	QULWAL	QCOND	TNKTM	VOLPROP	VOLULG
2	4	0.0003	0.0000	0.0000	36.0000	**********	924.8683

E.2.1 LC-39 Perlite Sample Output Plots

LC-39 perlite propellant path solid node temperature prediction, ullage inner sphere solid node temperature prediction, propellant path heat transfer rates, and boiloff rate output plots are shown in figures 35–38, respectively.

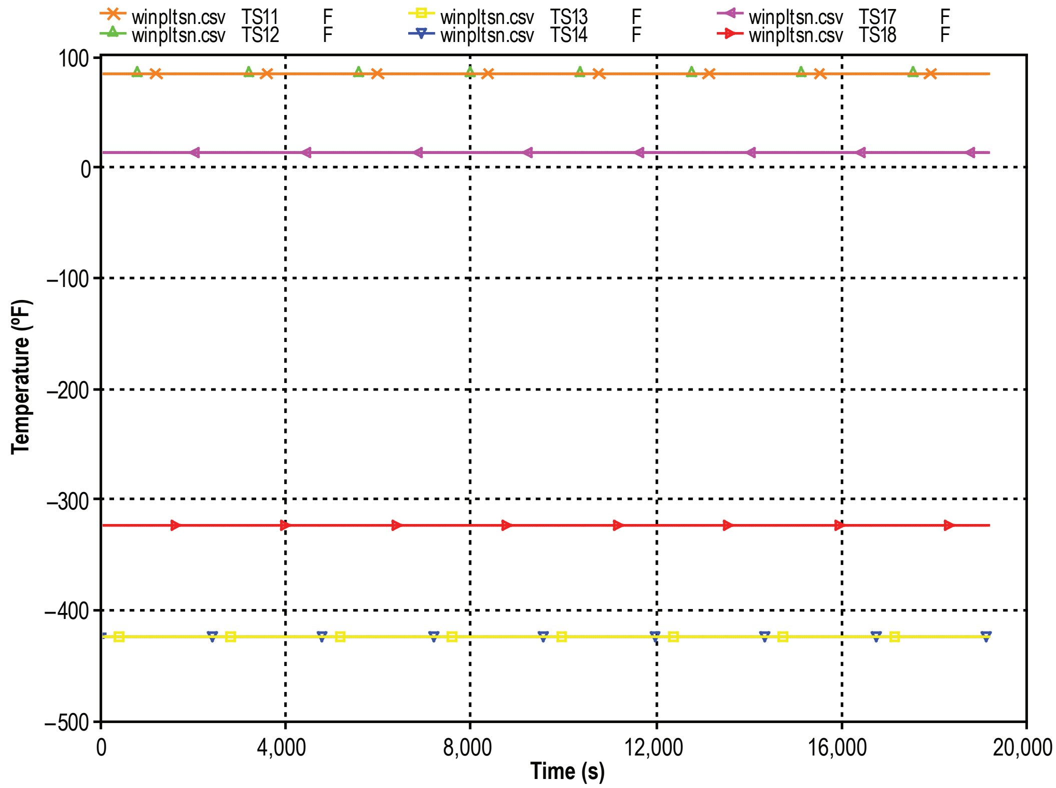

Figure 35. LC-39 perlite propellant path solid node temperature predictions.

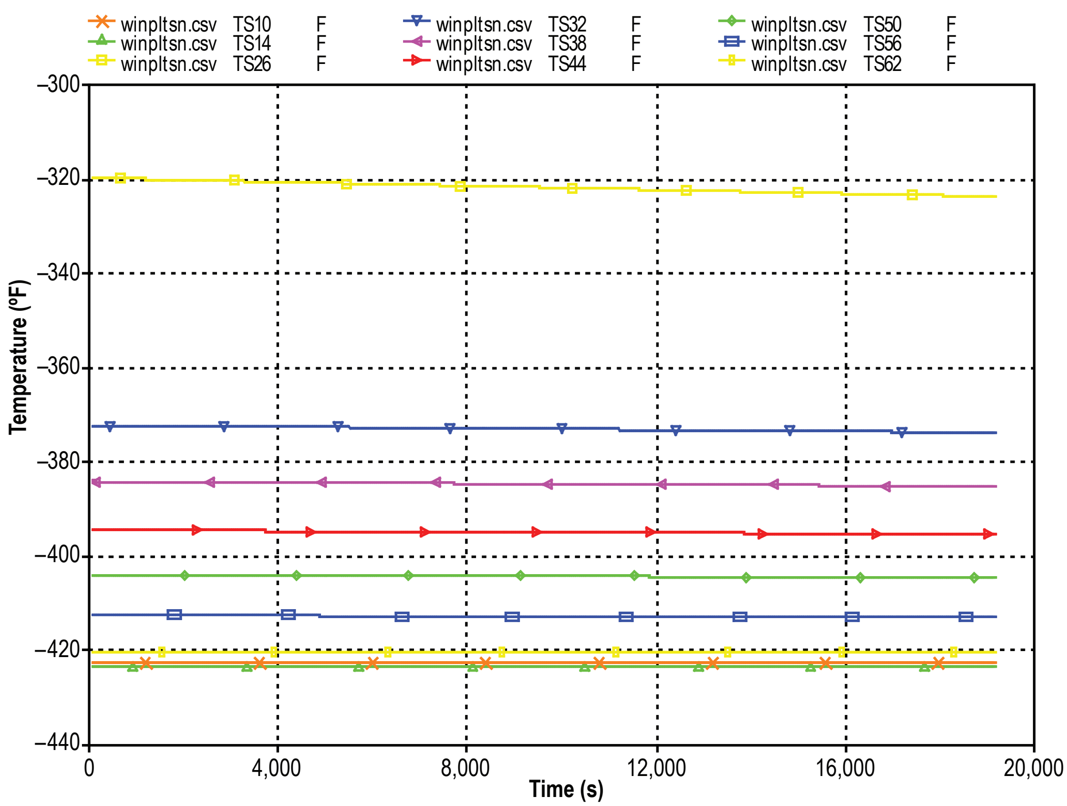

Figure 36. LC-39 perlite ullage inner sphere solid node temperature predictions.

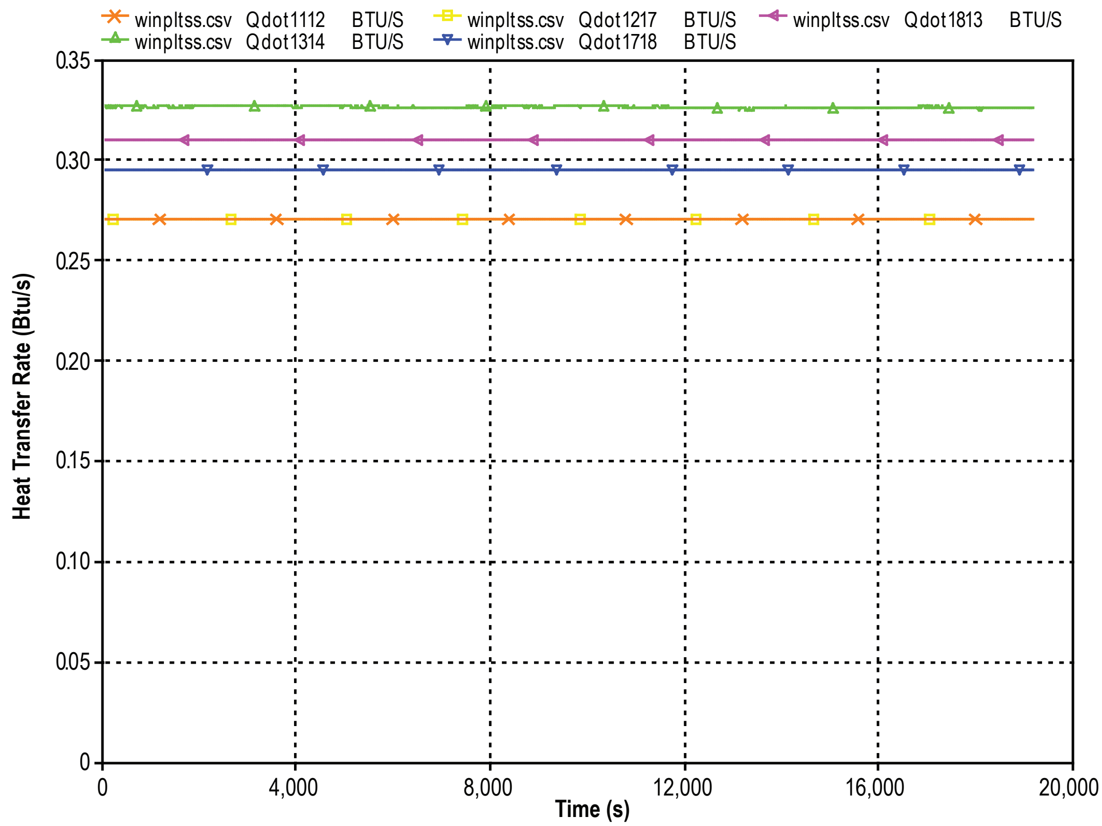

Figure 37. LC-39 perlite propellant path heat transfer rates.

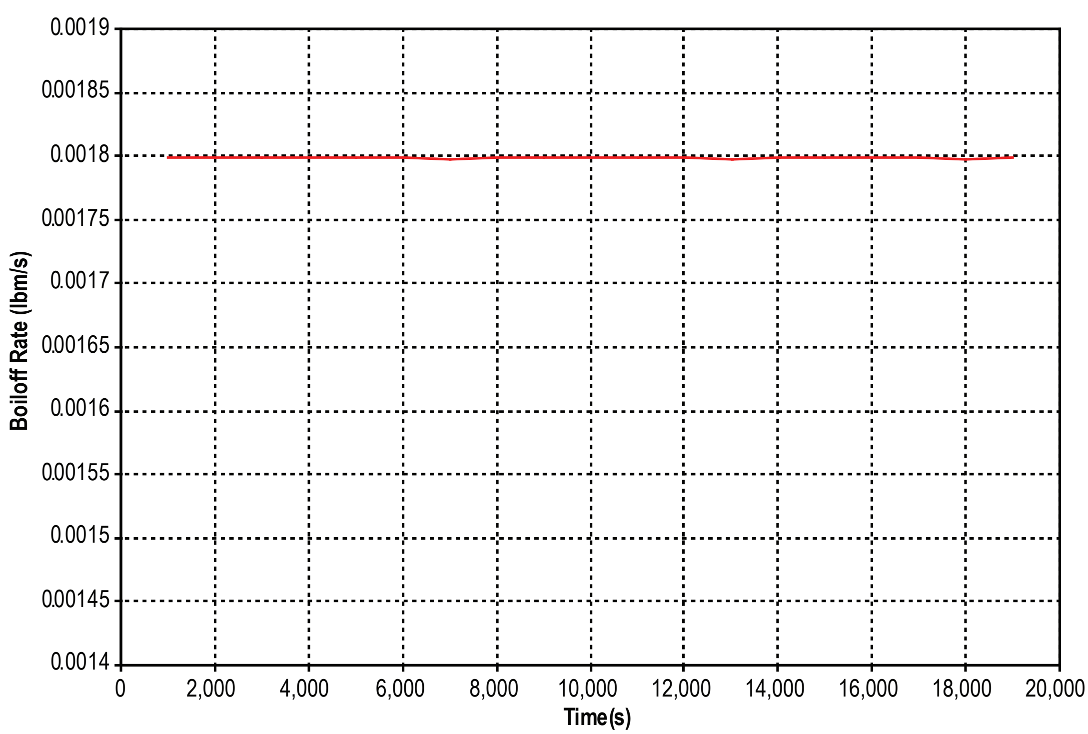

Figure 38. LC-39 perlite boiloff rates.

E.3 LC-39 Glass Bubbles Input Data File

```
GFSSP VERSION
   500
GFSSP INSTALLATION PATH
   C:\Program Files\GFSSP\
ANALYST
   Todd Steadman
INPUT DATA FILE NAME
   D:\KSC_Cryotank\Full_scale_tank\LC39B_LH2_glas06.dat
OUTPUT FILE NAME
   LC39B_LH2_glas06.out
TITLE
   LC-39 Liquid Hydrogen Tank - 85% Full by Height

USETUP
   F
DENCON      GRAVITY   ENERGY     MIXTURE    THRUST    STEADY    TRANSV    SAVER
   F        T         T          F          F         F         T         T
HEX         HCOEF     REACTING   INERTIA    CONDX     ADDPROP   PRINTI    ROTATION
   F        F         F          F          F         F         F         F
BUOYANCY    HRATE     INVAL      MSORCE     MOVBND    TPA       VARGEO    TVM
   T        T         T          F          F         F         F         F
SHEAR       PRNTIN    PRNTADD    OPVALVE    TRANSQ    CONJUG    RADIAT    WINPLOT
   F        F         T          F          F         T         T         T
PRESS       INSUC     VARROT     CYCLIC     CHKVALS
   T        F         F          F          T
NORMAL      SIMUL     SECONDL    NRSOLVT
   F        F         F          T
NNODES      NINT      NBR        NF
   11       9         9          1
RELAXK      RELAXD    RELAXH     CC         NITER
   1        0.5       0.01       1e-06      500
DTAU        TIMEF     TIMEL      NPSTEP
   10       45000     0000       300
NFLUID(I), I = 1, NF
   10

NODE     INDEX     DESCRIPTION
   1     2         "Vent Exit (Ambient)"
   2     1         "Ullage Node 8"
   3     2         "LH2 Tank Pseudo Node"
   4     1         "LH2 Propellant Volume"
   19    1         "Ullage Node 1"
   21    1         "Ullage Node 3"
   22    1         "Ullage Node 4"
   23    1         "Ullage Node 5"
   24    1         "Ullage Node 6"
   25    1         "Ullage Node 7"

REFERENCE NODE FOR DENSITY
   19

NODE     PRES     TEMP     MASS     HEAT     THRST    NODE-VOLUME
         (PSI)    (DEGF)   SOURC    SOURC    AREA
   2     14.7     -421     0        0        0        1.5982e+06
```

4	16.3	-423.6	0	0	0	1.9767e+08
19	14.7	-421	0	0	0	1.5982e+06
20	14.7	-421	0	0	0	1.5982e+06
22	14.7	-421	0	0	0	1.5982e+06
23	14.7	-421	0	0	0	1.5982e+06
24	14.7	-421	0	0	0	1.5982e+06
25	14.7	-421	0	0	0	1.5982e+06

ln2prsh1.dat
lh2prsh3.dat

INODE	NUMBR	NAMEBR	
2	1	252	
4	1	34	
19	2	1920	191
20	2	2021	1920
21	2	2122	2021
22	2	2223	2122
23	2	2324	2223
24	2	2425	2324
25	2	252	2425

BRANCH	UPNODE	DNNODE	OPTION	DESCRIPTION
34	3	4	2	“Propellant Surface (Pseudo Branch)”
252	25	2	1	“Pipe 252”
2425	24	25	1	“Pipe 2425”
2324	23	24	1	“Pipe 2324”
2223	22	23	1	“Pipe 2223”
2122	21	22	1	“Pipe 2122”
2021	20	21	1	«Pipe 2021»
1920	19	20	1	«Pipe 1920»
191	19	1	1	«Vent Line»

BRANCH	OPTION -2	FLOW COEFF	AREA			
34		0	1e-05			
BRANCH	OPTION -1	LENGTH	DIA	EPSD	ANGLE	AREA
252		7.79	511.82	0	0	2.0574e+05
BRANCH	OPTION -1	LENGTH	DIA	EPSD	ANGLE	AREA
2425		8.34	494.59	0	0	1.9212e+05
BRANCH	OPTION -1	LENGTH	DIA	EPSD	ANGLE	AREA
2324		9.07	474.71	0	0	1.7699e+05
BRANCH	OPTION -1	LENGTH	DIA	EPSD	ANGLE	AREA
2223		10.07	451.17	0	0	1.5987e+05
BRANCH	OPTION -1	LENGTH	DIA	EPSD	ANGLE	AREA
2122		11.57	422.14	0	0	1.3996e+05
BRANCH	OPTION -1	LENGTH	DIA	EPSD	ANGLE	AREA
2021		14.27	383.83	0	0	1.1571e+05
BRANCH	OPTION -1	LENGTH	DIA	EPSD	ANGLE	AREA
1920		45.81	325.3	0	0	83109
BRANCH	OPTION -1	LENGTH	DIA	EPSD	ANGLE	AREA
191		897	12.39	6.4568e-05	90	120.57

INITIAL FLOWRATES IN BRANCHES FOR UNSTEADY FLOW

34	0.0001
252	0

```
     2425        0
     2324        0
     2223        0
     2122        0
     2021        0
     1920        0
     191         0.0001

NUMBER OF PRESSURIZATION PROPELLANT TANKS IN CIRCUIT
     1
TNKTYPE     NODUL       NODULB      NODPRP      IBRPRP      TNKAR         TNKTH
     0      2           3           4           34          2.5666e+05    0.625
TNKRHO      TNKCP       TNKCON      ARHC        FCTHC       TNKTM
     467    0.07        0.0017      2.1816e+05  0.00265     -423.6
RESTART NODE INFORMATION FILE
   FNDLC39B.DAT
RESTART BRANCH INFORMATION FILE
   FBRLC39B.DAT
NSOLID      NAMB      NSSC      NSFC      NSAC      NSSR
     54     1         93        9         9         0

NODESL  MATRL SMASS          TS           NUMSS   NUMSF   NUMSA   NUMSSR DESCRIPTION
   7    44    1933.78000     85.00000     3       0       1       0      «Sec 8 OS Outer»
NAMESS
   78   711   677
NAMESA
   67
   8    44    1933.78000     85.00000     4       0       0       0      «Sec 7 OS Inner»
NAMESS
   78   812   815            668
   9    29    1477.42000     -417.00000   4       0       0       0      «Sec 8 IS Outer»
NAMESS
   910  913   169            639
   10   29    1477.42000     -418.00000   3       1       0       0      «Sec 8 IS Inner»
NAMESS
   910  1014  6210
NAMESF
   102
   11   44    173893.00000   85.00000     2       0       1       0      «Outer Half of Propellant
                                                                            Outer Tank Wall»
NAMESS
   1112 711
NAMESA
   611
   12   44    173893.00000   85.00000     3       0       0       0      «Inner Half of Propellant
                                                                            Outer Tank Wall»
NAMESS
   1112 812   1217
   13    29   122995.00000   -423.60000   3       0       0       0      «Outer Half of Propellant-
                                                                            Tank Wall»
NAMESS
   1314 913   1813
   14   29    122995.00000   -423.60000   2       1       0       0      «Inner Half of Propellant
                                                                            Tank Wall»
```

NAMESS								
1314	1014							
NAMESF								
144								
15	43	1073.27000	28.00000	4	0	0	0	«Sec 8 Ins Outer»
NAMESS								
815	1516	1517	6515					
16	43	1073.27000	-294.00000	4	0	0	0	«Sec 8 Ins Inner»
NAMESS								
1516	169	1618	6416					
17	43	93001.30000	14.00000	3	0	0	0	«Outer Half of Propellant Insulation»
NAMESS								
1217	1718	1517						
18	43	93001.30000	-324.00000	3	0	0	0	«Inner Half of Propellant Insulation»
NAMESS								
1718	1813	1618						
26	29	7195.20000	-408.00000	2	1	0	0	«Sec 1 IS Inner»
NAMESS								
2726	2632							
NAMESF								
2619								
27	29	7195.20000	-408.00000	3	0	0	0	«Sec 1 IS Outer»
NAMESS								
2726	2827	2733						
28	43	9078.26000	-294.00000	3	0	0	0	«Sec 1 Ins Inner»
NAMESS								
2827	2928	2834						
29	43	9078.26000	28.00000	3	0	0	0	«Sec 1 Ins Outer»
NAMESS								
2928	3029	2935						
30	44	22683.70000	85.00000	3	0	0	0	«Sec 1 OS Inner»
NAMESS								
3029	3130	3036						
31	44	22683.70000	85.00000	2	0	1	0	«Sec 1 OS Outer»
NAMESS								
3130	3137							
NAMESA								
631								
32	29	3146.34000	-409.00000	3	1	0	0	«Sec 2 IS Inner»
NAMES								
3332	2632	3238						
NAMESF								
3220								
33	29	3146.34000	-409.00000	4	0	0	0	«Sec 2 IS Outer»
NAMESS								
3332	3433	2733	3339					
34	43	2285.53000	-294.00000	4	0	0	0	«Sec 2 Ins Inner»
NAMESS								
3433	3534	2834	3440					
35	43	2285.53000	28.00000	4	0	0	0	«Sec 2 Ins Outer»
NAMESS								
3534	3635	2935	3541					

```
  36    44    4117.99000    85.00000    4    0    0    0    «Sec 2 OS Inner»
NAMES
  3635  3736  3036          3642
  37    44    4117.99000    85.00000    3    0    1    0    «Sec 2 OS Outer»
NAMESS
  3736  3137  3743
NAMESA
  637
  38    29    2448.33000    -410.00000  3    1    0    0    «Sec 3 IS Inner»
NAMESS
  3938  3238  3844
NAMESF
  3821
  39    29    2448.33000    -410.00000  4    0    0    0    «Sec 3 IS Outer»
NAMESS
  3938  4039  3339          3945
  40    43    1778.59000    -294.00000  4    0    0    0    «Sec 3 Ins Inner»
NAMESS
  4039  4140  3440          4046
  41    43    1778.59000 28.00000       4    0    0    0    «Sec 3 Ins Outer»
NAMESS
  4140  4241  3541          4147
  42    44    3204.60000    85.00000    4    0    0    0    «Sec 3 OS Inner»
NAMESS
  4241  4342  3642          4248
  43    44    3204.60000    85.00000    3    0    1    0    «Sec 3 OS Outer»
NAMESS
  4342  3743  4349
NAMESA
  643
  44    29    2088.37000    -411.00000  3    1    0    0    «Sec 4 IS Inner»
NAMESS
  4544  3844  4450
NAMESF
  4422
  45    29    2088.37000    -411.00000  4    0    0    0    «Sec 4 IS Outer»
NAMESS
  4544  4645  3945  4551
  46    43    1517.01000    -294.00000  4    0    0    0    «Sec 4 Ins Inner»
NAMESS
  4645  4746  4046          4652
  47    43    1517.01000    28.00000    4    0    0    0    «Sec 4 Ins Outer»
NAMESS
  4746  4847  4147          4753
  48    44    2733.29000    85.00000    4    0    0    0    «Sec 4 OS Inner»
NAMESS
  4847  4948  4248          4854
  49    44    2733.29000    85.00000    3    0    1    0    «Sec 4 OS Outer»
NAMESS
  4948  4349  4955
NAMESA
  649
  50    29    1859.02000    -412.00000  3    1    0    0    «Sec 5 IS Inner»
```

```
NAMESS
  5150      4450      5056
NAMESF
  5023
  51        29        1859.02000    -412.00000   4    0    0    0    «Sec 5 IS Outer»
NAMESS
  5150      5251      4551          5157
  52        43        1350.40000    -294.00000   4    0    0    0    “Sec 5 Ins Inner”
NAMESS
  5251      5352      4652          5258
  53        43        1350.40000    28.00000     4    0    0    0    “Sec 5 Ins Outer”
NAMESS
  5352      5453      4753          5359
  54        44        2433.11000    85.00000      4   0    0    0    “Sec 5 OS Inner”
NAMESS
  5453      5554      4854          5460
  55        44        2433.11000    85.00000      3   0    1    0    “Sec 5 OS Outer”
NAMESS
  5554      4955      5561
NAMESA
  655
  56        29        1696.69000    -413.00000   3    1    0    0    “Sec 6 IS Inner”
NAMESS
  5756      5056      5662
NAMESF
  5624
  57        29        1696.69000    -413.00000   4    0    0    0    “Sec 6 IS Outer”
NAMESS
  5756      5857      5157          5763
  58        43        1232.48000    -294.00000   4    0    0    0    “Sec 6 Ins Inner”
NAMESS
  5857      5958      5258          5864
  59        43        1232.48000    28.00000     4    0    0    0    “Sec 6 Ins Outer”
NAMESS
  5958      6059      5359          5965
  60         44       2220.64000    85.00000     4    0    0    0    “Sec 6 OS Inner”
NAMESS
  6059      6160      5460          6066
  61        44        2220.64000    85.00000     3    0    1    0    “Sec 6 OS Outer”
NAMESS
  6160      5561      6167
NAMESA
  661
  62        29        1574.14000    -414.00000   3    1    0    0    “Sec 7 IS Inner”
NAMESS
  6362      5662      6210
NAMESF
  6225
  63        29        1574.14000    -414.00000   4    0    0    0    “Sec 7 IS Outer”
NAMESS
  6362      6463      5763          639
  64        43        1143.46000    -294.00000   4    0    0    0    “Sec 7 Ins Inner”
NAMESS
  6463      6564      5864          6416
```

65	43	1143.46000	28.00000	4	0	0	0	"Sec 7 Ins Outer"

NAMESS

6564	6665	5965	6515

66	44	2060.25000	85.00000	4	0	0	0	"Sec 7 OS Inner"

NAMESS

6665	6766	6066	668

67	44	2060.25000	85.00000	3	0	1	0	"Sec 7 OS Outer"

NAMESS

6766	6167	677

NAMESA

667

NODEAM	TAMB	DESCRIPTION
6	85.00000	"Ambient Condition"

ICONSS	ICNSI	ICNSJ	ARCSIJ	DISTSIJ	DESCRIPTION
78	7	8	19879.20000	0.34000	"Sec 8 OS In-Out Conduction"
910	9	10	17494.40000	0.31000	"Sec 8 IS In-Out Conduction"
1112	11	12	1787620.00000	0.34000	"Propellant Surface Area at Midpoint of Outer Tank Wall"
1314	13	14	1456350.00000	0.31000	"Propellant Surface Area at Midpoint of Tank Wall"
1014	10	14	724.84000	5.34857	"Sec 8-Prp IS Inner"
913	9	13	725.45000	5.35309	"Sec 8-Prp IS Outer"
812	8	12	906.02100	6.07775	"Sec 8-Prp OS Inner"
711	7	11	906.76400	6.08273	"Sec 8-Prp OS Outer"
815	8	15	19862.90000	12.59000	"Sec 8 Ins-OS Conduction"
1516	15	16	18686.10000	24.84000	"Sec 8 Ins In-Out Conduction"
169	16	9	17509.20000	12.58000	"Sec 8 IS-Ins Conduction"
1217	12	17	1785250.00000	12.59000	"Propellant Outer Sphere-Insulation Interface Area"
1718	17	18	1617900.00000	24.84000	"Propellant Surface Area at Midpoint of Insulation"
1813	18	13	1458310.00000	12.58000	"Propellant Inner Sphere-Insulation Interface Area"
1517	15	17	63514.80000	5.89529	"Sec 8-Prp Ins Outer"
1618	16	18	59636.70000	5.53533	"Sec 8-Prp Ins Inner"
2726	27	26	88392.50000	0.31000	"Sec 1 IS In-Out Conduction"
2827	28	27	89193.00000	12.58000	"Sec 1 IS-Ins Conduction"
2928	29	28	156764.00000	24.84000	"Sec 1 Ins In-Out Conduction"
3029	30	29	232091.00000	12.59000	"Sec 1 Ins-OS Conduction"
3130	31	30	233187.00000	0.34000	"Sec 1 OS In-Out Conduction"
3332	33	32	37254.40000	0.31000	"Sec 2 IS In-Out Conduction"
3433	34	33	37286.00000	12.58000	"Sec 2 IS-Ins Conduction"
3534	35	34	39792.10000	24.84000	"Sec 2 Ins In-Out Conduction"
3635	36	35	42298.20000	12.59000	"Sec 2 Ins-OS Conduction"
3736	37	36	42332.90000	0.34000	"Sec 2 OS In-Out Conduction"
3938	39	38	28991.20000	0.31000	"Sec 3 IS In-Out Conduction"
4039	40	39	29015.70000	12.58000	"Sec 3 IS-Ins Conduction"
4140	41	40	30966.00000	24.84000	"Sec 3 Ins In-Out Conduction"
4241	42	41	32916.20000	12.59000	"Sec 3 Ins-OS Conduction"
4342	43	42	32943.20000	0.34000	"Sec 3 OS In-Out Conduction"
4544	45	44	24727.40000	0.31000	"Sec 4 IS In-Out Conduction"
4645	46	45	24748.30000	12.58000	"Sec 4 IS-Ins Conduction"
4746	47	46	26411.80000	24.84000	"Sec 4 Ins In-Out Conduction"
4847	48	47	28075.20000	12.59000	"Sec 4 Ins-OS Conduction"
4948	49	48	28098.20000	0.34000	"Sec 4 OS In-Out Conduction"
5150	51	50	22011.70000	0.31000	"Sec 5 IS In-Out Conduction"
5251	52	51	22030.40000	12.58000	"Sec 5 IS-Ins Conduction"

5352	53	52	23511.10000	24.84000	"Sec 5 Ins In-Out Conduction"
5453	54	53	24991.80000	12.59000	"Sec 5 Ins-OS Conduction"
5554	55	54	25012.30000	0.34000	"Sec 5 OS In-Out Conduction"
5756	57	56	20089.60000	0.31000	"Sec 6 IS In-Out Conduction"
5857	58	57	20106.60000	12.58000	"Sec 6 IS-Ins Conduction"
5958	59	58	21458.00000	24.84000	"Sec 6 Ins In-Out Conduction"
6059	60	59	22809.50000	12.59000	"Sec 6 Ins-OS Conduction"
6160	61	60	22828.20000	0.34000	"Sec 6 OS In-Out Conduction"
6362	63	62	18638.60000	0.31000	"Sec 7 IS In-Out Conduction"
6463	64	63	18654.40000	12.58000	"Sec 7 IS-Ins Conduction"
6564	65	64	19908.20000	24.84000	"Sec 7 Ins In-Out Conduction"
6665	66	65	21162.00000	12.59000	"Sec 7 Ins-OS Conduction"
6766	67	66	21179.40000	0.34000	"Sec 7 OS In-Out Conduction"
2632	26	32	724.83700	185.78600	"Sec 1-2 IS Inner"
3238	32	38	724.83700	28.05150	"Sec 2-3 IS Inner"
3844	38	44	724.83700	20.39420	"Sec 3-4 IS Inner"
4450	44	50	724.83700	16.53240	"Sec 4-5 IS Inner"
5056	50	56	724.83700	14.12770	"Sec 5-6 IS Inner"
5662	56	62	724.83700	12.46210	"Sec 6-7 IS Inner"
6210	62	10	724.83700	11.22990	"Sec 7-8 IS Inner"
2733	27	33	725.45000	185.94300	"Sec 1-2 IS Outer"
3339	33	39	725.45000	28.07530	"Sec 2-3 IS Outer"
3945	39	45	725.45000	20.41150	"Sec 3-4 IS Outer"
4551	45	51	725.45000	16.54640	"Sec 4-5 IS Outer"
5157	51	57	725.45000	14.13970	"Sec 5-6 IS Outer"
5763	57	63	725.45000	12.47270	"Sec 6-7 IS Outer"
639	63	9	725.45000	11.23940	"Sec 7-8 IS Outer"
2834	28	34	59636.70000	192.27400	"Sec 1-2 Ins Inner"
3440	34	40	59636.70000	29.03110	"Sec 2-3 Ins Inner"
4046	40	46	59636.70000	21.10640	"Sec 3-4 Ins Inner"
4652	46	52	59636.70000	17.10970	"Sec 4-5 Ins Inner"
5258	52	58	59636.70000	14.62110	"Sec 5-6 Ins Inner"
5864	58	64	59636.70000	12.89730	"Sec 6-7 Ins Inner"
6416	64	16	59636.70000	11.62200	"Sec 7-8 Ins Inner"
2935	29	35	63514.80000	204.77700	"Sec 1-2 Ins Outer"
3541	35	41	63514.80000	30.91890	"Sec 2-3 Ins Outer"
4147	41	47	63514.80000	22.47890	"Sec 3-4 Ins Outer"
4753	47	53	63514.80000	18.22230	"Sec 4-5 Ins Outer"
5359	53	59	63514.80000	15.57180	"Sec 5-6 Ins Outer"
5965	59	65	63514.80000	13.73600	"Sec 6-7 Ins Outer"
6515	65	15	63514.80000	12.37780	"Sec 7-8 Ins Outer"
3036	30	36	906.02100	211.11500	"Sec 1-2 OS Inner"
3642	36	42	906.02100	31.87590	"Sec 2-3 OS Inner"
4248	42	48	906.02100	23.17460	"Sec 3-4 OS Inner"
4854	48	54	906.02100	18.78630	"Sec 4-5 OS Inner"
5460	54	60	906.02100	16.05380	"Sec 5-6 OS Inner"
6066	60	66	906.02100	14.16110	"Sec 6-7 OS Inner"
668	66	8	906.02100	12.76090	"Sec 7-8 OS Inner"
3137	31	37	906.76400	211.28800	"Sec 1-2 OS Outer"
3743	37	43	906.76400	31.90200	"Sec 2-3 OS Outer"
4349	43	49	906.76400	23.19360	"Sec 3-4 OS Outer"
4955	49	55	906.76400	18.80170	"Sec 4-5 OS Outer"
5561	55	61	906.76400	16.06700	"Sec 5-6 OS Outer"

6167	61	67	906.76400	14.17270	"Sec 6-7 OS Outer"
677	67	7	906.76400	12.77140	"Sec 7-8 OS Outer"

ICONSF	ICS	ICF	MODEL	ARSF	HCSF	EMSFS	EMSFF	DESCRIPTION
102	10	2	0	1.74796e+04	1.00000e+00	0.00000e+00	0.00000e+00	«Sec 8 IS Ullage Wall»
144	14	4	0	1.45439e+06	0.00000e+00	0.00000e+00	0.00000e+00	«Propellant-Tank Wall Surface Area»
2619	26	19	0	8.75930e+04	1.00000e+00	0.00000e+00	0.00000e+00	«Sec 1 IS Ullage Wall»
3220	32	20	0	3.72229e+04	1.00000e+00	0.00000e+00	0.00000e+00	«Sec 2 IS Ullage Wall»
3821	38	21	0	2.89667e+04	1.00000e+00	0.00000e+00	0.00000e+00	«Sec 3 IS Ullage Wall»
4422	44	22	0	2.47065e+04	1.00000e+00	0.00000e+00	0.00000e+00	«Sec 4 IS Ullage Wall»
5023	50	23	0	2.19931e+04	1.00000e+00	0.00000e+00	0.00000e+00	«Sec 5 IS Ullage Wall»
5624	56	24	0	2.00726e+04	1.00000e+00	0.00000e+00	0.00000e+00	«Sec 6 IS Ullage Wall»
6225	62	25	0	1.86228e+04	1.00000e+00	0.00000e+00	0.00000e+00	«Sec 7IS Ullage Wall»

ICONSA	ICSAS	ICSAA	ARSA	HCSA	EMSAS	EMSAA	DESCRIPTION
67	7	6	1.98955e+04	4.44000e-04	7.00000e-01	7.00000e-01	"Sec 8 OS-Amb Convection"
611	11	6	1.78999e+06	4.44000e-04	7.00000e-01	7.00000e-01	"Propellant Space Outer Surface of Outer Tank"
631	31	6	2.34285e+05	4.44000e-04	7.00000e-01	7.00000e-01	"Sec 1 OS-Amb Convection"
637	37	6	4.23676e+04	4.44000e-04	7.00000e-01	7.00000e-01	"Sec 2 OS-Amb Convection"
643	43	6	3.29702e+04	4.44000e-04	7.00000e-01	7.00000e-01	"Sec 3 OS-Amb Convection"
649	49	6	2.81212e+04	4.44000e-04	7.00000e-01	7.00000e-01	"Sec 4 OS-Amb Convection"
655	55	6	2.50328e+04	4.44000e-04	7.00000e-01	7.00000e-01	"Sec 5 OS-Amb Convection"
661	61	6	2.28469e+04	4.44000e-04	7.00000e-01	7.00000e-01	"Sec 6 OS-Amb Convection"
667	67	6	2.11967e+04	4.44000e-04	7.00000e-01	7.00000e-01	"Sec 7 OS-Amb Convection"

E.4 LC-39 Glass Bubbles Sample Output Data File

ISTEP =1500 TAU = 0.60000E+05

BOUNDARY NODES

NODE	P (PSI)	TF (F)	Z (COMP)	RHO (LBM/FT^3)	QUALITY
1	0.1470E+02	0.8500E+02	0.0000E+00	0.5065E-02	0.1000E+01
3	0.1631E+02	-0.4241E+03	0.0000E+00	0.4458E+01	0.0000E+00

SOLUTION

INTERNAL NODES

NODE	P (PSI)	TF (F)	Z (COMP)	RHO (LBM/FT^3)	EM (LBM)	QUALITY
2	0.1470E+02	-0.4228E+03	0.9076E+00	0.8264E-01	0.7643E+02	0.1000E+01
4	0.1345E+02	-0.4236E+03	0.1584E-01	0.4438E+01	0.5077E+06	0.5202E-06
19	0.1470E+02	-0.2606E+03	0.1001E+01	0.1387E-01	0.1283E+02	0.1000E+01
20	0.1470E+02	-0.3344E+03	0.9982E+00	0.2209E-01	0.2043E+02	0.1000E+01
21	0.1470E+02	-0.3571E+03	0.9954E+00	0.2707E-01	0.2504E+02	0.1000E+01
22	0.1470E+02	-0.3746E+03	0.9911E+00	0.3279E-01	0.3033E+02	0.1000E+01
23	0.1470E+02	-0.3885E+03	0.9846E+00	0.3945E-01	0.3649E+02	0.1000E+01
24	0.1470E+02	-0.4004E+03	0.9740E+00	0.4792E-01	0.4432E+02	0.1000E+01
25	0.1470E+02	-0.4112E+03	0.9550E+00	0.5980E-01	0.5531E+02	0.1000E+01

NODE	H BTU/LB	ENTROPY BTU/LB-R	EMU LBM/FT-SEC	COND BTU/FT-S-R	CP BTU/LB-R	GAMA
2	0.8304E+02	0.7340E+01	0.7653E-06	0.2637E-05	0.2784E+01	0.1869E+01

4	-0.1105E+03	0.1907E+01	0.9179E-05	0.1579E-04	0.2250E+01	0.1698E+01
19	0.5334E+03	0.7340E+01	0.2985E-05	0.1460E-04	0.3413E+01	0.1409E+01
20	0.3104E+03	0.7340E+01	0.2171E-05	0.8381E-05	0.2666E+01	0.1602E+01
21	0.2515E+03	0.7340E+01	0.1861E-05	0.6841E-05	0.2535E+01	0.1663E+01
22	0.2074E+03	0.7340E+01	0.1603E-05	0.5754E-05	0.2505E+01	0.1692E+01
23	0.1725E+03	0.7340E+01	0.1383E-05	0.4893E-05	0.2531E+01	0.1703E+01
24	0.1421E+03	0.7340E+01	0.1182E-05	0.4150E-05	0.2566E+01	0.1724E+01
25	0.1141E+03	0.7340E+01	0.9868E-06	0.3441E-05	0.2626E+01	0.1762E+01

BRANCHES

BRANCH	KFACTOR (LBF-S^2/ (LBM-FT)^2)	DELP (PSI)	FLOW RATE (LBM/SEC)	VELOCITY (FT/SEC)	REYN. NO.	MACH NO.	ENTROPY GEN. BTU/(R-SEC)	LOST WORK LBF-FT/SEC
34	0.000E+00	0.286E+01	0.624E-11	0.202E-04	0.284E-02	0.167E-07	0.000E+00	0.000E+00
252	0.000E+00	0.274E-03	-0.126E-02	-0.107E-04	0.492E+02	0.736E-08	0.000E+00	0.000E+00
2425	0.000E+00	0.207E-03	-0.125E-02	-0.156E-04	0.391E+02	0.987E-08	0.000E+00	0.000E+00
2324	0.000E+00	0.170E-03	-0.124E-02	-0.210E-04	0.337E+02	0.122E-07	0.000E+00	0.000E+00
2223	0.000E+00	0.144E-03	-0.123E-02	-0.282E-04	0.302E+02	0.150E-07	0.000E+00	0.000E+00
2122	0.000E+00	0.123E-03	-0.123E-02	0.387E-04	0.278E+02	0.189E-07	0.000E+00	0.000E+00
2021	0.000E+00	0.107E-03	-0.122E-02	0.560E-04	0.261E+02	0.252E-07	0.000E+00	0.000E+00
1920	0.000E+00	0.152E-03	-0.119E-02	0.930E-04	0.257E+02	0.354E-07	0.000E+00	0.000E+00
191	0.153E+02	-0.531E-06	0.117E-02	0.101E+00	0.484E+03	0.384E-04	0.115E-10	0.178E-05

SOLID NODES

NODESL	CPSLD BTU/LB F	TS F
7	0.110E+00	0.850E+02
8	0.110E+00	0.850E+02
9	0.107E+00	-0.420E+03
10	0.107E+00	-0.420E+03
11	0.110E+00	0.850E+02
12	0.110E+00	0.850E+02
13	0.107E+00	-0.424E+03
14	0.107E+00	-0.424E+03
15	0.190E+00	0.275E+02
16	0.190E+00	-0.295E+03
17	0.190E+00	0.140E+02
18	0.190E+00	-0.324E+03
26	0.116E+00	-0.257E+03
27	0.116E+00	-0.257E+03
28	0.190E+00	-0.293E+03
29	0.190E+00	0.280E+02
30	0.110E+00	0.850E+02
31	0.110E+00	0.850E+02
32	0.112E+00	-0.333E+03
33	0.112E+00	-0.333E+03
34	0.190E+00	-0.294E+03
35	0.190E+00	0.279E+02
36	0.110E+00	0.850E+02
37	0.110E+00	0.850E+02
38	0.110E+00	-0.356E+03
39	0.110E+00	-0.356E+03
40	0.190E+00	-0.294E+03

41	0.190E+00	0.279E+02
42	0.110E+00	0.850E+02
43	0.110E+00	0.850E+02
44	0.109E+00	-0.374E+03
45	0.109E+00	-0.374E+03
46	0.190E+00	-0.294E+03
47	0.190E+00	0.279E+02
48	0.110E+00	0.850E+02
49	0.110E+00	0.850E+02
50	0.109E+00	-0.388E+03
51	0.109E+00	-0.388E+03
52	0.190E+00	-0.294E+03
53	0.190E+00	0.279E+02
54	0.110E+00	0.850E+02
55	0.110E+00	0.850E+02
56	0.108E+00	-0.400E+03
57	0.108E+00	-0.400E+03
58	0.190E+00	-0.294E+03
59	0.190E+00	0.279E+02
60	0.110E+00	0.850E+02
61	0.110E+00	0.850E+02
62	0.107E+00	-0.411E+03
63	0.107E+00	-0.411E+03
64	0.190E+00	-0.294E+03
65	0.190E+00	0.279E+02
66	0.110E+00	0.850E+02
67	0.110E+00	0.850E+02

SOLID TO SOLID CONDUCTOR

ICONSS	CONDKIJ BTU/S FT F	QDOTSS BTU/S
78	0.750E-02	0.155E-02
910	0.255E-02	0.391E-01
1112	0.750E-02	0.161E+00
1314	0.255E-02	0.281E+00
1014	0.255E-02	0.961E-01
913	0.255E-02	0.962E-01
812	0.750E-02	0.161E-03
711	0.750E-02	0.161E-03
815	0.192E-06	0.145E-02
1516	0.960E-07	0.194E-02
169	0.192E-06	0.279E-02
1217	0.192E-06	0.161E+00
1718	0.960E-07	0.176E+00
1813	0.192E-06	0.185E+00
1517	0.960E-07	0.117E-02
1618	0.960E-07	0.251E-02
2726	0.275E-02	0.111E+00
2827	0.192E-06	-0.412E-02
2928	0.960E-07	0.162E-01
3029	0.192E-06	0.168E-01
3130	0.750E-02	0.168E-01
3332	0.267E-02	0.167E-01
3433	0.192E-06	0.186E-02

3534	0.960E-07	0.412E-02
3635	0.192E-06	0.307E-02
3736	0.750E-02	0.307E-02
3938	0.264E-02	0.124E-01
4039	0.192E-06	0.229E-02
4140	0.960E-07	0.321E-02
4241	0.192E-06	0.239E-02
4342	0.750E-02	0.239E-02
4544	0.262E-02	0.845E-02
4645	0.192E-06	0.251E-02
4746	0.960E-07	0.274E-02
4847	0.192E-06	0.204E-02
4948	0.750E-02	0.204E-02
5150	0.260E-02	0.537E-02
5251	0.192E-06	0.263E-02
5352	0.960E-07	0.244E-02
5453	0.192E-06	0.181E-02
5554	0.750E-02	0.182E-02
5756	0.258E-02	0.433E-02
5857	0.192E-06	0.271E-02
5958	0.960E-07	0.223E-02
6059	0.192E-06	0.166E-02
6160	0.750E-02	0.167E-02
6362	0.257E-02	0.568E-02
6463	0.192E-06	0.276E-02
6564	0.960E-07	0.206E-02
6665	0.192E-06	0.154E-02
6766	0.750E-02	0.158E-02
2632	0.271E-02	0.668E-01
3238	0.266E-02	0.131E+00
3844	0.263E-02	0.139E+00
4450	0.261E-02	0.135E+00
5056	0.259E-02	0.134E+00
5662	0.258E-02	0.134E+00
6210	0.256E-02	0.132E+00
2733	0.271E-02	0.668E-01
3339	0.266E-02	0.131E+00
3945	0.263E-02	0.139E+00
4551	0.261E-02	0.135E+00
5157	0.259E-02	0.134E+00
5763	0.258E-02	0.134E+00
639	0.256E-02	0.132E+00
2834	0.960E-07	0.842E-06
3440	0.960E-07	0.274E-05
4046	0.960E-07	0.246E-05
4652	0.960E-07	0.224E-05
5258	0.960E-07	0.229E-05
5864	0.960E-07	0.252E-05
6416	0.960E-07	0.311E-04
2935	0.960E-07	0.390E-06
3541	0.960E-07	0.272E-08
4147	0.960E-07	0.195E-08
4753	0.960E-07	0.178E-08
5359	0.960E-07	0.199E-08

5965	0.960E-07	0.675E-07
6515	0.960E-07	0.135E-04
3036	0.750E-02	0.459E-06
3642	0.750E-02	0.161E-06
4248	0.750E-02	0.566E-06
4854	0.750E-02	0.229E-05
5460	0.750E-02	0.785E-05
6066	0.750E-02	0.237E-04
668	0.750E-02	0.649E-04
3137	0.750E-02	0.458E-06
3743	0.750E-02	0.161E-06
4349	0.750E-02	0.566E-06
4955	0.750E-02	0.229E-05
5561	0.750E-02	0.784E-05
6167	0.750E-02	0.237E-04
677	0.750E-02	0.648E-04

SOLID TO FLUID CONDUCTOR

ICONSF	QDOTSF	HCSF	HCSFR
	BTU/S	BTU/S FT**2 F	BTU/S FT**2 F
102	-0.755E-01	0.249E-03	0.000E+00
144	-0.376E+00	0.113E-02	0.000E+00
2619	-0.225E+00	0.105E-03	0.000E+00
3220	-0.315E-01	0.871E-04	0.000E+00
3821	-0.225E-01	0.917E-04	0.000E+00
4422	-0.144E-01	0.933E-04	0.000E+00
5023	-0.811E-02	0.915E-04	0.000E+00
5624	-0.594E-02	0.959E-04	0.000E+00
6225	-0.857E-02	0.120E-03	0.000E+00

SOLID TO AMBIENT CONDUCTOR

ICONSA	QDOTSA	HCSA	HCSAR
	BTU/S	BTU/S FT**2 F	BTU/S FT**2 F
67	0.164E-02	0.444E-03	0.166E-03
611	0.161E+00	0.444E-03	0.166E-03
631	0.168E-01	0.444E-03	0.166E-03
637	0.307E-02	0.444E-03	0.166E-03
643	0.239E-02	0.444E-03	0.166E-03
649	0.204E-02	0.444E-03	0.166E-03
655	0.182E-02	0.444E-03	0.166E-03
661	0.169E-02	0.444E-03	0.166E-03
667	-0.473E-01	0.444E-03	0.166E-03

NUMBER OF PRESSURIZATION SYSTEMS = 1

NODUL	NODPRP	QULPRP	QULWAL	QCOND	TNKTM	VOLPROP	VOLULG
2	4	0.0003	0.0000	0.0000	36.0000	**********	924.8683

E.5.1 LC-39 Glass Bubbles Sample Output Plots

LC-39 glass bubbles propellant path solid node temperature prediction, ullage inner sphere solid node temperature prediction, propellant path heat transfer rates, and boiloff rate output plots are shown in figures 39–42, respectively.

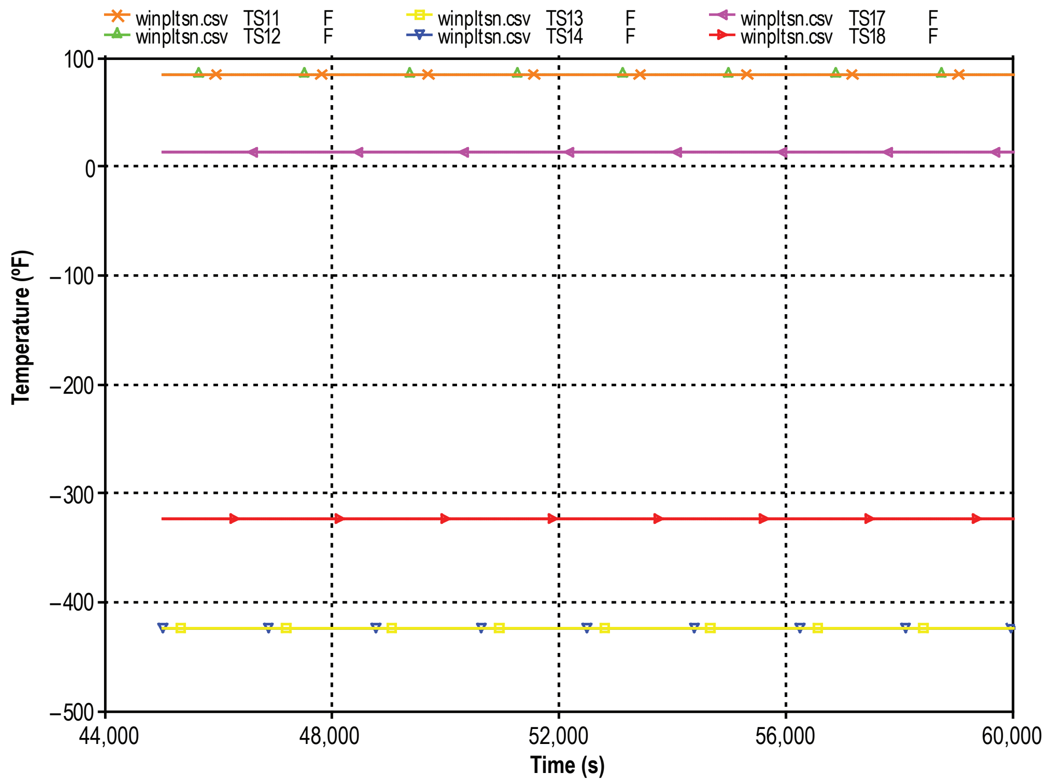

Figure 39. LC-39 glass bubbles propellant path solid node temperature predictions.

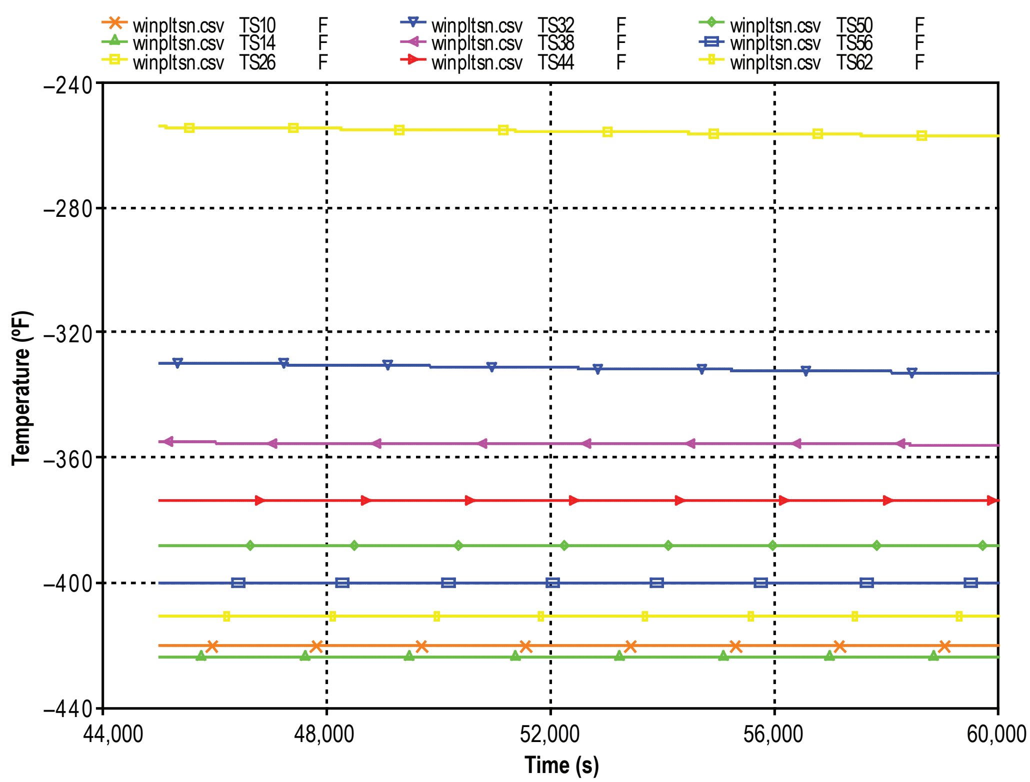

Figure 40. LC-39 glass bubbles ullage inner sphere solid node temperature predictions.

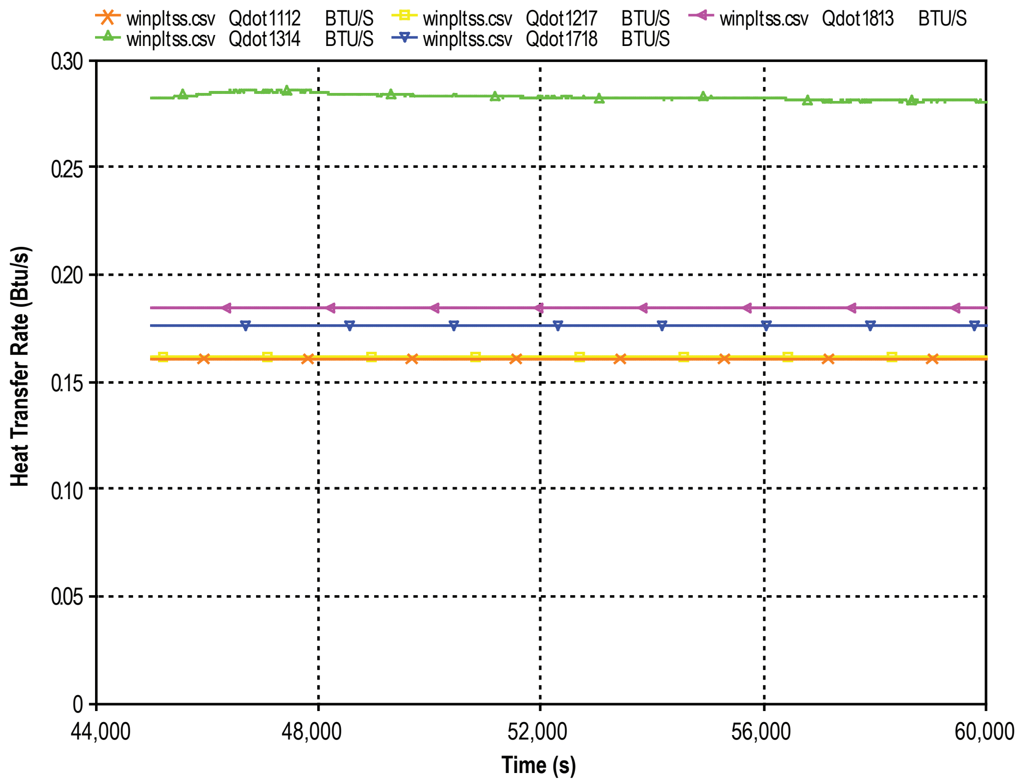

Figure 41. LC-39 glass bubbles propellant path heat transfer rates.

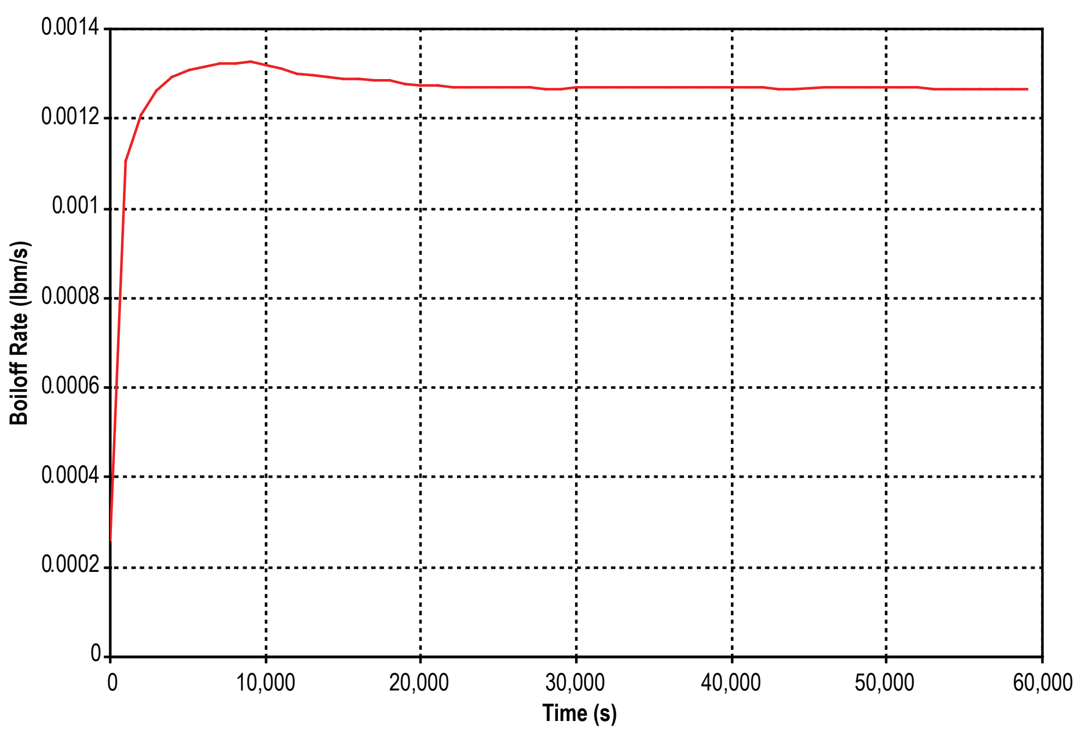

Figure 42. LC-39 glass bubbles boiloff rates.

REFERENCES

1. Fesmire, J.E.; and Augustynowicz, S.D.: "Thermal Performance Testing of Glass Microspheres Under Cryogenic Vacuum Conditions," *Paper No. CEC C2-C-04*, Cryogenic Engineering Conference, Anchorage, AL, September 22–26, 2003.

2. Fesmire, J.E.; Augustynowicz, S.D.; Nagy, Z.F.; et al.: "Vibration and Thermal Cycling Effects on Bulk-Fill Insulation Materials for Cryogenic Tanks," *Paper No. CEC C2-T-04*, Cryogenic Engineering Conference, Keystone, CO, August 29–September 2, 2005.

3. Majumdar, A.K.: "A Second Law Based Unstructured Finite Volume Procedure for Generalized Flow Simulation," *Paper No. AIAA 99-0934*, 37th AIAA Aerospace Sciences Meeting Conference and Exhibit, Reno, NV, January 11–14, 1999.

4. Majumdar, A.K.; and Steadman, T.: "Numerical Modeling of Pressurization of a Propellant Tank," *Journal of Propulsion and Power*, Vol. 17, No. 2, pp. 385–391, March–April 2001.

5. Majumdar, A.K.: "Numerical Modeling of Conjugate Heat Transfer in Fluid Network," Thermal Fluid Analysis Workshop, Jet Propulsion Laboratory, Pasadena, CA, August 30–September 3, 2004.

6. Hendricks, R.C.; Baron, A.K.; and Peller, I.C.: "GASP—A Computer Code for Calculating the Thermodynamic and Transport Properties for Ten Fluids: Parahydrogen, Helium, Neon, Methane, Nitrogen, Carbon Monoxide, Oxygen, Fluorine, Argon, and Carbon Dioxide," *NASA-TN-D-7808*, Glenn Research Center, February 1975.

7. Hendricks, R.C.; Peller, I.C.; and Baron, A.K.: "WASP—A Flexible FORTRAN IV Computer Code for Calculating Water and Steam Properties," *NASA-TN-D-7391*, Glenn Research Center, November 1973.

8. Cryodata Inc., *User's Guide to GASPAK, Version 3.20*, November 1994.

9. Van Hooser, K.; Bailey, J.W.; and Majumdar, A.K.: "Numerical Prediction of Transient Axial Thrust and Internal Flows in a Rocket Engine Turbopump," *Paper No. AIAA 99-2189*, 35th AIAA/ASME/SAE/ASEE Joint Propulsion Conference, Los Angeles, CA, June 20–24, 1999.

10. Holt, K.; Majumdar, A.; Steadman, T.; and Hedayat, A.: "Numerical Modeling and Test Data Comparison of Propulsion Test Article Helium Pressurization System," *Paper No. AIAA-2000-3719*, 36th AIAA /ASME /SAE /ASEE Joint Propulsion Conference and Exhibit, Huntsville, AL, July 16–19, 2000.

11. Sass, J.P.; Fesmire, J.E.; Morris, D.L.; et al.: "Thermal Performance Comparison of Glass Microsphere and Perlite Insulation Systems for Liquid Hydrogen Storage Tanks," *Paper No. C3-K-05,* Cryogenic Engineering Conference and International Cryogenic Materials Conference, Chattanooga, TN, July 16–20, 2007.

12. Fesmire, J.E.; Sass, J.P.; Morris, D.L.; et al.: "Cost-Efficient Storage of Cryogens," *Paper No. C3-K-06*, Cryogenic Engineering Conference and International Cryogenic Materials Conference, Chattanooga, TN, July 16–20, 2007.

REPORT DOCUMENTATION PAGE			*Form Approved* *OMB No. 0704-0188*
Public reporting burden for this collection of information is estimated to average 1 hour per response, including the time for reviewing instructions, searching existing data sources, gathering and maintaining the data needed, and completing and reviewing the collection of information. Send comments regarding this burden estimate or any other aspect of this collection of information, including suggestions for reducing this burden, to Washington Headquarters Services, Directorate for Information Operation and Reports, 1215 Jefferson Davis Highway, Suite 1204, Arlington, VA 22202-4302, and to the Office of Management and Budget, Paperwork Reduction Project (0704-0188), Washington, DC 20503			
1. AGENCY USE ONLY *(Leave Blank)*	2. REPORT DATE November 2007	3. REPORT TYPE AND DATES COVERED Technical Memorandum	
4. TITLE AND SUBTITLE Numerical Modeling of Propellant Boiloff in Cryogenic Storage Tank			5. FUNDING NUMBERS
6. AUTHORS A.K. Majumdar, T.E. Steadman,* and J.L. Maroney*			
7. PERFORMING ORGANIZATION NAME(S) AND ADDRESS(ES) George C. Marshall Space Flight Center Marshall Space Flight Center, AL 35812			8. PERFORMING ORGANIZATION REPORT NUMBER M–1206
9. SPONSORING/MONITORING AGENCY NAME(S) AND ADDRESS(ES) National Aeronautics and Space Administration Washington, DC 20546–0001			10. SPONSORING/MONITORING AGENCY REPORT NUMBER NASA/TM—2007–215131
11. SUPPLEMENTARY NOTES Prepared by the Propulsion Systems Department, Engineering Directorate *Sverdrup Technology, Inc., Huntsville, AL			
12a. DISTRIBUTION/AVAILABILITY STATEMENT Unclassified-Unlimited Subject Category 14 Availability: NASA CASI 301–621–0390			12b. DISTRIBUTION CODE
13. ABSTRACT *(Maximum 200 words)* This Technical Memorandum (TM) describes the thermal modeling effort undertaken at Marshall Space Flight Center to support the Cryogenic Test Laboratory at Kennedy Space Center (KSC) for a study of insulation materials for cryogenic tanks in order to reduce propellant boiloff during long-term storage. The Generalized Fluid System Simulation program has been used to model boiloff in 1,000-L demonstration tanks built for testing the thermal performance of glass bubbles and perlite insulation. Numerical predictions of boiloff rate and ullage temperature have been compared with the measured data from the testing of demonstration tanks. A satisfactory comparison between measured and predicted data has been observed for both liquid nitrogen and hydrogen tests. Based on the experience gained with the modeling of the demonstration tanks, a numerical model of the liquid hydrogen storage tank at launch complex 39 at KSC was built. The predicted boiloff rate of hydrogen has been found to be in good agreement with observed field data. This TM describes three different models that have been developed during this period of study (March 2005 to June 2006), comparisons with test data, and results of parametric studies.			
14. SUBJECT TERMS cryogenic tanks, thermal insulation, propellant boiloff, finite volume method, conjugate heat transfer			15. NUMBER OF PAGES 102
			16. PRICE CODE
17. SECURITY CLASSIFICATION OF REPORT Unclassified	18. SECURITY CLASSIFICATION OF THIS PAGE Unclassified	19. SECURITY CLASSIFICATION OF ABSTRACT Unclassified	20. LIMITATION OF ABSTRACT Unlimited

NSN 7540-01-280-5500

Standard Form 298 (Rev. 2-89)
Prescribed by ANSI Std. 239-18
298-102

National Aeronautics and
Space Administration
IS20
George C. Marshall Space Flight Center
Marshall Space Flight Center, Alabama
35812